The roles of specific Monodehydroascorbate Reductases in the Arabidopsis thaliana antioxidative system.

Dongdong Xu

université PARIS-SACLAY

Roles of specific monodehydroascorbate reductases in the antioxidant system of *Arabidopsis thaliana*

Les rôles de spécifique monodéhydroascorbate réductases dans le système antioxydant chez Arabidopsis thaliana

Thèse de doctorat de l'université Paris-Saclay

École doctorale n° 567 SEVE, Science du Végétal : du gène à l'écosystème
Spécialité de doctorat : Sciences Végétales
Graduate School : Biosphera. Référent : Faculté des sciences d'Orsay

Thèse préparée à l'institut des sciences des plantes de Paris- Saclay (Université d'Evry-Val-d'Essonne, Université Paris-Saclay, CNRS, Université Paris Cité, INRAE)
Sous la direction de **Graham NOCTOR**, professeur de l'Université Paris-Saclay,
la co-direction de **Emmanuelle ISSAKIDIS-BOURGUET**, chargée de recherches

Thèse soutenue à Paris-Saclay, le 13 Décembre 2024, par

Dongdong XU

Composition du Jury

Membres du jury avec voix délibérative

Dr. Valérie GEFFROY Directrice de recherches, Univ. Paris-Saclay, IPS2	Présidente
Dr. Anne REPELLIN Professeure, Univ. Paris-Est Créteil, IEES Paris	Rapportrice & Examinatrice
Dr. Ivan COUEE Professeur, Univ. Rennes, Ecobio Rennes	Rapporteur & Examinateur
Dr. Arnould SAVOURE Professeur, Univ. Sorbonne, IEES Paris	Examinateur

THÈSE DE DOCTORAT

NNT : 2024UPASB071

Acknowledgements

As I approach the end of my four-year PhD journey, I would like to express my gratitude to everyone who has supported me along the way.

First and foremost, I am deeply grateful to my supervisor Pr. Graham Noctor for giving me the opportunity to join his group and pursue my PhD research, for his supervision with immense knowledge and rigorous attitude towards scientific research. Deep thanks are also due to my co-supervisor Dr. Emmanuelle Issakidis-Bourguet for her important scientific guidance, as well as for her kind and thoughtful encouragement during both the professional and personal challenges of my PhD journey. I am immensely thankful to both of them for their invaluable scientific guidance throughout my PhD.

My special appreciation is given to Gilles Châtel-Innocenti and Christophe Espinasse for their assistance and mentoring in scientific skills, which were crucial to the successful completion of this work. The insightful discussions shared with colleagues Mathias, Lug and Tao, have greatly enriched the research experience. I would also like to express my gratitude to Hélène Vanacker for her valuable guidance and contributions to my work.

I want to express my appreciation to everyone who helped me, both within the CCARS team and outside of it. Your encouragement and assistance, especially in providing crucial experimental materials, have been invaluable to my research. Heartfelt appreciation goes to the fellow Chinese colleagues: Siqi, Fengquan, Jing (former post-doc), Zhengyang, Yanyan, Xiaoning, Yonghua, Yangyang, Xiaoyu, Lili, Fei, and many others. Thank you for the wonderful times we shared, you filled these four years with joy and warmth.

I am also deeply grateful to the committee members Dr. Cécile Raynaud, Dr. Pierre Crozet, and Dr. Mathieu Jossier, as well as to Dr. Marianne Delarue from the doctoral school for their guidance and advices.

Lastly, I would like to extend my deepest gratitude to the China Scholarship Council (CSC), French Agence Nationale de la Recherche grants ANR-17-CE20-0025 (HIPATH) and the Institut Universitaire de France (IUF) for their unwavering support. Without their financial supporting, my PhD in France would not have been possible.

Finally, I wish to thank my family in China. I am forever grateful for my parents' unconditional support for my decision to pursue a PhD in France. I am also deeply thankful to my husband, Mr. Haizhou Liu, for his understanding and support which gave me the resilience and courage in my study.

Thank you to everyone who contributed to this unforgettable journey.

Abbreviations

ACOX	Acyl-CoA oxidase
AO	Ascorbate oxidase
APX	Ascorbate peroxidase
AQPs	Aquaporins
Asc	Ascorbate
CAT	Catalase
CDPK	Ca^{2+}-dependent protein kinase
cICDH	Cytosolic NADP-dependent isocitrate dehydrogenase
CIPK	Calcineurin B-like-interacting protein kinase
CO_2	Carbon dioxide
Cys	Cysteine
DAB	3,3'-diaminobenzidine
DHA(R)	Dehydroascorbate (reductase)
DMSO	Dimethyl sulfoxide
DNA	Deoxyribonucleic acid
E.coli	*Escherichia coli*
EF	Extended finger
EMS	Ethyl methane sulfonate
EPR	Electron paramagnetic resonance
ETI	Effector-triggered immunity
FAD	Flavin adenine dinucleotide
FNR	Ferredoxin-$NADP^+$ oxidoreductase
FTR	Ferredoxin-thioredoxin reductase
GFP	Green fluorescent protein
GOX	Glycolate oxidase
GPX	Glutathione peroxidase
GR	Glutathione reductase
GRX	Glutaredoxin
GSH/GSSG	Reduced/oxidized glutathione
GSTs	Glutathione S-transferases
GTP	Guanosine triphosphate
G6PDH	Glucose-6-phosphate dehydrogenase
His	Histidine
H_2O_2	Hydrogen peroxide
HPCA1	Hydrogen peroxide-induced calcium increases
HPLC	High performance liquid chromatography
HR	Hypersensitive response
IAA	3-indoleacetic acid
ICDH	Isocitrate dehydrogenase
ICS1	Isochorismate synthase1

IPTG	Isopropyl β-D-1-thiogalactopyranoside
JA	Jasmonic acid
LD	Long-day
LHC	Light-harvesting antenna complex
MAPK	Mitogen-activated protein kinase
ME	Malic enzyme
mBBr	Monobromobimane
MDA	Malondialdehyde
MDHA	Monodehydroascorbate
MDHAR	Monodehydroascorbate reductase
Met	Methionine
mETC	Mitochondrial electron transport chain
NAD(H)	Nicotinamide adenine dinucleotide
NADP(H)	Nicotinamide adenine dinucleotide phosphate
NADP-ME	NADP-dependent malic enzyme
NLRs	Nucleotide-binding domain leucine-rich repeat receptors
NO	Nitric oxide
NPR1	Nonexpresser of *PR* gene 1
NTR	NADPH-thioredoxin reductase
$O_2^{\bullet-}$	Superoxide radical
$OH^{\bullet}$	Hydroxyl radical
OST1	Open stomata 1
OXI1	Oxidative signal-inducible 1
PA	Phosphatidic acid
PAL	Phenylalanine ammonia-lyase
PAMPs	Pathogen-associated molecular patterns
PAP	3′-phosphoadenosine 5′-phosphate
PARP	Poly (ADP-ribose) polymerase
PCD	Programmed cell death
PCR	Polymerase chain reaction
PDK1	3-phosphoinositide-dependent protein kinase 1
PGA	3-phosphoglycerate
Phe	Phenylalanine
PIP2;1	Plasma membrane intrinsic protein 2;1
PLD	Phospholipase D
PPIs	Protein-protein interactions
PP2	Protein phosphatase 2
PQ	Plastoquinone
PR	Pathogenesis-related
PRRs	Pattern recognition receptors
PRX	Peroxiredoxin
PSI/II	Photosystem I/II
PTI	Pattern-triggered immunity or PAMP-triggered immunity

PTS1	Peroxisomal targeting sequence 1
qPCR	Quantitative polymerase chain reaction
QTL	Quantitative trait loci
RBOH	Respiratory burst oxidase homolog
RETC	Respiratory electron transport chain
RLK	Receptor-like kinase
RNA	Ribonucleotide acid
RNR	Ribonucleotide reductase
roGFP	Reduction/oxidation-sensitive green fluorescent protein
ROP	Rho of plants
ROS	Reactive oxygen species
Rubisco	Ribulose-1,5-bisphosphate carboxylase/oygenase
RuBP	Ribulose-1,5-bisphosphate
SA	Salicylic acid
SAG	SA glucoside
SD	Short-day
SDS-PAGE	Sodium dodecyl sulfate-polyacrylamide gel electrophoresis
SGE	SA glucose ester
SOD	Superoxide dismutase
spy	Spindly
Sugar-P	Sugar phosphate
TBS	Tris-buffered saline
TCA	Tricarboxylic acid cycle
T-DNA	Transfer-DNA
TF	Transcription factor
TNT	2,4,6-Trinitrotoluene
Trp	Tryptophan
TRX	Thioredoxin
Tyr	Tyrosine
UV	Ultraviolet
Y2H	Yeast two-hybrid
XOD	Xanthine oxidase
$^{1}O_2$	Singlet oxygen
2-VPD	2-Vinylpyridine
$^{1/3}$Chl	Single/triplet state excited chlorophyll
6PGDH	6-Phosphogluconate dehydrogenase

TABLE OF CONTENTS

CHAPTER 1 GENERAL INTRODUCTION

CHAPTER 1 GENERAL INTRODUCTION

1.1 Climate change and stress

Relationships between plants and humans are extremely intricate. Plants provide food and oxygen to humans and to domesticated animals, as well as numerous compounds of medical benefit. To generate these compounds, plants convert CO_2 into organic matter using light energy. Currently, atmospheric CO_2 levels are rising, which in itself can be beneficial to plants. However, the physicochemical properties of CO_2, together with an increase in other so-called 'greenhouse gases', are also leading to a gradual heating of our planet, driving an alarming trend of continual increase in global temperature. Increased thermal energy in the atmosphere is predicted to change weather patterns, leading to increasingly severe periods of prolonged stress that threatens plant survival and/or yield (Eckardt et al., 2023; Zandalinas et al., 2021). Almost all stresses have in common the increased production and/or accumulation of reactive oxygen species (ROS) within plant tissues.

As plants are generally sessile, they cannot migrate like animals to more favorable environments to alleviate or solve the problems caused by stresses such as drought, freezing, high light intensity, pathogen attack, and heavy metal poisoning. To respond to environmental changes, plants have evolved biochemical mechanisms to favor stress resistance or adaptation. Key among such mechanisms are those that enable improved management of ROS to avoid excessive oxidative stress (Noctor, 2015; Noctor et al., 2014; Paiva & Bozza, 2014; Shin et al., 2013).

Efforts over recent decades have reported several approaches to improving stress resistance capacity in plants. These have included improving photosynthesis (Cardona et al., 2018) and/or reducing photorespiration (Wang et al., 2020), improving nitrogen uptake ratio (Anas et al., 2020; Liu et al., 2022), and increasing water use efficiency (Ruggiero et al., 2017). In addition to these approaches, intensive effort has focused on trying to understand the physiological outcome of ROS signaling, since this process plays a crucial role in plant acclimation to the environment and plant development. The intensity of ROS signaling is dependent on rates of ROS production but also the capacity and efficacity of antioxidative enzymes that remove ROS (Noctor et al., 2018). In my research, I have investigated the specific roles of a set of plant enzymes involved in the complex antioxidative system, in order to assess their roles in controlling cell redox state and their influence in controlling ROS signaling.

1.2 Reactive Oxygen Species (ROS)

1.2.1 Definition of ROS

ROS are inevitable by-products of the normal metabolism of oxygen in aerobic organisms. The term ROS englobes derivatives that are more reactive than ground-state oxygen, formed either by physical excitation to produce singlet oxygen ($^1O_2$) or by addition of electrons, chemical reactions that lead to compounds such as superoxide, hydrogen peroxide (H_2O_2) or the hydroxyl radical (Fujii et al., 2022). While these compounds can be formed by non-enzymatic reactions, superoxide and H_2O_2 formation can also result from oxidase-type enzymes (eg, NADPH oxidases, glycolate oxidases). Ultimately, the vast majority of the ROS formed in cells are converted to water (Figure 1.1). It should be noted that other compounds can be secondarily produced from these ROS and that the term ROS should not be considered synonymous with free radical: some ROS are radicals while others are not.

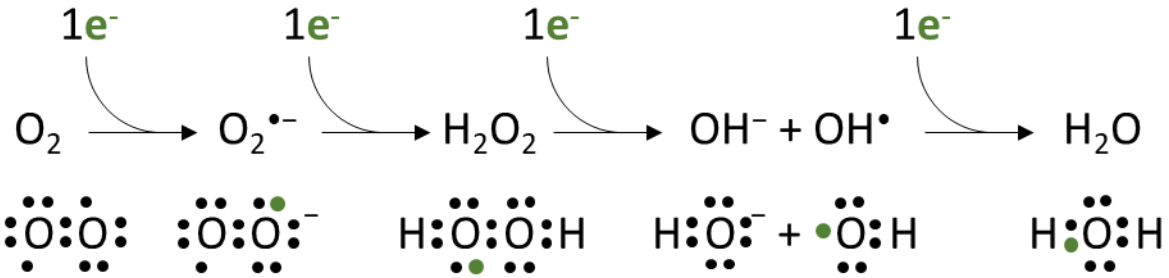

Figure 1.1. Transformation from oxygen to water by progressive univalent addition of electrons involving production of ROS (superoxide, hydrogen peroxide, hydroxyl radical)

Together, all these ROS make up the reactive oxygen family. Once considered to be anecdotal in biological systems, it is now known that ROS are produced and metabolised in almost all cells. For several reasons, they are particularly important in plants. Many plant cells operate within an oxygen-rich environment, particularly in photosynthetic tissues, and high-energy intermediates involved in photosynthesis mean that energy or electron transfer to produce ROS inevitably occurs at relatively high rates. ROS are also produced by various plant metabolic pathways or generated, in a 'programmed' manner, by NADPH oxidases. We now know that ROS production and accumulation can act as signals of environmental change. At the same time, however, efficient antioxidative systems must police ROS to avoid excessive accumulation that can lead to undesirable or excessive oxidation of essential cell components such as lipids, proteins, RNA, DNA and many small molecules (Mittler et al., 2022). Indeed,

H_2O_2 concentrations in particular are subject to fine control by the actions of several enzymatic systems, including some that are the focus of this thesis.

1.2.1.1 Singlet oxygen ($^1O_2$)

While ground state oxygen is a bi-radical, it can lose this radical state by transition to the singlet state, which is much more reactive. This transition requires energy, which in various systems is often ultimately attributable to light. In humans, singlet oxygen is reported to be an oxidant that is induced by longwave (UV) radiation (UVA: 320 – 400 nm), photoaging the skin cells. However, this reactive species is also responsible for tumour-killing during photodynamic therapy (Krutmann, 2000). Singlet oxygen can produce a variety of biochemical effects, including oxidation of lipid fatty acid chains as well as DNA. In plants, singlet oxygen is notably produced when light is in excess of that required for photosynthesis. In these conditions, the lifetime of triplet chlorophyll increases, favoring energy transfer to ground-state oxygen. Production of singlet oxygen through this mechanism can lead to photo-oxidation but the molecule has also received considerable attention as an activator of signaling pathways (Lokdarshi et al., 2020). In some cases, signaling may occur by detection of the accumulation of compounds that result from singlet oxygen -induced oxidation of functionally useful compounds, such as carotenoids (Havaux, 2014).

1.2.1.2 Superoxide radical ($O_2^{\bullet-}$)

Superoxide is produced by the one-electron reduction of the oxygen molecule. This ROS is considered to be both a free radical and a charged anion (Andrés et al., 2023). Superoxide is highly soluble in water, and at low pH values is protonated to preferentially form the hydroperoxide radical ($HO_2^{\bullet}$). The superoxide anion is generated by numerous systems, including electron transport chains and various enzymes such as Respiratory Burst Oxidase Homologs (RBOH-type NADPH oxidases; Figure 1.2).

$$NADPH + 2O_2 \xrightarrow[\text{oxidase}]{\text{NADPH}} NADP^+ + 2O_2^{\bullet-}$$

Figure 1.2. Production of superoxide by RBOH-type NADPH oxidases.

Once formed, superoxide can accept another electron to form the peroxide anion, whose protonation leads to H_2O_2 (Figure 1.1), a somewhat more stable ROS. However, the major fate of superoxide is thought to be dismutation, which also leads to H_2O_2 but with one superoxide being re-oxidized to O_2

(Figure 1.3). Although dismutation can occur spontaneously, the reaction is greatly accelerated by superoxide dismutase (SOD). This enzyme plays an important role in most cells, since superoxide can be toxic since if allowed to accumulate.

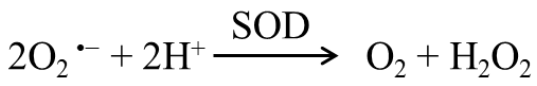

Figure 1.3. Superoxide dismutation. The reaction can occur spontaneously or, as shown, be catalysed by SOD.

Because of its strong instability, superoxide has a short lifetime in cells (Hayyan et al., 2016). This property, together with the presence of SOD and reducing compounds, makes this ROS difficult to accurately quantify in organisms in many conditions (Georgiou et al., 2008; Johnston et al., 2015). Superoxide signals can, however, be monitored semi-quantitatively by electron paramagnetic resonance (EPR) spectroscopy, a method that allows detection of radicals with unpaired electrons (Johnston et al., 2015).

1.2.1.3 Hydrogen peroxide (H_2O_2)

As well as being secondarily produced from superoxide H_2O_2 can be directly produced by enzymes such as glycolate oxidases (GOX; Figure 1.4), some of which play important roles in photorespiration.

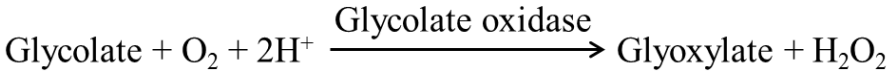

Figure 1.4. Hydrogen peroxide from molecular oxygen catalysed by glycolate oxidase.

H_2O_2 is stable in abiotic environments at ambient temperature and neutral pH (Mahaseth & Kuzminov, 2017; Rhee, 2006) but its oxidizing properties mean that its lifetime in cells is short. Indiscriminate reactions with cellular components are limited by a battery of antioxidative enzymes that can decompose H_2O_2 to water and/or O_2 (see below). In addition to its intrinsic oxidizing properties, H_2O_2 can give rise the highly reactive hydroxyl radical ($OH^{\bullet}$) by cleavage of the molecule that occurs subsequent to accepting an electron (Figure 1.1). This is a further reason to explain the existence of so many H_2O_2-metabolizing enzymes. Indeed, despite its chemical stability in metal-free abiotic environments, H_2O_2 can be highly reactive in cells, particularly if free transition metals are available in the reduced state. Metals such as Fe^{2+} or Cu^{2+} are rapidly oxidized by H_2O_2 in the so-called Fenton

reaction, producing a hydroxide anion and the hydroxyl radical (Mahaseth & Kuzminov, 2017). Because of its extremely rapid chemical reactivity, the generation of the latter must be minimized.

It has become clear over recent years that, like superoxide, H_2O_2 accumulation can also have positive physiological effects in plants. One well-studied example is in plant responses to pathogens (Chaouch et al., 2010) but H_2O_2 serves a vital function in numerous procedures, encompassing signal transduction, the fortification of the cell wall through lignification, fostering plant growth, the formation of root hairs, and xylem diversification, as well as coordinating root-shoot interactions and regulating stomatal responses (Cheeseman, 2007). Among all ROS, H_2O_2 seems best suited to act as a signaling molecule because of its relative stability, ability to cross membranes (Bienert et al., 2007; Tian et al., 2016), and role in posttranslational modification of cysteine and methionine residues in target proteins (Waszczak et al., 2014, 2015; Jacques et al., 2015).

Although various methods have been used to quantify H_2O_2, question marks remain over the accuracy of some of them and the huge range of tissue contents reported in plants suggests that further effort may be required to develop improved protocols (Queval et al., 2008; Noctor et al., 2016). Such efforts may include roGFP-based biosensors (Lew et al., 2020), although so far it has not proved possible to use these methods to quantify concentrations, notably because of the extremely rapid destruction by cellular antioxidant systems of the added H_2O_2 required to standardise the signal.

1.2.1.4 Hydroxyl radical (OH˙)

Considered as one of the most powerful oxidants in biological systems, the hydroxyl radical can be generated through oxidative metabolism, inflammation, or ionizing radiation (Wang & Wei, 2023), as well as by the Fenton reaction mentioned above (Mahaseth & Kuzminov, 2017). Although an extremely short-lived ROS whose production is generally minimised, the hydroxyl radical has nevertheless been implicated as a beneficial actor in some processes; for example, as an effector in calcium homeostasis (Demidchik et al., 2003), root hair development (Foreman et al., 2003), as well as cell wall metabolism and stress signaling in general (Chung et al., 2008; Laohavisit et al., 2013). However, the molecule is certainly the most potentially damaging of all the ROS, able among other things to initiate lipid peroxidation chain reactions, modify proteins, and react with nucleobases resulting in DNA damage. Because of these properties, the hydroxyl radical has been implicating in aging and pathologies such as cancers or neurological diseases (Guptasarma et al., 1992; Kristensen et al., 2021; Wang & Wei, 2023).

1.2.2 Localization of ROS generation

Because the environment fluctuates, the concentrations and effects of ROS within organisms are not constant. Changes in ROS can determine, or at least significantly influence, plant responses to the environment. It is important to note that excessive accumulation of ROS is considered unlikely, given that these molecules rapidly engage the rich and complex plant antioxidative systems, some of which are, furthermore, induced by increased ROS concentrations (Foyer & Noctor, 2005). Moreover, the once-prevalent idea that ROS concentrations should be kept as low as possible has been superseded by the realisation that these molecules are crucial signaling molecule in cellular regulation.

Within cells, ROS production occurs in different compartments, and may play diverse physiological roles (Figure 1.5). Processes that can produce quite high amounts of ROS include photosynthesis in chloroplasts, respiration in mitochondria, photorespiration in peroxisomes, and systems at the plasma membrane and apoplast. The contribution of each compartment to ROS generation will depend on the physiological activity or developmental stage of the organism, as well as the environmental conditions (Hayyan et al., 2016; Mhamdi & Van Breusegem, 2018; Mittler et al., 2022; Noctor et al., 2018).

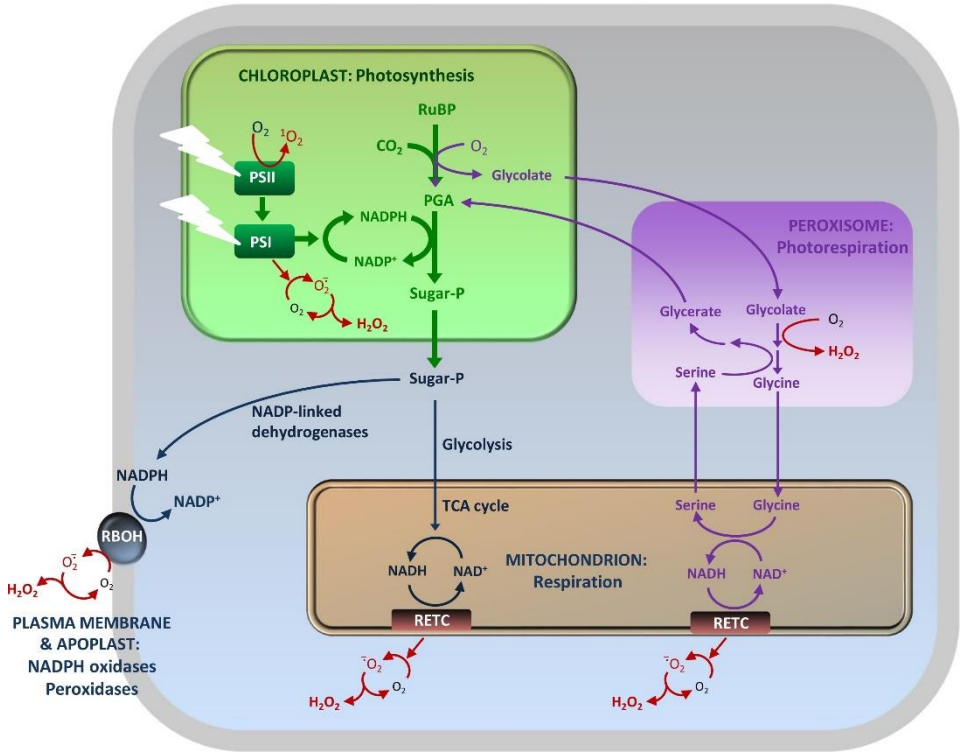

Figure 1.5. ROS producing pathways in plants

PGA, 3-phosphoglycerate. PSI/II, Photosystem I/II. RBOH, respiratory burst oxidase homolog. RETC, respiratory electron transport chain. RuBP, ribulose 1,5-bisphosphate. Sugar-P, sugar phosphate. Scheme taken from Noctor et al. (2018).

1.2.2.1 ROS dynamics in chloroplasts

Photosynthesis is the dominant physiological function in leaves and a potentially important source of ROS production. In the light, the growth of plants is sustained by the energetic processes of photosynthesis, in which oxygen and ROS are continuously generated in response to excitation of pigments and the electron transfer that results from this (Noctor et al., 2018).

In the chloroplast, both photosystem I (PSI) and photosystem II (PSII) are major sites for producing ROS (Foyer & Hanke, 2022; Li & Kim, 2022; Noctor et al., 2018). In PSII, excess light can cause an increase in the lifetime of chlorophyll excited states, favoring the probability of formation of triplet state excited chlorophyll (^{3}Chl) in the light-harvesting antenna complex (LHC) and reaction centre (Havaux, 2014). Unlike singlet state excited chlorophyll (^{1}Chl), the triplet form readily interacts with ground-state oxygen to produce the excited, more reactive singlet form (Møller, 2001). Singlet oxygen can react with components in close proximity, notably to oxidize pigments such as β-carotene as well as proteins such as D1, and must be de-excited by physical or chemical reactions, if photo-oxidation of the photosystem is to be avoided (Havaux, 2014). While PSII and plastoquinone can also lead to reduction of oxygen to superoxide, production of superoxide and H_2O_2 is probably highest at PSI, due to the highly reductive nature of the terminal electron acceptors such as iron-sulphur centres and ferredoxin. There is a competition between oxidation of PSI acceptors by ferredoxin-$NADP^+$ oxidoreductase (FNR), which produces NADPH from $NADP^+$, and oxygen, which produces ROS. While reduction of oxygen can have beneficial effects (eg, relieving electron pressure or by allowing ATP formation independent of NADP formation), superoxide accumulation must be limited. Here, iron-SODs (FeSODs) and copper/zinc-SODs (Cu/ZnSODs) can convert superoxide to H_2O_2 (Li & Kim, 2022).

Production of H_2O_2 by the electron transport chain may play an important signaling role in response to light and or changes in metabolic status (Foyer & Noctor, 2005a,b). Like superoxide, however, H_2O_2 accumulation must be controlled. In this context, several enzymes play key roles. These include thylakoid membrane-associated and stromal ascorbate peroxidases (APXs) as well as peroxiredoxins (Apel & Hirt, 2004; Awad et al., 2015). These enzymes allow oxygen reduction to form an electron sink (also called the water–water cycle) that can be critical to balancing oxidation and reduction of the electron transport chain to maximize photosynthetic efficiency (Asada, 2006).

Of the chemically distinct ROS produced in chloroplasts, evidence has been presented that singlet oxygen is primarily responsible for photodamage to proteins and lipids (Triantaphylidès & Havaux, 2009). Indeed, singlet oxygen differs from H_2O_2 in that it has a notably brief existence and limited

diffusion range, which restricts its movement. Amino acid residues such as tryptophan (Trp), tyrosine (Tyr), phenylalanine (Phe), histidine (His), methionine (Met), and cysteine (Cys) are recognized targets of singlet oxygen (Li & Kim, 2022).

1.2.2.2 Peroxisomes: ROS factories in metabolism and signaling

Peroxisomes are single-membrane organelles found in nearly all eukaryotic cells that play roles in various physiological processes. They are characterized by the presence of various oxidases, as well as high concentrations of catalase, and are significant sources of ROS. The primary metabolic activities responsible for the generation of H_2O_2 in different types of peroxisomes include the photorespiratory GOX reaction (green tissues), fatty acid β-oxidation, and the dismutation of superoxide radicals that can be formed by some enzymatic systems or electron transfer reactions (Del Río et al., 2006; Foyer & Noctor, 2003; Mhamdi et al., 2012; Andrés et al., 2023). Studies in pea and watermelon have provided evidence that superoxide can be formed both in the peroxisome matrix, by systems such as xanthine oxidase (XOD), and in the peroxisomal membranes by NADPH-dependent electron transfer reactions (Del Río et al., 2002; Sandalio et al., 1988).

Photorespiration occurs in C_3 plants under light conditions. In this process, ribulose-1,5-bisphosphate (RuBP) reacts with O_2, producing 2-phosphoglycolate, a reaction catalysed by ribulose-1,5-bisphosphate carboxylase/oxygenase (RuBisCo). The glycolate produced subsequently is transferred to the peroxisomes, where it is mainly oxidised to glyoxylate by GOX, accompanied by the production of H_2O_2 (Noctor et al., 2018). Because photorespiration can be among the most rapid plant metabolic processes in certain conditions, H_2O_2 production in peroxisomes due to GOX has been estimated to be greater than that in chloroplasts and mitochondria, although the relative rates of production will be dependent on conditions (Foyer et al., 2009).

Another peroxisomal ROS-producing pathway is fatty acid β-oxidation, which notably occurs in the early state of germination of oil-storing seeds, enabling fatty acids to be converted to sugars to support growth of the developing seedling. The degradation of fatty acids involves formation of acyl-CoA, which is subsequently oxidised by acyl-CoA oxidase (ACOX). Peroxisomal ACOX proteins are flavin adenine dinucleotide (FAD)-dependent proteins, with the electrons transferred from the FAD group to oxygen to generate H_2O_2. Similar to that produced in photorespiration, this H_2O_2 is mainly removed by catalase, although other H_2O_2-metabolising enzymes also exist in peroxisomes (Wanders et al., 2016).

Peroxisomal ROS contribute to redox signaling cascades that regulate developmental processes such as seed germination, root development, and leaf senescence (Corpas et al., 2001; Del Río & López-Huertas, 2016). Peroxisomes also play a crucial role in adjusting the balance of chemicals in the cell, forming an important interface between metabolism and the environment (Nyathi & Baker, 2006). The dual role of peroxisomal ROS in both metabolism and signaling highlights the interconnectedness of these functions within a single organelle.

1.2.2.3 ROS production and signaling in mitochondria

Mitochondria are, like chloroplasts, organelles with a double external membrane. Mitochondria are considered to be cellular powerhouses, particularly in heterotrophic cells, and are crucial for cellular respiration and energy production. Superoxide and H_2O_2 are generated as by-products of electron transport within the mitochondrial respiratory chain (mETC), located on the inner membrane of this organelle (Sweetlove et al., 2002). This complex cascade involves the shuttling of electrons between protein complexes, using diverse substrates, and involves several sites that can produce ROS by electron transfer to oxygen (Turrens, 2003). In particular, complexes I and III of the mETC are considered to be significant contributors to ROS generation under many conditions (Cadenas et al., 1977; Chandel et al., 2000; Foyer & Noctor, 2005a; Muller et al., 2004).

At complex I, reducing equivalents from the NADH/NAD^+ pool enter respiration through the flavin mononucleotide in the NADH-binding site, site I_F, which has long been known as a site of superoxide production (Cadenas et al., 1977). Complex III, also known as the cytochrome bc_1 complex, receives electrons from the ubiquinol pool, and carries out the Q-cycle, before electrons are transferred to cytochrome *c*. During this process, electrons 'leak' and react with molecular oxygen, producing superoxide. The specific site on complex III responsible for this process is known as the III_{Qo} site, or the 'outer quinol-oxidizing site' (Korge et al., 2017; Kushnareva et al., 2002; Sarewicz & Osyczka, 2015).

In mitochondria, superoxide can be directly eliminated by reduced ASC or GSH, potentially inducing changes in these antioxidant pools that serve as signaling cues. Within the mitochondrial matrix, superoxide is transformed to H_2O_2, either spontaneously or via mitochondrial Mn-SOD (Finkemeier et al., 2005). Thereafter, several types of peroxidases (see Section 1.3) can efficiently scavenge H_2O_2, and plant mitochondria house most of the enzymes involved in the ascorbate-glutathione cycle (Chew et al., 2003). Mitochondrial ROS are involved in redox signaling cascades that modulate energy metabolism, cellular respiration, and stress responses (Suzuki et al., 2012). Striking a balance between

ATP production and ROS generation is crucial for maintaining cellular health and optimizing stress responses.

1.2.2.4 The plasma membrane and NADPH oxidases

In addition to the intracellular ROS production sites discussed above, these molecules are also produced at the cell surface and in the apoplast. For example, extracellular $OH^{\bullet}$ generation has been detected in isolated plasma membranes (Heyno et al., 2011; Mojović et al., 2004). Moreover, on the plasma membrane, specialized enzymes called NADPH oxidases are involved in generation of ROS, notably during immune responses. These NADPH oxidases are also called respiratory burst oxidase homologs (RBOHs), as they are homologous to the enzymes that function in oxidative bursts that are part of the animal immune response. RBOHs play an important role in regulating ROS contents in response to many different stresses, triggering the formation of ROS signaling at the apoplast.

ROS generation by RBOHs can be regulated by various ways. Apart from expression levels, one way is the binding of Ca^{2+} to extended finger (EF)-hand domains in their cytosolic amino-terminal region, phosphorylation/dephosphorylation of their cytosolic amino or carboxy terminals, and binding of other factors such as phosphatidic acid and Rho of plants (ROP) small GTP-binding proteins. Other possible regulatory mechanisms are ubiquitylation, persulfidation, nitrosylation, glutathionylation and/or endocytosis. As transmembrane proteins, RBOHs draw on the cytosolic NADPH pool, transferring electrons to oxygen to generate superoxide in the apoplast according to the equation shown above in Figure 1.2 (Foreman et al., 2003; Kaya et al., 2014; Torres et al., 2002). The physiological functions of RBOH-dependent ROS production are numerous, including roles in phytohormone signaling and pathogen recognition. In the latter case, ROS produced by NADPH oxidases participate in defence signaling, facilitating the activation of downstream immune responses and the synthesis of secondary metabolites (Denness et al., 2011).

1.2.3 Movement of ROS inside and outside the cell

Elevated concentrations of ROS can lead to modified compartmental redox balance arising from the engagement of ROS generation-scavenging systems. However, although most ROS are removed by these systems, some can be transferred to the nucleus, initiating adaptation and acclimation responses (Figure 1.6). While ROS-signaling pathways remain to be fully elucidated, it is thought that the initial sensing of oxidation occurs via ROS- and redox-responsive proteins or by the direct oxidation of cellular metabolites, such as β-carotene.

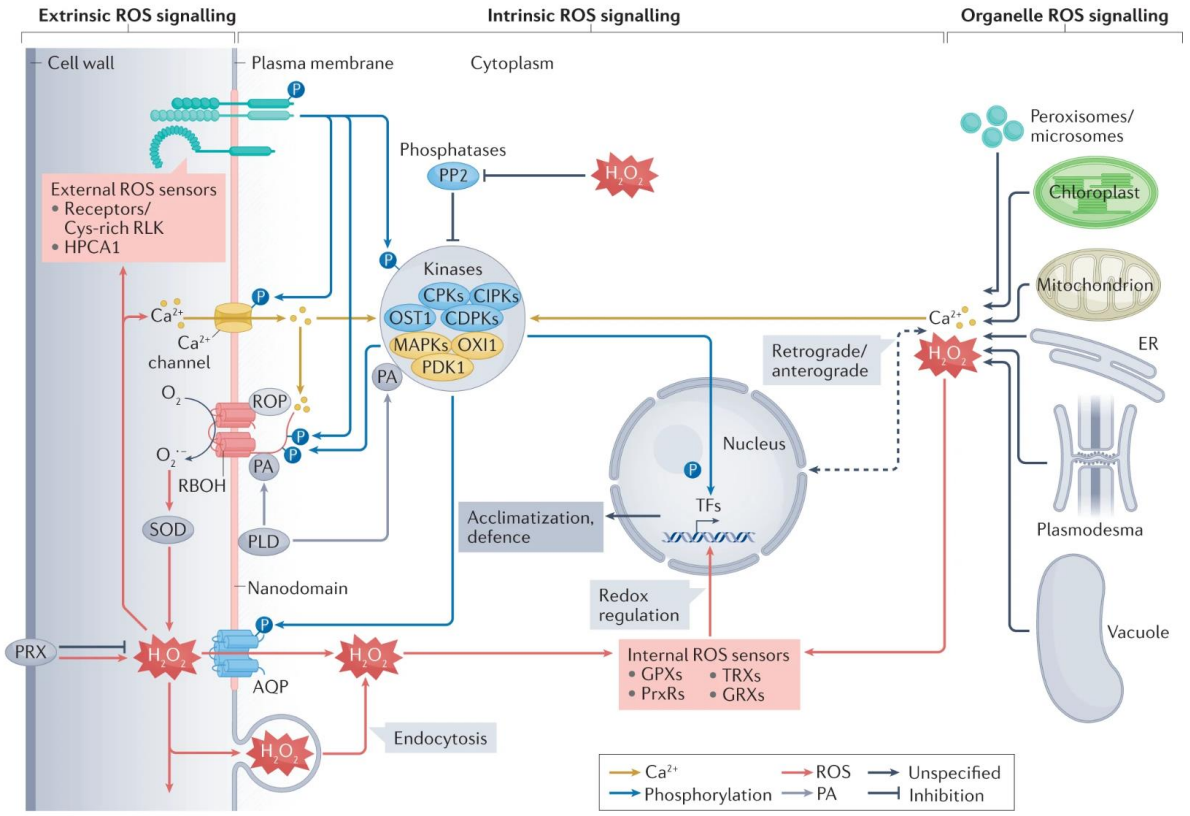

Figure 1.6. ROS signaling in plants can be divided into extrinsic, intrinsic and organelle-localized pathways. These are integrated through the function of respiratory burst oxidase homologues (RBOHs), aquaporins (AQPs), various Ca^{2+} channels, receptors and various kinases and phosphatases that link ROS signaling with calcium, phosphorylation, phosphatidic acid (PA) and redox signaling, and trigger transcriptional responses to stress. apoROS, apoplastic reactive oxygen species; CDPK, Ca^{2+}-dependent protein kinase; chlROS, chloroplastic reactive oxygen species; CIPK, calcineurin B-like-interacting protein kinase; CPK, Ca^{2+}-dependent protein kinase; cytROS, cytosolic reactive oxygen species; ER, endoplasmic reticulum; erROS, endoplasmic reticulum-associated reactive oxygen species; GPX, glutathione peroxidase; GRX, glutaredoxin; HPCA1, HYDROGEN PEROXIDE-INDUCED CALCIUM INCREASES 1; MAPK, mitogen-activated protein kinase; mitROS, mitochondrial reactive oxygen species; nucROS, nuclear reactive oxygen species; OST1, OPEN STOMATA 1; OXI1, OXIDATIVE SIGNAL-INDUCIBLE 1; P, phosphate; PA, phosphatidic acid; pdROS, plasmodesmatal reactive oxygen species; perROS, peroxisomal reactive oxygen species; PRX, peroxidase; PrxR, peroxiredoxin; PDK1, 3-PHOSPHOINOSITIDE-DEPENDENT PROTEIN KINASE 1; PLD, phospholipase D; PP2, protein phosphatase 2; RLK, receptor-like kinase; ROP, Rho of plants; SOD, superoxide dismutase; TF, transcription factor; TRX, thioredoxin; vacROS, vacuolar reactive oxygen species; vesROS, vesicular reactive oxygen species. Scheme taken from Mittler et al. (2022).

Chloroplastic ROS production leads to the accumulation of chloroplastic 3'-phosphoadenosine 5'-phosphate (PAP) accumulation, which acts as the second messenger transferring redox state information to the nucleus (Figure 1.6). However, whether signaling events can be initiated by direct H_2O_2 translocation from chloroplasts to nucleus is not clear (Estavillo et al., 2011). A similar process can occur in mitochondria, due to the dual targeting of the PAP catabolism enzyme PAP phosphatase (SAL1). Accumulation of ROS in the apoplast sparks a rapid cytosolic Ca^{2+} surge. However, mechanisms for apoplastic ROS sensing and the identity of ROS-linked Ca^{2+} channels remain elusive.

ROS accumulated in the apoplast can interact with receptors, either directly or indirectly via redox-transducing proteins. For instance, H_2O_2-induced calcium increases 1 (HPCA1), various antioxidants, as well as Ca^{2+} and K^+ channels, might undergo oxidation or regulation as a consequence (Figure 1.6; Mittler et al., 2022). While H_2O_2 generated in the apoplast can enter cells via both aquaporins (AQPs) PLASMAMEMBRANE INTRINSIC PROTEIN 2;1 (PIP2;1) and by the way of endocytosis, cell wall-bound peroxidases can also produce or scavenge ROS under different conditions, and have been shown to regulate apoplastic ROS levels in response to different stimuli (Mittler et al., 2022). Hence, even in the apoplast, where ROS-scavenging systems are considered somewhat less powerful than in many intracellular compartments, only part of the ROS that is produced is allowed to accumulate.

1.2.4 Dual nature of ROS: from damage to signaling

As noted above, ROS is an encompassing term for a diverse group of active oxygen molecules, each of which presents unique characteristics and varying levels of reactivity. Occurring under both optimal and stress-induced conditions such as intense light, water scarcity, heavy metal exposure, cold temperatures, and the presence of pathogens, the intricate generation of these multifaceted ROS, tightly intertwined with reactions that ensure their control, contributes to the dynamic ROS milieu.

Because ROS are potent oxidizing agents, their uncontrolled accumulation poses the danger of excessive oxidation that could be harmful to organisms. Consequently, organisms have evolved mechanisms to counterbalance this by employing reducing agents like glutathione and ascorbate, in conjunction with enzymes such as peroxidase, catalase, and SOD, to efficiently neutralize ROS. However, in less favorable environmental conditions, intracellular ROS production escalates, and controlled accumulation of ROS acts as a signal to trigger appropriate plant responses. This orchestrated response aids plants in adopting effective strategies when confronted with adversity (Mittler et al., 2011, 2022; Noctor et al., 2018).

It has become clear over recent years that the significance of ROS signaling in plant biology cannot be overstated. Their dual nature, whereby ROS can be both harmful and beneficial, is reflective of the intricate balance that defines life itself. Deciphering the cellular communication that is influenced by ROS and antioxidants is a key aim to gain insights into the strategies that plants employ to the challenges, thus paving the way for enhanced agricultural practices and a deeper understanding of the interplay between plants and their environment (D'Autréaux & Toledano, 2007; Del Río & López-Huertas, 2016).

1.2.4.1 ROS signaling and ROS homeostasis in cells

Throughout the long-term evolutionary processes, in order to avoid overly stressful conditions, organisms have become adapted to using ROS as stress signals. The quick and ever-changing ROS signaling in cells arises from the opposing actions of ROS generation and removal (Foyer & Noctor, 2005b). Since these two actions continuously happen together within cells, any shift in the equilibrium between the rates of removal and generation would promptly lead to swift changes in ROS quantities, triggering a signaling response (Mittler et al., 2011). Indeed, it has been shown that ROS signals can be auto-propagating from cell to cell, a signal that is reported to be disseminated at a rate of about 8.4 cm/min in *Arabidopsis thaliana* (Miller et al., 2009).

ROS and redox signaling are critical players in cellular communication and in the response of plants to abiotic stress (Foyer & Noctor, 2003, 2005;). Redox signaling helps plants to maintain a balance; for example, in order to prevent excessive accumulation of ROS, the glutathione-ascorbate pathway (also called Foyer–Asada–Halliwell pathway) is engaged to allow removal of excess H_2O_2 in cells. As discussed in more detail below, this pathway is found in several subcellular compartments in plants, where it plays a key role in defence against excessive H_2O_2 accumulation. Indeed, the ratio of reduced glutathione (GSH) and oxidized glutathione (GSSG) can be taken as an indicator of the redox state of the cell (Mittler et al., 2022).

As noted above, ROS can be transferred between different cell compartments and activate signal transduction at specific locations (Ding et al., 2019; Exposito-Rodriguez et al., 2017). Hence, when plants encounter stressful situations like heat or drought, ROS and redox signaling intensify their involvement, but this may involve several different cellular compartments.

1.2.4.2 Links between ROS signaling and other signaling pathways

ROS play an irreplaceable role in various physiological processes involved in plant development. The levels of ROS are regulated through a delicate equilibrium between generation and degradation, managed by intricate antioxidant mechanisms (Mittler et al., 2011). These interdependent systems, alongside the precise oversight of pathways linked to ROS, shape the adaptability and resilience of plants to varying circumstances. Consequently, they exert command over both plant growth and survival (Mhamdi & Van Breusegem, 2018).

ROS can intricately interlink with diverse signaling pathways, thus amplifying their role as multifaceted cellular communicators, to trigger an acclimation response. Among the numerous pathways that ROS

engage with, interactions with calcium and protein phosphorylation networks have elicited significant attention. This is prominently illustrated in the context of the RBOH-type NADPH oxidase proteins responsible for ROS generation. Notably, RBOH proteins encompass domains like EF-calcium binding and phosphorylation domains, which underscore their direct connections with calcium and protein phosphorylation-based signaling pathways (Ogasawara et al., 2008). These intertwining interactions create a sophisticated orchestration of cellular responses.

Moreover, the orchestration of ROS extends to the cellular redox landscape. This intricate linkage is exemplified through molecules like thioredoxins (TRX), peroxiredoxins (PRX), glutaredoxins (GRX), and NADPH (Kobayashi et al., 2007). These redox-active molecules serve as intermediaries, harmonizing ROS-induced signals with the broader redox environment of the cell. The intricate interplay between ROS and these redox players creates a network system that goes beyond isolated signaling events to facilitate a continuous cellular response that is deeply rooted in the cellular redox environment.

According to our current knowledge, ROS are pivotal participants in cellular communication. Their ability to interface with calcium, protein phosphorylation networks, and the cellular redox environment reveals their critical role in complex signaling. These interconnected pathways underscore not only the complexity of ROS-mediated signaling but also the highly integrated nature of cellular responses, in which ROS act as dynamic messengers bridging seemingly disparate signaling domains into harmonious cellular behaviour (Dietz et al., 2010; Moon et al., 2002; Rouhier, 2010).

ROS accumulation was found to activate the mitogen-activated protein kinase (MAPK) cascades, which are pivotal in transmitting external cues from the cellular membrane to the nucleus through a sequence of phosphorylation events. This signaling cascade is under the negative control of MAPK phosphatases (MKPs) (Boutros et al., 2008). Studies found that the numerous cellular stimuli that induce ROS production can also activate MAPK pathways, and direct exposure of cells to H_2O_2 induces MAPK pathway activation (Dabrowski et al., 2000; Li et al., 2001; Ruffels et al., 2004; Son et al., 2011; Torres, 2003). ROS-responsive MAPKKK MEKK1, MPK3, MPK4 and MPK6 are particularly important. In Arabidopsis protoplasts, MEKK1 kinase activity and protein amounts were both significantly elevated by H_2O_2 treatment. In Col-0 plants, MPK3, MPK4 and MPK6 were highly stimulated by H_2O_2 treatment, while MEKK1 also can mediate the activation of MPK4 in response to ROS (Nakagami et al., 2006).

ROS signals have also been identified as key contributors to the upstream processes driving abscisic acid (ABA)-induced stomatal closure. Moreover, the robust expression of MPK9 and MPK12 within guard cells proves indispensable for orchestrating this induction. Notably, both ABA and H_2O_2

treatments stimulate MPK12 activity, further underlining its regulatory role in this pathway (Jammes et al., 2009).

There is also a tight relationship between ROS signaling and primary cellular metabolism. One example concerns the tricarboxylic acid cycle (TCA), a metabolic hub vital for energy generation and biosynthesis in the mitochondria. ROS accumulation can inhibit the TCA cycle while concurrently upregulating glycolysis and oxidative pentose phosphate pathways. This dynamic coupling underscores the role of ROS as not just transient metabolic products but also pivotal regulatory cues that orchestrate metabolic responses tailored to the ever-evolving cellular environment (Del Río et al., 2006; Foyer & Noctor, 2003).

Another link between ROS and primary metabolic pathways occurs in chloroplasts. Within these cellular energy factories, ROS signaling interfaces with the redox state of the plastoquinone (PQ) pool. As both ROS source and target, the PQ pool is a key for ROS-mediated signaling. This dynamic interplay allows plants to launch responses to environmental changes, thereby conferring adaptability to shifting light conditions and external stressors (Foyer & Hanke, 2022; Foyer & Noctor, 2003; Li & Kim, 2022). This responsive calibration underscores the plant's ability to finely modulate photosynthetic machinery, adapting it to the complex of changing surroundings.

Finally, it should be noted that organisms can use ROS as a defensive weapon against stress. For example, macrophages can generate substantial quantities of ROS to effectively eliminate pathogens (Mendoza-Aguilar et al., 2013). Like animals, an oxidative burst also occurs in plant cells challenged with pathogens or molecules derived from interactions with pathogens. As well as signaling the presence of the pathogen, ROS accumulation may in itself be beneficial in weakening growth and division of the invader. However, one key interaction in this context is the impact of H_2O_2 and redox factors on salicylic acid (SA) accumulation and signaling. Given its relevance to this work, this interaction will now be discussed in more detail.

1.2.4.3 H_2O_2 and the Salicylic Acid (SA) pathway

Salicylic acid, a naturally occurring phenolic compound containing an aromatic benzene ring, is produced as a secondary metabolite in plants and some microorganisms. This molecule plays crucial roles in the regulation of different biochemical and physiological processes, and serves as a linchpin in orchestrating plant responses to biotic and abiotic stresses (Mishra & Baek, 2021). However, it has received most attention for its role in plant responses to certain pathogens.

The involvement of SA in plant defence against pathogens, including bacteria, fungi, and viruses, was first reported in the 1990s (Malamy et al., 1990; Mittler et al., 1999). The application of exogenous SA to tobacco leaves can induce the expression of pathogenesis-related (*PR*) genes that have long been considered to enhance resistance against infections caused by tobacco mosaic virus (TMV) and other organisms (Antoniw & White, 1980; Mittler et al., 1999; White, 1979). Furthermore, the important role that SA plays in various processes, including growth, flowering, photosynthesis, development, and antioxidant enzymes and plant immunity, has been extensively documented (De Vos et al., 2005; Myers Jr et al., 2023; Rivas-San Vicente & Plasencia, 2011; Saleem et al., 2021). SA activates a cascade of defence responses, leading to the expression of genes associated with pathogen resistance and hypersensitive responses (Rivas-San Vicente & Plasencia, 2011).

One established route of SA biosynthesis in plants is through isochorismate synthase (ICS). This pathway has been shown to be essential for SA accumulation during Arabidopsis responses to pathogens (Nawrath & Métraux, 1999; Wildermuth et al., 2001). Another pathway, which can also be considered to start from chorismic acid, is via phenylalanine ammonia-lyase (PAL). In Arabidopsis, the ICS pathway is considered to be the primary pathway of SA synthesis (Mishra & Baek, 2021; Rekhter et al., 2019). Once synthesized, SA can be found in both free and conjugated forms, particularly *O*-glucosylated conjugates. Two well-studied SA conjugates are SA glucoside (SAG) and SA glucose ester (SGE), which are stored in vacuoles and are considered to be inactive reserves of SA. Under stress conditions such as pathogen attack, all these forms can accumulate rapidly, with free SA being important for activation of resistance pathways, both locally and systemically (Dean et al., 2003; Snoeren et al., 2010). A key resistance mechanism is the SA-dependent induction of three *PR* genes (*PR1*, *PR2*, and PR5) although many other genes can also be induced by SA. Studies using ozone treatment or catalase-deficient plants clearly show that one of the effects of ROS accumulation is induction of the SA pathway (Chaouch et al., 2010; Mhamdi et al., 2010a).

Recent evidence highlights a complex interplay between H_2O_2 and SA (Lukan & Coll, 2022). During pathogen attack, pattern-triggered immunity (PTI) is facilitated by surface-localized pattern recognition receptors (PRRs), which identify conserved pathogenic molecular motifs known as pathogen-associated molecular patterns (PAMPs). In addition, intracellular receptors known as nucleotide-binding domain leucine-rich repeat receptors (NLRs) can detect effector proteins produced by pathogens within cells, leading to the initiation of effector-triggered immunity (ETI). The involvement of the ROS-producing RBOHD has been demonstrated in both PTI and ETI pathways. SA can act to regulate ROS production by modulating RBOH transcription.

Once SA accumulates, redox regulation also intervenes in its signaling pathways. Elevated SA levels and changes in cytosolic redox state cause the monomerization of nonexpresser of *PR* gene 1 (NPR1) (Mou et al., 2003). This monomerized NPR1 translocates to the nucleus and facilitates NPR1-dependent gene expression by directly interacting with TGA transcription factors that regulate the expression of *PR* genes. Interestingly, H_2O_2 present between cells can inhibit SA accumulation and HR in neighbouring cells (Lukan & Coll, 2022).

H_2O_2 produced in the chloroplast might play a role in signaling HR-mediated cell death and in regulating associated plant immune responses involving SA. This could involve reprogramming gene transcription related to the pathogen response. Retrograde signals, either through stromules or via cytosolic entry, might be responsible for transmitting these effects. Within the nucleus, gene expression control primarily relies on the activity of transcription factors (TFs) interacting with oxidative stress-responsive *cis*-regulatory elements in gene promoters. The interconnected functions of ROS and SA in immunity exhibit dependence on the specific system and the particular isoform of RBOH involved (Lukan & Coll, 2022).

Whatever the role of the chloroplast, investigations in Arabidopsis have revealed a potential role for H_2O_2 generated in the peroxisomes in influencing SA levels. In the oxidative stress-mimicking model CATALASE-deficient mutant, *cat2*, a scenario emerges in which peroxisomal H_2O_2 accumulates due to the absence of efficient H_2O_2 scavenging enzymes under conditions where photorespiration is active (air, moderate light). In these conditions, leaf lesions are observed when plants are grown under long-day (LD) conditions, and these lesions are dependent on an active ICS pathway to produce SA (Chaouch et al., 2010). Intriguingly, neither a lesion phenotype nor SA accumulation is observed under short-day (SD) conditions, even though gene expression patterns and biochemical markers suggest that oxidative stress is not weaker than in LD (Figure 1.7) (Mhamdi et al., 2010a). Most importantly, no oxidative stress or lesions are observed when *cat2* plants are grown in high CO_2, underlining the key role of H_2O_2 produced by photorespiration in triggering these responses (Queval et al., 2007).

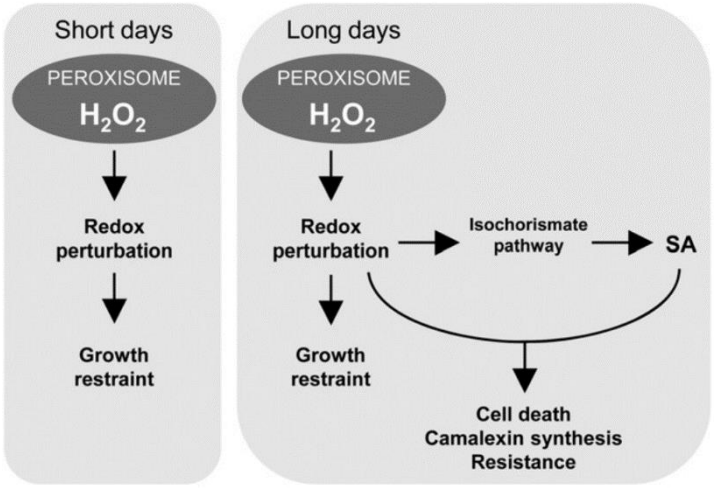

Figure 1.7. Role of day length and SA pathway in the control of responses driven by peroxisomal H_2O_2. Scheme taken from Chaouch et al. (2010).

It should be noted that, despite the importance of catalase in metabolising photorespiratory H_2O_2, the *cat2* mutation is far from lethal. In air, *cat2* grows and flowers, even at relatively high light intensities, although plants are substantially smaller than wild-type grown in the same conditions. The lack of lethality can be explained by the engagement of other antioxidative pathways that mitigate the extent of oxidative stress in this system, notably the ascorbate-glutathione pathway. In addition to their roles in limiting oxidative stress when catalase activity is low, it seems that the engagement of these pathways could have a signaling role in linking H_2O_2 to SA accumulation. Indeed, it has been shown that lines doubly deficient in both *cat2* and either glutathione reductase 1 (GR1) or dehydroascorbate reductase (DHAR) show weakened induction of the SA pathway and leaf lesions (Mhamdi et al., 2010b; Rahantaniaina et al., 2017). Such findings might be considered surprising, since the double mutants should be more oxidatively stressed than the single *cat2* mutant, and is one motivation for the work reported here on monodehydroascorbate reductase. The following section focuses on the major enzymes within the complex plant antioxidative system that act to remove H_2O_2 and, hence, control the accumulation of this oxidizing signaling molecule.

1.3 Control of H_2O_2 in plants

Plants contain an unusually complex antioxidative system. Indeed, it is not easy to define exactly which enzymes might be considered antioxidative since the systems include many supporting players that do not directly interact with ROS. Among the different ROS, most enzymes have evolved to remove H_2O_2, either by dismutation (catalase) or by reduction to water. The second case involves peroxidases which,

unlike catalase, require a reductant. Plants contain several kinds of peroxidase, and these enzymes are supported by various enzymes that ensure reductants are present for ongoing activity. The discussion below will focus on catalase and the ascorbate-glutathione pathway, which is a peroxidase-based system.

1.3.1 Catalase

Catalase (EC 1.11.1.6) is a heme-based enzyme encountered in almost all oxygen-exposed living beings, including bacteria, plants, and animals (Cheeseman, 2007). It is one of a multitude of enzymes within the antioxidative system that act to preserve cellular redox equilibrium. Catalase acts to facilitate the decomposition of H_2O_2 into water and oxygen, effectively limiting the accumulation of this ROS (Chelikani et al., 2004). This mechanism is crucial in sustaining cellular equilibrium and averting the emergence of diseases linked to oxidative stress (Zamocky et al., 2008).

1.3.1.1 Subcellular localization and classification of catalase

In plants, subcellular fractionation and *in situ* activity staining studies have confirmed that peroxisomes possess a high degree of catalase activity (Mullen et al., 1997). The entry of catalases to peroxisomes is typically facilitated through the peroxisomal targeting sequence 1 (PTS1) pathway, which involves non-cleaved tripeptide sequences located at the extreme C-terminus of the polypeptide (Brown & Baker, 2008; McNew & Goodman, 1994). While catalase has a somewhat atypical PTS1, the protein is found to localize primarily in peroxisomes, although there is evidence that it might also be found in the cytosol and nucleus (Bai & Cederbaum, 2001; Mhamdi et al., 2012; Al-Hajaya et al., 2022).

Most plants studied so far contain three genes encoding catalases (Scandalios et al., 1997; Willekens et al., 1995), which can be divided into three classes according to expression patterns and functional analysis (Mhamdi et al., 2010a). This tripartite classification was first proposed during studies on the maize and tobacco catalases (Scandalios et al., 1997; Willekens et al., 1995). It should be noted that this has resulted in an inconsistent nomenclature for the catalases themselves, which has been further complicated by a separate naming system for the subsequently characterized genes in rice. Whatever the names used in different species, it is considered that Class I denotes the gene predominantly expressed in photosynthetic tissues whereas Class II catalases are principally linked with vascular tissues. Class III catalases have a significant presence in seeds and reproductive tissues (Willekens et al., 1995). In Arabidopsis, where the nomenclature was based on the previously characterized maize genes, class I, class II and class III refer to *CAT2*, *CAT3*, and *CAT1*, respectively (Table 1.1).

Table 1.1. Classification of the three CATs found in different plant species (table taken from Mhamdi et al., 2010a). The division into three classes is based on the classification introduced by Willekens et al. (1995).

	Class I	Class II	Class III
Tobacco	Cat1	Cat2	Cat3
Arabidopsis	CAT2	CAT3	CAT1
Maize	Cat2	Cat3	Cat1
Pumpkin	cat2	cat3	cat1
Rice	CatC	CatA	CatB

These isoforms have different tissue-specific expression patterns and may have different functions in plant development and stress responses. These three catalases share high sequence similarity, which could suggest similarity in biochemical properties. However, the exact functional and biochemical distinctions may not be entirely revealed by sequence similarity alone (Yang et al., 2019). Based on analysis of Arabidopsis T-DNA mutants of *cat1*, *cat2* and *cat3*, it was reported that *cat2* has the most important effect on activity in leaves, and also impacts catalase activity in young roots (Mhamdi et al., 2010a; Yang et al., 2019).

1.3.1.2 The Arabidopsis *cat2* mutant: an oxidative stress mimic system in plants

Catalases are distinguished by their high specificity for H_2O_2. In Arabidopsis, CAT2 primarily functions in photosynthetic tissues. As a Class I catalase, *CAT2* shows an expression pattern typical of genes associated with photosynthesis. Disabling *CAT2* expression in Arabidopsis knockout mutants causes extractable leaf activity to decrease to about 20% of the wild-type value (Mhamdi et al., 2010a). As discussed in the next section, this has important effects on plant function when plants are grown under typical conditions (moderate light in air). However, such effects are not observed when plants are grown at high CO_2 to decrease photorespiration, where *cat2* shows a wild-type phenotype (Queval et al., 2007). These observations underline the key role of *CAT2* in removing H_2O_2 produced in photorespiration (see Figure 1.5) and also reveal that *cat2* is a conditional mutant in which oxidative stress can be controlled by manipulating external conditions (Mhamdi et al., 2010a).

1.3.1.3 SA pathway activation in CAT2-deficient lines

The first links between catalase deficiency and cell death were observed in a barley catalase mutant identified in a photorespiratory screen (Kendall et al., 1983). Subsequently, antisense tobacco plants

with decreased expression of *CAT1* (homologue of Arabidopsis *CAT2*; Table 1) were used to further study the influence of H_2O_2 generated intracellularly on plant function (Dat et al., 2001). It was shown that tobacco *CAT1* deficiency triggered the initiation of certain pathogenesis-associated processes such as lesion formation, salicylic acid (SA) accumulation, and activation of pathogenesis-related (PR) genes expression (Mittler et al., 1999). However, the relationship between these different processes was not elucidated.

In Arabidopsis, the rosette size of the *cat2* mutant is smaller than that of the wild-type (Mhamdi et al., 2010a). The loss of CAT2 functionality induces lesion formation under LD conditions, a phenomenon not observed in SD settings. Notably, salicylic acid (SA) and the phytoalexin camalexin exhibit heightened accumulation in *cat2* plants during LD conditions, yet maintain levels comparable to wild-type in SD conditions. Therefore, activation of the SA and the phytoalexin camalexin pathways due to CAT2 deficiency is day length-dependent in Arabidopsis (Queval et al., 2007). Knocking out *CAT1* or *CAT3* expression does not produce such effects, and the functional importance of these catalases remains much less clear (Mhamdi et al., 2010a; Yang et al., 2019).

To establish whether SA accumulation in Arabidopsis was caused directly by CAT2 deficiency and whether this accumulation was necessary for the *cat2* lesion phenotype, *cat2* was crossed with the *sid2* mutant, which is defective in isochorismate synthase 1 (ICS1), the enzyme essential for producing SA in Arabidopsis exposed to pathogens. This analysis revealed that *cat2 sid2* did not accumulate SA or show lesion formation (Chaouch et al., 2010). The conclusions that could be drawn from this study are (1) decreasing CAT2 in Arabidopsis can mimic biotic stress responses such as SA accumulation and hypersensitive-like cell death; (2) CAT2 deficiency induces SA accumulation through the ICS1 pathway; and (3) blocking SA accumulation by disabling ICS1 function is sufficient to avoid cell death, as well as other related features of *cat2* that are related to lesion formation, such as the induction of defence genes.

1.3.1.4 Redox perturbation in *cat2* plants

Although H_2O_2 is not an easy compound to measure accurately in plants, increased diaminobenzidine (DAB) staining in the roots of the *cat2* mutant indicates that catalase deficiency is associated with an increase in this molecule, as might indeed be predicted (Bueso et al., 2007). However, attempts to quantify H_2O_2 in *cat2* leaves have yielded somewhat contrasting results. One study revealed a highly reproducible two-fold elevation in measurable H_2O_2 levels in *cat2* (Hu et al., 2010) but repeated attempts in our laboratory to quantify such increases has produced data that are less clear, even in

conditions in which the cell redox state is clearly disrupted (Noctor et al., 2015). In any case, even a two-fold increase would be a very small fraction of the H_2O_2 generated in photorespiration in our growth conditions in air, suggesting that any elevation in the levels of this molecule is probably transient, localised and/or minor, due to effective processing by other pathways that can metabolise H_2O_2. This conclusion is supported by transcriptomic and biochemical changes that accompany the oxidative stress-triggered phenotype. Most notably, at the biochemical level, *cat2* shows a heightened accumulation of oxidized glutathione (GSSG) and a decreased glutathione reduction state (Mhamdi et al., 2010b), effects that are observed when plants are grown in air in either LD or SD growth conditions (Chaouch et al., 2010). This observation implicates pathways involving glutathione as particularly important players when catalase activity is compromised (see next section).

1.3.2 The ascorbate-glutathione pathway

Ascorbate and glutathione act as some the cell's most important defenses against ROS. They are key regulators of redox balance and influence vital physiological functions like cell division, cell death, light perception, and pathogen-triggered responses (Foyer & Noctor, 2011; Hasanuzzaman et al., 2019). Hence, ascorbate and glutathione can synergize within the "redox hub", notably *via* their close association in the ascorbate-glutathione pathway, while also operating independently through distinct mechanisms (Foyer & Noctor, 2011). The ascorbate-glutathione pathway is shown schematically in Figure 1.8, which also emphasizes the potentially co-operative relationship between catalase and this pathway in avoiding excessive accumulation of H_2O_2. According to this scheme, decreases in catalase activity might be predicted to enhance flux through ascorbate peroxidase (APX) and, hence, at least some of the other three enzymes of the ascorbate-glutathione pathway.

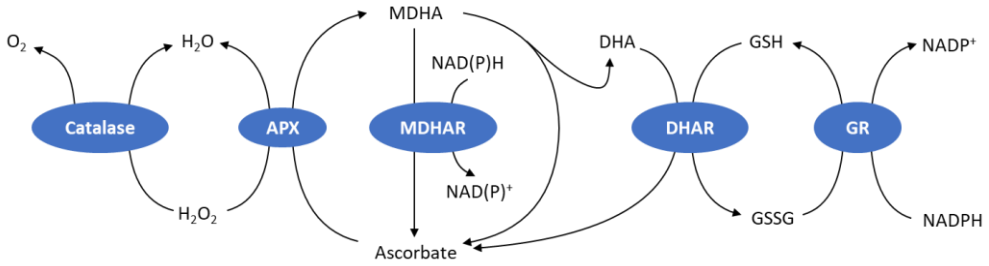

Figure 1.8. Relationship between catalase and the ascorbate-glutathione pathway in H_2O_2 removal. APX, ascorbate peroxidase; MDHA(R), monodehydroascorbate (reductase); DHA(R), dehydroascorbate (reductase); GSH, glutathione; GSSG, glutathione disulfide; GR, glutathione reductase. Schema taken from Foyer and Noctor (2009).

As well as APX, which catalyses the conversion of H_2O_2 to water using ascorbate as the electron donor (Caverzan et al., 2012), two enzymes within the pathway are involved in ascorbate regeneration. These are monodehydroascorbate reductase (MDHAR) and dehydroascorbate reductase (DHAR). The fourth enzyme of the pathway is glutathione reductase (GR), which regenerates GSH. These enzymes play an essential role in maintaining the balance of redox reactions in cells, thus offering defence against oxidative stress (Foyer & Noctor, 2009). It should be noted, however, that the so-called ascorbate-glutathione pathway can operate fully or partly, with MDHAR, DHAR, and GR making different contributions depending on conditions and, especially, flux rate. For example, kinetic modelling suggests that if APX activity is relatively low, ascorbate regeneration might not require DHAR or GR (Tuzet et al., 2019). In this case, MDHAR could largely or completely suffice to regenerate ascorbate for APX activity and ascorbate would function independently of glutathione (Tuzet et al., 2019).

1.3.2.1 Ascorbate

As the most abundant antioxidant in plants, ascorbate (vitamin C) is present in concentrations ranging from 10 to 300 mM (Smirnoff & Wheeler, 2000). Among many functions, it is a co-factor in the ascorbate-glutathione pathway (Figure 1.8). It is predominantly biosynthesized *via* galactose in the Smirnoff-Wheeler pathway, with the final step occurring within the mitochondria (Wheeler et al., 1998; Szarka et al., 2013). Ascorbate plays pivotal roles in numerous cellular activities in plant cells, ranging from roles within the cell cycle to facilitating cell growth and senescence (Xiao et al., 2021). Synthesis, regeneration, and transport are key components in maintaining the equilibrium of ascorbate levels, in ever-fluctuating environmental conditions (Szarka et al., 2013). The ascorbate level is an important indicator of cellular redox state, and is influenced by environmental variations, notably light intensity, and by genetic control of its biosynthesis, recycling and degradation (Fotopoulos & Kanellis, 2013).

1.3.2.2 Ascorbate peroxidase

Ascorbate peroxidase (APX) is commonly found in photosynthetic eukaryotes. Genome-wide studies in higher plants revealed that APX belongs to a multigenic family, with Arabidopsis having nine genes, rice having eight, and tomato seven (Li, 2023). These APX gene clusters can be categorized into three subfamilies based on their subcellular locations: chloroplastic, cytosolic, and microbody isoenzymes (Asada, 1992).

APX acts as an enzyme in the ascorbate-glutathione pathway, and has been implicated in numerous plant growth and development processes, including lateral root growth, nodule development, leaf senescence, seed germination, and programmed cell death (PCD) (Li, 2023). In the plant antioxidative

system, APX is distinguished by its capacity of reducing H_2O_2 to water. This specificity and efficiency makes APX a crucial component in the plant defence strategy against oxidative stress (Asada, 1992).

1.3.2.3 Mechanisms of ascorbate regeneration

In removing ROS, ascorbate donates a single reducing equivalent and is oxidized to the monodehydroascorbate (MDHA) radical. As a short-lived intermediate, MDHA can spontaneously form the fully oxidized species, dehydroascorbate (DHA) by a dismutation reaction, with the other MDHA molecule being converted to ascorbate (Figure 1.9). Two main enzymes are involved in ascorbate regeneration. The first is MDHAR, which reduces MDHA to ascorbate in an NAD(P)H-dependent reaction (Njus et al., 2020) and which will be discussed in detail in section 1.4. If MDHAR is fully effective in reducing all the MDHA, none would dismutate, DHA would not be formed, and the 'ascorbate-glutathione' pathway would in fact consist of a glutathione-independent cycling of ascorbate through APX and MDHAR (Figure 1.8). In reality, however, at least some of the MDHA will escape reduction and so a second ascorbate-regenerating enzyme, DHAR, can intervene to convert DHA to ascorbate at the expense of GSH (Figure 1.9). It should be noted that DHA can also be reduced to ascorbate through a chemical reaction with GSH, and that DHA-reducing mechanisms also exist at the expense of other thiols such as TRX (Foyer & Mullineaux, 1998). However, studies of *cat2 dhar* multiple mutants suggest that isoforms of DHAR are essential for effective defence in oxidative stress conditions (Rahantaniaina et al., 2017).

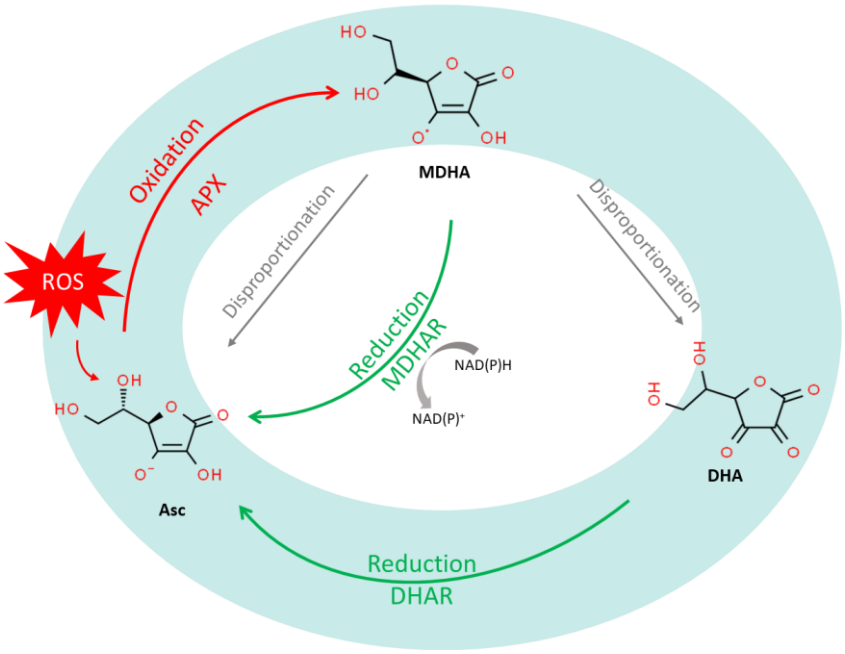

Figure 1.9. The ascorbate oxidation and regeneration cycle involving MDHA and DHA. Asc, ascorbate; APX, ascorbate peroxidase; MDHA, monodehydroascorbate; DHA, dehydroascorbate; MDHAR, monodehyroascorbate reductase.

1.3.2.4 Glutathione and glutathione reductase in plants

Glutathione is a tripeptide synthesized from three amino acids (ϒ-Glu-Cys-Gly). Most of the multiple functions of glutathione involve the Cys sulfhydryl group. Indeed, glutathione is the primary non-protein thiol found in many plants. This molecule is crucial for plant well-being and function, and knockout mutants that lack the first dedicated enzyme of the glutathione biosynthesis pathway are embryo-lethal (Cairns et al., 2006).

Glutathione notably acts as a reducing agent, donating electrons to other molecules from its thiol group (–SH). This allows glutathione to neutralize ROS (notably free radicals) by donating a hydrogen atom, favoring formation of GSSG, in which two glutathione molecules are linked by a disulfide bond (–S–S–). To allow ongoing antioxidant activity, the disulfide form must be converted back to reduced glutathione (GSH) by the enzyme glutathione reductase (GR), using NADPH as an electron donor (Figure 1.8) (Noctor et al., 2011, 2012, 2013).

Glutathione and related thiols are widely recognized for their role in response to pathogens, such as triggering the activation of *PR* genes and the production of phytoalexins (Gomez et al., 2004; Hess et

al., 2005; Vanacker et al., 2000). In the development of the shoot meristem, glutathione plays an overlapping role with TRX systems (Reichheld et al., 2007; Bashandy et al., 2010).

As mentioned above, GR is a major enzyme in the ascorbate-glutathione cycle. Like MDHAR, it is an FAD-dependent enzyme. GR catalyzes reduction of the GSSG disulfide bond, using NADPH as a cofactor, to produce two molecules of GSH (Figure 1.8). This action maintains GSH at a concentration of about 1-10 mM in the cell, with a high ratio of GSH:GSSG, at least in the absence of stress. Two GRs are found in Arabidopsis: GR1 and GR2. The chloroplast/mitochondrial isoform GR2 deficiency results in embryonic lethality in Arabidopsis (Marty et al., 2009; Mhamdi et al., 2010b). By contrast, the cytosolic/peroxisomal isoform, GR1, shows no phenotype under standard growth conditions, although it does show a lower GSH:GSSG ratio than the wild-type (Marty et al., 2009; Mhamdi et al., 2010b). Under conditions of oxidative stress, GR1 is essential for avoiding excessive oxidation of the glutathione pool and favoring growth (Mhamdi et al., 2010b). Expression of this enzyme also seems to be required for activation of phytohormone synthesis and signaling in response to oxidative stress (Mhamdi et al., 2010b). This last observation, together with studies conducted on *cat2 dhar* mutants (Rahantaniaina et al., 2017), discussed further below, point to some role of the ascorbate-glutathione pathway in linking oxidative stress to downstream signaling, and is an important motivation for part of the work described in this thesis.

It is interesting to compare the responses of ascorbate and glutathione pools to enhanced intracellular availability, as can occur in the *cat2* background. Increasing levels of intracellular H_2O_2 seem to have a greater effect on overall ascorbate reserves than on the ascorbate redox balance. However, neither of these effects are as marked as the impact on glutathione, which can increase several fold, largely in the form of GSSG (Chaouch et al., 2010; Mhamdi et al., 2010a). Factors that explain the accumulation of glutathione include enhanced biosynthesis in response to H_2O_2 as well as the sequestration of GSSG in the vacuole, where it is relatively stable (Queval et al., 2009, 2011). Given the difficulty of direct quantification of H_2O_2, glutathione content and redox state are useful markers of the intensity of intracellular oxidative stress (Noctor et al., 2015).

1.3.2.5 Dehydroascorbate reductase

As mentioned above, DHAR catalyses the conversion of DHA to ascorbate, using reducing equivalents from glutathione (Chen & Gallie, 2004). In *Arabidopsis thaliana*, three genes encode DHAR1 and DHAR2 in the cytosol and DHAR3 in the chloroplasts. As also observed for *gr1*, single *dhar* mutations in Arabidopsis do not cause an effect on phenotype (Rahantaniaina et al., 2017). However, in

Arabidopsis lines deficient in catalase, additional mutations in cytosolic and chloroplastic DHAR decrease accumulation of SA and SA-dependent gene expression, as well as leaf lesion formation (Rahantaniaina et al., 2017). Despite this, no effect on ascorbate status was observed. Considering that ascorbate is found in various cellular compartments and there are multiple pathways to facilitate its recycling, one might anticipate that disruptions in a single recycling route would be compensated by the actions of the other pathways (Foyer & Noctor, 2011; Ding et al., 2020). Indeed, this has been experimentally observed: even in a quadruple *cat2 dhar1 dhar2 dhar3* mutant, ascorbate contents and redox status were not markedly different from the wild-type, although the absence of the DHARs did affect the response of the glutathione pool (Rahantaniaina et al., 2017). The roles of the different MDHARs in conditions of oxidative stress have not yet been examined in detail: they are the subject of a large part of this thesis.

1.3.3 Other enzymes involved in plant antioxidative systems

As has been discussed in previous sections, several enzymes contribute to keeping ROS at levels compatible with cell function. While SOD acts to remove superoxide, H_2O_2 formed by superoxide dismutation or more directly by two-electron reduction of oxygen can be processed by catalase or APX. However, plant antioxidative systems extend beyond these enzymes (Figure 1.10) and include several others that can, like APX, act to convert H_2O_2 to water. These notably include PRX, glutathione peroxidase-like enzymes (GPX-like), and glutathione S-transferases (GSTs), some of which can have GSH-dependent peroxidase activity as well as or instead of their classical activity of conjugation (Dixon et al., 2009). Alongside these proteins, TRX and GRX play roles in the regulation of protein structure and function, in some cases through antioxidative reactions that remove ROS or that re-reduce oxidized protein residues (Reichheld et al., 2007; Tarrago et al., 2009; Rouhier, 2010).

PRXs reduce peroxides, such as H_2O_2, organic hydroperoxides, and peroxynitrite, using reducing equivalents derived from TRX or other electron donors (Dietz, 2003). By doing so, PRXs help to protect cells from oxidative damage and modulate signaling pathways involving peroxides. PRXs are classified into several types, including 1-Cys and 2-Cys PRX, based on the number and position of conserved cysteine residues involved in the catalytic cycle. Their ability to sense and respond to oxidative stress makes them important players in cellular defense mechanisms (Jurado-Flores et al., 2020). In addition to PRX, plants contain several genes encoding so-called glutathione peroxidases (GPX). However, these enzymes use a different mechanism to animal GPXs and several studies have shown that they use TRX rather than GSH as reductant (Herbette et al., 2002; Iqbal et al., 2006; Navrot et al., 2006). Therefore,

the term GPX is misleading and it has been proposed that a more accurate term would be GPX-like (Attacha et al., 2017).

As well as supplying reductant to certain PRX and GPX-like proteins, TRXs modulate various proteins by reducing their cysteine residues, thereby altering their redox state (Vanacker et al., 2018). Like TRXs, GRXs are small, ubiquitous proteins that play complementary roles in maintaining cellular redox homeostasis. GRXs primarily function by catalyzing the reduction of disulfide bonds in proteins and glutathionylation/deglutathionylation processes, which can regulate the activity of various target proteins (Vanacker et al., 2018). This activity is crucial in protecting cells from oxidative damage, as it helps to repair proteins that have been oxidized by ROS. GRXs are also involved in the regulation of iron-sulfur cluster assembly and signal transduction pathways, further highlighting their importance in cellular function and stress responses (Rouhier, 2010; Ogata et al., 2021). Both TRX and GRX can also donate reducing equivalents to regenerate methionine sulfoxide reductases that are important in repairing oxidized protein methionine residues (Tarrago et al., 2009).

GSTs constitute a large family of proteins (encoded by 55 genes in Arabidopsis) that play multiple roles in cellular detoxification processes. Classically, GSTs catalyse the conjugation of the tripeptide glutathione to a wide variety of endogenous and exogenous electrophilic compounds (Dixon et al., 2009). This reaction facilitates the neutralization and solubilization of these compounds, tagging them for transport into the vacuole and/or aiding in their subsequent elimination from the cell. In addition to this detoxifying role, at least some GSTs also exhibit peroxidase activity, helping to reduce lipid peroxides and protect against oxidative damage. GSTs are involved in the regulation of apoptosis and stress response pathways, further underscoring their multifunctional nature in maintaining cellular health (Takahashi, 1992; Vaish et al., 2020).

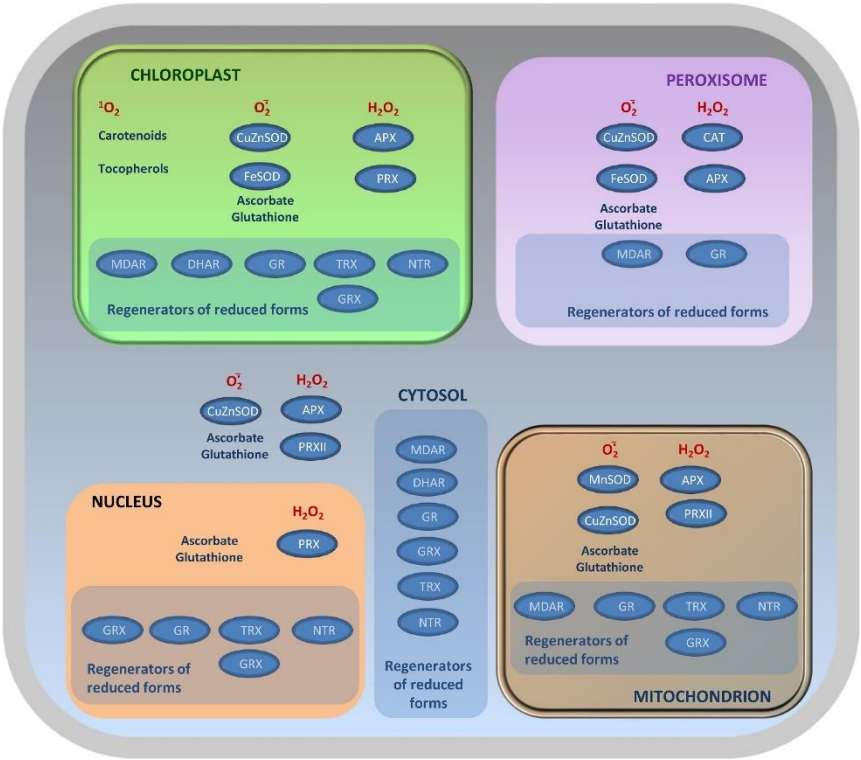

Figure 1.10. Overview of the principal plant antioxidative systems and where they are found within the cell The figure summarizes available information for Arabidopsis on the subcellular localization of antioxidative enzymes and related proteins. The information is not exhaustive, and other proteins may be involved. APX, ascorbate peroxidase. CAT, catalase. DHAR, dehydroascorbate reductase. GR, glutathione reductase. GRX, glutaredoxin. MDAR, monodehydroascorbate reductase. NTR, NADPH-thioredoxin reductase. PRX, peroxiredoxin. SOD, superoxide dismutase. TRX, thioredoxin. Scheme taken from Noctor et al. (2018).

As is the case for two of the three catalase and several enzymes involved in the ascorbate-glutathione pathway, the exact importance of individual isoforms of these other antioxidative enzymes remains to be elucidated. In particular, it is not clear why plants need so many types of enzymes to eliminate peroxides. However, a key point may be that, while catalase and APX are quite specific to H_2O_2, PRX, GST, and GPX-like enzymes are also able to reduce organic peroxides that can arise from lipid peroxidation. Therefore, GRXs, PRXs, and GSTs complement the activities of other antioxidative components, creating a robust network that ensures cellular protection against oxidative stress. While these systems should not be overlooked, the focus of this thesis is on the role of MDHARs, and so these enzymes will now be discussed in more detail.

1.4 Monodehydroascorbate reductase

MDHAR is an FAD-containing oxidoreductase that is considered to be part of the ascorbate-glutathione pathway (Hossain & Asada, 1985; Tanaka et al., 2021). In catalyzing the conversion of MDHA to

ascorbate, the enzyme can utilize either NADH or NADPH as electron donors (Endo et al., 1997; Hossain et al., 1984; Hossain & Asada, 1985). MDHAR has also been identified in some prokaryotic systems, such as cyanobacteria (Tanaka et al., 2021). The functional and evolutionary implications of this distribution pattern remain to be explored (Tanaka et al., 2021).

Several isoforms of MDHAR are found in plants, encoded by different genes. The isoforms number four in maize (*Zea mays*), five in rice (*Oryza sativa*), five in *Brachypodium distachyon,* and six in Arabidopsis (Tanaka et al., 2021). The isoforms range from 47 to 54 kDa in molecular mass and differ in their cellular localization, expression patterns, and regulatory mechanisms under various stress conditions, suggesting a tailored response of each enzyme to diverse stress factors (Johnston et al., 2015; Li et al., 2020; Park et al., 2019; Shin et al., 2013; Truffault et al., 2016; Yeh et al., 2019).

1.4.1 Subcellular localization of MDHAR in Arabidopsis

In *Arabidopsis*, the six AtMDHAR isoforms are encoded by five distinct *MDAR* genes and are targeted to different subcellular compartments. AtMDHAR1 and AtMDHAR4 are peroxisomal isoforms, AtMDAHR1 possesses a C-terminal AKI tripeptide that resembles a PTS1 motif for targeting to the peroxisomal matrix while AtMDHAR4 has a targeting signal that addresses the protein to the peroxisomal membrane (Lisenbee et al., 2005). MDHAR2 and MDHAR3 were found to be localized in the cytosol (Lisenbee et al., 2005; Tanaka et al., 2021). The single *MDAR5/6* gene has two different transcription starts in the N-terminus, leading to two transcripts of slightly different length. The mRNA of *mdar6* is 21 bases shorter than *mdar5*, allowing MDHAR6 to be addressed to chloroplasts while MDHAR5 is found in the mitochondria (Obara et al., 2002).

1.4.2 Biochemical and structural characterization of MDHAR

As well as activity against MDHA, at least some MDHARs have been shown to be active against compounds like ferricyanide, 2,6-dichlorophenolindophenol, and *p*-benzoquinone (Hossain & Asada, 1985). The FAD prosthetic group is situated in a Rossmann-fold domain in the protein structure, bound by hydrogen bonds and Van der Waal's forces to amino acid residues that are highly conserved across different species (Eltayeb et al., 2007; Park et al., 2016).

As previously noted, the catalytic activity of MDHAR is dependent on both NADH and NADPH. The kinetic properties of MDHAR, such as its affinity for substrates and cofactors, can vary considerably among species and even among isoforms within a single species (Hossain & Asada, 1985). Generally, research indicates that MDHAR uses NADH more efficiently compared to NADPH *in vitro*, with lower

K_M values for the former (Table 1.2). This is true even for MDHAR6, an isoform that operates in the chloroplast where NADPH synthesis is occurring via the electron transport chain in the light (Hossain & Asada, 1985; Murthy & Zilinskas, 1994; Sano et al., 1995, 2005).

Table 1.2. MDHARs affinity and activity for cofactor NADH/NADPH in different species

	MDHAR	Molecular weight	K_M (μM)		V_{max}		Origin
			NADH	NADPH	NADH	NADPH	
1	**Spinach chloroplast**	53 kDa	**6.3**	**430**	200 unit/mg	300 unit/mg	Sano *et al*., 2005
2	**Potato mitochondria**	54 kDa	**12.3**	**57.3**	4.2 unit/mg	ND	De Leonardis *et al*., 1995
3	**Potato cytosol**	42 kDa	**7.7**	**30**	61 μmol/min/mg	ND	Borraccino *et al*., 1986
4	**Cucumber**	47 kDa	**4.4**	**210**	300 unit/mg	ND	Sano *et al*., 1995
5	**Spinach leaf**	53 kDa	**7**	**22**	200 unit/mg	300 unit/mg	Hossain *et al*., 1984
6	**Cucumber fruit**	47 kDa	**4.6**	**23**	200 μmol/min/mg	150 μmol/min/mg	Hossain *et al*., 1985
7	**Pea**	47 kDa	**5.3**	**22**	312 μmol/min/mg	40.9 μmol/min/mg	Murthy *et al*., 1994
8	**Soybean root nodule**	43 kDa	**5.6**	**150**	288 μmol/min/mg	ND	Dalton *et al*., 1992

The catalytic mechanism of MDHAR has been studied in rice. Based on the structures of NADH and NADPH (Figure 1.11), it is hypothesized that an extra hydrogen bond with the ADP-ribose moiety of NAD facilities the formation of the MDHAR-NAD complex in rice.. Furthermore, the Glu196 residue of OsMDHAR plays an important role in selecting NAD (Park et al., 2016).

The reaction kinetics of MDHAR is supposed to be a ping-pong mechanism (Hossain & Asada, 1985), During this reaction, the enzyme-bound FAD (E-FAD) undergoes reduction by NADH, resulting in the formation of a charge-transfer complex (E-$FADH_2 \cdot NAD^+$). The reduced enzyme transfers electrons to MDHA through two consecutive single-electron transfers, with the intermediate thought to be the semiquinone form (E-$FAD \cdot NAD^+$). The rate constant for the enzyme-bound FAD reduction by NADH was assessed using stopped-flow analysis as about 10^8 M^{-1} s^{-1} (Hossain & Asada, 1985).

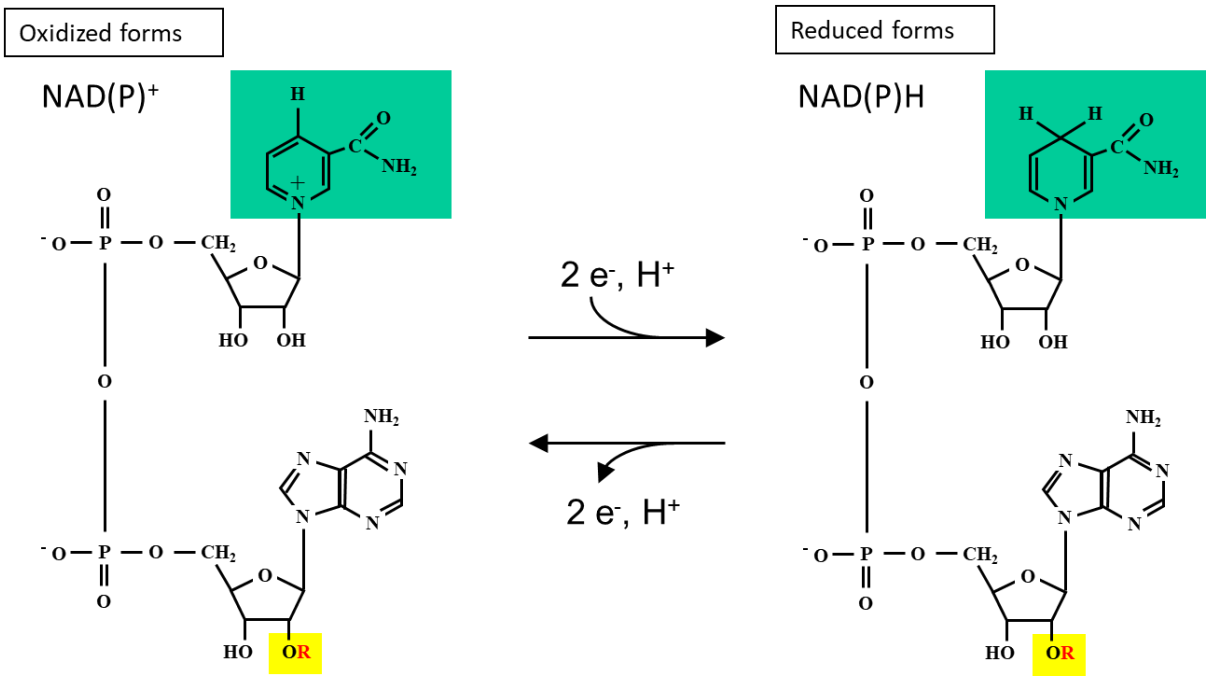

Figure 1.11. Oxidized and reduced forms of NAD(H) and NADP(H). Green shading indicates the redox-active nicotinamide group while yellow indicates the different between NAD(H) and NADP(H). In NAD(H), R = H while in NADP(H), R = phosphate.

1.4.3 Functional studies of MDHAR in plants

While the catalytic mechanism of the enzyme is quite well understood, much remains to be elucidated on the physiological significance of the different isoforms within the plant. If the primary biochemical function of MDHAR is clear (recycling MDHA to ascorbate at the expense of NADH or NADPH), less is known about the physiological importance of this function. Several studies have reported on MDHAR activity or expression of the genes under different conditions. For instance, a correlation has been established between MDHAR activity and tolerance to salinity, drought, and temperature stresses in several plant species (Eltayeb et al., 2007; Kwon et al., 2003; Leterrier et al., 2005; Park et al., 2019).

Genes encoding MDHAR (known as *MDAR*) have been cloned from several plant species, including cucumber (*Cucumis sativus*) (Sano & Asada, 1994), pea (*Pisum sativum L.*) (Murthy & Zilinskas, 1994) tomato (*Solanum lycopersicum*) fruit (Crantz' et al., 1995) and spinach leaves (Sano et al., 2005). The *MDAR* genetic sequence from *Brassica campestris* was identified and its mRNA expression was studied under conditions of oxidative stress (Yoon et al., 2004). Additionally, genome-wide analysis of *MDAR* gene family in cotton species suggests that MDHAR functions in fibre development via regulating ascorbate redox homeostasis (Zhou et al., 2021).

As well as information from correlative studies, approaches based on altered expression of *MDAR* expression have been conducted in several species. Based on RNAi and overexpression lines, cytosolic MDHAR (OsMDAR3) was reported to enhance stress adaptation and crop output in paddy fields of *Oryza sativa L. japonica* (Kim et al., 2017). Using a quantitative trait loci (QTL) approach, a link between MDAR expression levels and ascorbate content was reported in tomato fruit under chilling stress (Stevens et al., 2008). Also in tomato, altered expression of an isoform localized in the cytosol and peroxisomes led to the somewhat surprising conclusion that ascorbate content is negatively correlated with MDHAR activity (Gest et al., 2013).

In Arabidopsis, studies using loss-of-function mutants have identified specific functions for two *AtMDAR* genes. First, a mutant that required sugar for germination and early post-germination growth was identified as deficient in the peroxisomal membrane-bound AtMDHAR4 (Eastmond, 2007). This is presumably because reduction of MDHA to ascorbate by this enzyme is required to allow efficient removal of H_2O_2 generated during fatty acid β-oxidation in seedlings, which is the main source of carbon skeletons and energy when seedlings are growing in the absence of external sugar (Eastmond, 2007). More surprisingly, Arabidopsis lines deficient in mitochondrial MDHAR5 have been noted to thrive in soil treated with the explosive TNT whereas wild-type plants struggle to survive. This is attributed to TNT being a substrate with which the MDHAR protein interacts, leading to the production of superoxide from oxygen molecules (Johnston et al., 2015). This intriguing finding emphasizes the intricacy of the interplay between antioxidant systems and ROS, suggesting that in some conditions enzymes considered as antioxidative can in fact play pro-oxidant roles.

1.4.4 Thioredoxins and chloroplast MDHAR

TRXs are small ubiquitous disulfide reductase that play important roles in maintaining proteins in their reduced state within the context of photosynthesis. While certain TRXs function in antioxidant systems (see section 1.3.3), their primary function is to induce post-translational redox alterations in target proteins, a process that has been linked to virtually every cellular function. This leads to the transition of proteins into an active or inactive state when disulfide bonds are reduced (Sanz-Barrio et al., 2012). Plants TRXs are located in cytosol, mitochondria and chloroplasts. Cytosolic and mitochondrial TRX are reduced by a TRX reductase with NADPH as the electron donor (Arné & Holmgren, 2000). Chloroplastic TRX is reduced by ferredoxin/Trx reductase (FTR) utilizing electrons derived from the photosynthetic electron transport chain (Sanz-Barrio et al., 2012).

Cytosolic TRXs, TRX_{h3} and TRX_{h5} are reported to be involved in wounding, abscission, senescence, and pathogen attack, and several diverse oxidative stress conditions (Laloi et al., 2004). TRX_{h3} and TRX_{h5} catalyse the monomerization of NPR1 which is a key player in the SA signaling pathway (Chai et al., 2014). In plastids, both TRX_f and TRX_m act in photosynthetic tissues to regulate the activity of numerous other proteins (Sanz-Barrio et al., 2012). Chloroplastic AtMDHAR is one such protein, with TRX-dependent reduction of the enzyme leading to a doubling of the activity (Vanacker et al., 2018). Hence, the ability of MDHAR to regenerate ascorbate might be favored by reducing conditions *in vivo.* So far, data on redox regulation of MDHAR isoforms located in other compartments is less clear.

1.4.5 NADH and NADPH: important cofactors in the ascorbate-glutathione pathway

NADH and NADPH are principal cofactors involved in energy exchange in cells, notably playing key roles in essential processes such as photosynthesis and respiration. They also intervene in antioxidative reactions (Hossain et al., 1984; Endo et al., 1997; Foyer & Noctor, 2011). The oxidized forms of NADH and NADPH have two electrons and one proton fewer than the reduced forms and are called NAD^+ and $NADP^+$, respectively (Figure 1.11). While there is some overlap between the functions of NADH and NADPH (as shown in Table 1.2 for MDHAR), NADH generally intervenes in catabolic (energy-generating) processes such as respiration, where it is formed in glycolysis and the tricarboxylic acid cycle and re-oxidized by the respiratory electron transport chain (Gakière et al., 2018). By contrast, NADPH is generally involved in anabolic (energy-requiring) biosynthetic pathways such as photosynthesis, in which $NADP^+$ is converted to NADPH by the photosynthetic electron transport chain then re-oxidized, notably, during the CO_2 fixation process. The balance between the reduced and oxidized forms of these electron carriers is critical for maintaining the health and function of cells, and influences a multitude of cellular processes including DNA repair, cell signaling, and the regulation of circadian rhythms (Belenky et al., 2007; Noctor et al., 2006).

The core functions of both nucleotides are as electron exchangers in the soluble phase of the cell. NADPH is often considered particularly important in counteracting oxidative stress, as it is necessary to regenerate the key cellular antioxidant, GSH, from GSSG (as the cofactor of GR). This antioxidative function is particularly important, given that cells continuously produce reactive oxygen species (ROS) during metabolic processes, which, if deficient, can lead to cellular damage and a range of pathologies (Lim et al., 2020). NADPH can be generated through the oxidative pentose phosphate pathway. However, other enzymes, such as malic enzyme (ME) and isocitrate dehydrogenase (ICDH), can also contribute to cellular NADPH pools (Lim et al., 2020).

In isolated plant peroxisomes, the presence of three NADP-dehydrogenases was demonstrated, including glucose-6-phosphate dehydrogenase (G6PDH), 6-phosphogluconate dehydrogenase (6PGDH) and ICDH (Corpas et al., 1998). The localization of NADP-ICDH in Arabidopsis peroxisomes has been demonstrated by immunocytochemistry, and this dehydrogenase has been postulated to be involved in stomatal movement, suggesting that H_2O_2, NADPH and nitric oxide (NO) generated in peroxisomes are necessary for stomatal movements (Leterrier et al. 2016). Isoforms of these enzymes also exist in other compartments, such as the cytosol (Mhamdi et al., 2010c).

Within the ascorbate-glutathione pathway, NADH and NADPH are cofactors for two enzymes: MDHAR and GR. While GR shows a high specificity for NADPH, MDHAR can use both nucleotides. This dual usage raises an interesting question about the relative efficiency of these cofactors in enzyme function. Although Table 1.2 shows a preference for NADH, this finding does not provide definitive information on utilization of the two forms *in vivo.* This is because the preference for NADH is based on the assumption that the two nucleotides are present at similar concentration in plants, which might not be the case for certain compartments. One example is the cytosol, where NADH concentrations are thought to be very low (Heineke et al., 1991).

1.5 *Arabidopsis thaliana*: a model plant for understanding of plant functions

The use of model organisms has considerably enhanced scientific progress. In plants, Arabidopsis has been established for several years as a paradigmatic model (Weigel & Mott, 2009). This small flowering plant of the Brassicaceae family has gained attention due to its genetic tractability, ease of culture, prolific seed production, and short life cycle (Koenig & Weigel, 2015). These attributes make it an invaluable tool for illustrating complex molecular processes and understanding the fundamental principles governing plant function. With a life cycle of approximately six weeks in optimal conditions, Arabidopsis enables investigation of multiple generations within a relatively short timeframe (Koornneef et al., 1984). The rapid life cycle also facilitates the analysis of gene functions by allowing the observation of phenotypic changes in a brief period. Consequently, researchers can investigate a wide array of genetic, physiological, and environmental factors that influence plant growth and development (Eshed & Zamir, 1995).

Furthermore, Arabidopsis shares essential biological features with other plants, making findings potentially applicable to diverse species (Koornneef et al., 1984). The fact that basic life processes are similar in different plant groups means that what we learn from studying Arabidopsis could also apply to important crops (Alonso-Blanco et al., 2009; Kliebenstein & Osbourn, 2012). This is probably the

case for fundamental biochemical processes such as the redox-related pathways studied in the laboratory.

The ease of altering genes is a key feature that favors the choice of Arabidopsis for plant studies. Its detailed genetic map and genetic tools allow scientists to change the expression of specific genes to examine the phenotypic effects (reverse genetics). Methods like gene insertion and CRISPR editing help pinpoint and understand genes that are linked to certain traits or functions. This precise genetic control gives crucial insights into gene functions and helps improve crops for agriculture (Alonso et al., 2003). In particular, the availability of an array of T-DNA insertion lines within seed banks is a rich resource for reverse genetics studies, as is the ability to produce double mutants by simple crossing and genotypic selection. These features are fundamental to the work that has been conducted within this thesis.

1.6 Objectives of this research

Within the context of understanding the complex plant antioxidative systems and the interactions between them, the aim of this study was to explore the importance of the five genes encoding MDHAR in the model plant, Arabidopsis. The work extends previous studies in the laboratory focusing on redox regulation of the chloroplast MDHAR and the importance of specific isoforms of GR and DHAR, other enzymes in the ascorbate-glutathione pathway (Mhamdi et al., 2010b; Rahantaniaina et al., 2017; Vanacker et al., 2018). In particular, we sought to establish the functional importance of the five *MDAR* genes in Arabidopsis grown in optimal conditions and in conditions where increased availability of H_2O_2 is causing intracellular oxidative stress. To achieve this aim, available T-DNA mutants for each isoform that were available in the laboratory were used. Two types of double mutant were also studied. One type involved crosses between *mdar* mutants for the two isoforms found in the peroxisomes . This part of the work developed into a largely genetic study and is described in the second part of the results (Chapter 4). The major part of the work focused on producing and studying double mutants between each *mdar* mutant and *cat2*, with the aim of elucidating the role of the different MDHAR isoforms in conditions where increased availability of H_2O_2 leads to intracellular oxidative stress. The first part of the results (Chapter 3) describes the analyses of these mutants, in particularly the *cat2 mdar2* double mutants, at the phenotypic, molecular, biochemical, transcriptomic and proteomic levels.

CHAPTER 2 MATERIALS AND METHODS

2.1 Plant material

The model plant *Arabidopsis thaliana* was used for all studies. All the Arabidopsis mutants used in this study were in the genetic background of Colombia (Col-0). The mutations were obtained through the insertion of T-DNA at various genomic sites, resulting in loss-of-function mutations for the *mdar* mutants (SIGnAL Web site (http://signal.salk.edu)). For this study, the T-DNA mutants for the corresponding *MDAR* genes were available in the laboratory. All *mdar* mutants are knockout or severe knocked-down mutants. Multiple mutants were produced by crossings either in the wild-type *CAT2* background or in the *CAT2* deficient mutant background (*cat2*).

Arabidopsis *mdar* mutant lines used in this work were: *mdar1-2* (SALK_034893), *mdar1-3* (SAIL_720_H04), *mdar2* (SALK_028874), *mdar3* (SAIL_31-A09), *mdar4* (SALK_068667). The cat2 mutant was *cat2* (SALK_057998) (Queval et al., 2009).

2.2 Plant culture conditions

Because the *mdar4* mutant requires sugar for early root and photosystem development (Eastmond et al., 2007), all Arabidopsis seeds were as first step germinated germinated on 1/2 Murashige and Skoog solid medium (basal salt mixture; M0221; Duchefa. 0.8 % agar) in 9 cm x 9 cm plates, with the addition of 1% sucrose. After stratification in the dark at 4°C for two days, plates were placed under LD light conditions (16-hour light and 8-hour dark photoperiod) under a light intensity of 200 µmol photons·m^{-2}·s^{-1}, with a temperature of 22°C during the day and 20°C during the dark period. Relative humidity was maintained at 65 %. After 7 days, seedlings were transferred into soil in individual pots and further cultivated in the same conditions. In studies in which *mdar4* was not included,seeds were sometimes directly sown on soil.

For the genotyping work, 10-day-old seedlings grown on agar medium were sampled and frozen at -20°C for future analysis.

For all other analyses, young adult leaves from 3-4 week old plants were used.

2.3 High-throughput genotyping

A high-throughput DNA extraction protocol for PCR screening was developed based on the “quick & dirty” method (Edwards et al., 1991), using a 96-well plate.

Control samples (water, Col-0, and *mdar1-2*, *mdar1-3*, *mdar4*, and *cat2* single mutants) were always included along with PCR screened samples. Specific primers were designed for each gene

(oligonucleotide sequences are detailed in Tables S3.1 and 4.1).

To detect the presence of the T-DNA, a pair of primers was designed with one primer specific to the gene and the other primer specific to the T-DNA sequence. Specific hybridization temperature and elongation time were set for each primer pair using the Primer3 program (https://primer3.org).

The PCR products were analysed by electrophoresis in 0.8 % agarose gels prepared and run in TEA buffer (40 mM Tri-HCl pH 8.6, 1 mM EDTA, 20 mM acetate) and stained with ethidium bromide.

2.4 Gene expression level analyses

2.4.1 RNA extraction and reverse transcription (RT)

50-100 mg leaf samples were ground in liquid nitrogen using a mortar and a pestle (pre-chilled with liquid nitrogen). Total RNA was extracted from the ground powder with the NucleoSpin® RNA Plant and Fungi kit (REF 740122.50, Macherey Nagel). 1 µg RNA diluted with RNase-free water was hybridized with 0.5 µg dT oligo (70°C for 5 min and chill on ice) and reverse transcription was performed after addition of ribonuclease inhibitor and reverse transcriptase (Improm-II from Promega, 1 µL, in a 20 µL reaction volume), with the following incubation parameters: 5 min at 25°C, 60 min at 42°C, 15 min at 70°C and finally ice). 5 µL of the reverse transcription reaction products (diluted 25 times) were used for gene expression analyses by qPCR.

2.4.2 Reverse Transcription Quantitative Polymerase Chain Reaction (RT-qPCR)

The qPCR Light Cycler480 SYBR® Green I Master (Roche) buffer was used and the quantitative real-time reaction was performed in a LightCycler® 96 (Roche). Transcripts of the reference genes *ACTIN2* (At3g18780) and *PP2A* (At1g13320) or *Ubiquitin* (At4g36800) were used for normalization. Their sequences are listed in Table S3.1.

2.5 Recombinant MDHAR proteins

2.5.1 Plasmid construction

pGENI-MDAR expression plasmids were constructed from the *pGENI* plasmid (Bohrer et al., 2012) allowing the production of a recombinant protein fused to a strep-tag at its C-terminus. Each of the five Arabidopsis *MDAR* coding sequences (according to Araport11, without the STOP codon and mature form encoding sequence for MDHAR6) was inserted into *pGENI* by NcoI/XhoI cloning. To design the primers, the NEBuilder® Assembly Tool (www.neb.com) was utilized, and the plasmid construction

was carried out using the NEBuilder® HIFI Master Kit (New England Biolabs).

Integrity and sequence accuracy of the plasmid constructs were verified by sequencing (Eurofins).

2.5.2 Production of MDHAR recombinant proteins in *E.coli*

The *pGENI-MDHAR* plasmids were transferred into the *E. coli* BL21 (DE3) bacteria strain for the production of MDHAR recombinant proteins under the control of T7 bacteriophage RNA polymerase. Introduction of the plasmids was performed using DMSO competent cells, and a 30-sec heat shock (42°C) was applied to facilitate plasmid (100 ng) uptake by bacteria. Subsequently, the cells were cultured at 37°C for 35-45 min, and then plated on solid selective LB medium (ampicillin 100 mg/L). Only the bacteria carrying the plasmid were able to survive and form colonies in the presence of ampicillin.

To induce production of MDHAR proteins, 330 µM isopropyl β-D-1-thiogalactopyranoside (IPTG) was added to exponentially growing bacteria cultures (OD 0.5-0.6 at 600 nm). The culture was then incubated at an optimized temperature (37°C for 3-4 hours, or 30°C, 25°C, 18°C overnight) for production yield and solubility established for each MDHAR isoform.

Cells were harvested by centrifugation at 8000 rpm (BECKMAN COULTER Avanti JA-20 centrifuge equipped with a JLA 8.1000 rotor) during 30 min.

Cell pellets were frozen and stored at -80°C until protein extraction and purification.

2.5.3 Purification of MDHAR recombinant proteins

Cell pellets from an 800 mL bacteria culture were resuspended in 5-8 mL of extraction buffer TNE (Tris-HCl pH 7.9 30 mM, NaCl 150 mM, EDTA 1 mM) supplemented with the cocktail protease inhibitor (cOmplete Mini EDTA-free, Roche) (one tablet in 10 mL of extraction buffer). Extraction was performed by three passages through a French press at 10,000 P.S.I. (pre-cooled 5 mL pressure cell). After centrifugation (30 min at 4°C, 18,000 rpm, JA-20 rotor) MDHAR proteins were purified from the soluble crude bacteria extract by affinity chromatography using a Strep-Tactin column (1 mL, Strep-trap™ HP). After loading, the column was washed with TNE buffer, and then 0.1 mM desthiobiotin was used to elute the recombinant protein. Desthiobiotin was removed by diafiltration (Amicon unit 30 kDa cut-off, Millipore), and the purified protein preparation was concentrated to 1-2 mg/mL. Routinely, 5-10 mg of purified recombinant MDHAR protein was obtained from a volume of 800 mL bacteria culture. Purified samples were stored at -80°C, without any significant reduction in activity noticed after several months.

2.5.4 Quantification of purified proteins

Protein quantification was performed using the Qubit fluorometer (Qubit® 2.0 Fluorometer, LifeTechnologies; Qubit™ protein assay mix) in crude extracts or the NanoDrop microvolume spectrophotometer (Thermo Fisher Scientific) for final purified samples. Final samples concentrations were calculated on the basis of OD 280 nm with a calculated molar extinction coefficient of 43445 M^{-1} cm^{-1} for MDHAR1, of 56270 M^{-1} cm^{-1} for MDHAR2, of 56270 M^{-1} cm^{-1} for MDHAR3, of 53580 M^{-1} cm^{-1} for MDHAR6. MDHARs being flavin-containing enzymes (1 flavin per subunit), purified protein preparations were also quantified on the basis of OD at 450 nm with a molar extinction coefficient of 11.3 mM^{-1} cm^{-1} for flavin adenine dinucleotide (FAD).

2.5.5 SDS-PAGE

Purity of the enzyme preparations was assessed by SDS-PAGE and Coomassie blue staining using the NOVEX system from Thermo Fisher Scientific. Pre-cast gels (4-20% acrylamide-bis-acrylamide) were used according to the supplier (NuPAGE gels, Thermo Fisher Scientific). 10 µg protein samples were analyzed and MDHAR recombinant protein preparations were considered as purified to homogeneity upon detection of a single polypeptide of the expected size on SDS-PAGE gels stained with Coomassie blue.

2.5.6 Western blot

To set up the optimal temperature for production of recombinant MDHAR proteins, crude bacteria extracts (total after the French press, and soluble after centrifugation) were electrophoresed (as described above) and transferred onto a polyvinylidene difluoride (PVDF) membrane using the iBlot™ system (Thermo Fisher Scientific). The membrane was then blocked in TBS (Tris-buffered saline) supplemented with Tween-20 (0.1%, TBS-T) and 5% milk (low-fat, dry milk), at room temperature for about 1 hour or at 4°C overnight. The membrane was incubated with HRP-conjugated anti-streptavidin antibody (monoclonal anti-Strep tag II - HRP conjugated, from IBA, diluted 10^4 times in TBS-T) at room temperature for 2-3 h or at 4°C overnight. After three washes of 10 min in TBS-T at room temperature, the membrane was developed for Enhanced Chemiluminescence (ECL) using the ChemiDoc MP imaging system from Bio-Rad.

2.6 MDHAR activity assays

2.6.1 Purified recombinant enzyme

MDHAR enzyme activities were assayed using a spectrophotometer (BECKMAN Uvicon) and 1 mL UV-compatible plastic cuvettes to monitor MDHA-dependent NAD(P)H oxidation at 340 nm (the molar extinction coefficient for NAD(P)H at 340 nm is $E_{NAD(P)H}$ = 6.22 mM^{-1} cm^{-1}). The reaction mixture composition was: 2.5 mM Ascorbate (prepared in 20 mM NaH_2PO_4 pH 5.6), NAD(P)H at 250 µM, in Tris-HCl buffer 100 mM pH 7.5. Upon addition of 0.8 u ascorbate oxidase (AO) to generate MDHA from ascorbate, and MDHAR (purified protein *ca.* 0.1 µg), NAD(P)H oxidation kinetics were followed over 0.5 min.

The activity was measured as the initial rate of the reaction. To determine the K_M for NAD(P)H, the cofactor concentration varied from 0 to 100 µM for NADH, and from 0 to 250 µM for NADPH.

Michaelis-Menten curve fitting was computed by GraphPad, and Lineweaver-Burk plot analysis was employed to calculate the K_M (µM) values, V_{max} (µmol min^{-1} mg^{-1}), and catalytic activity K_{cat} (s^{-1}). V_{max} is calculated by the formula V_{max}= Vi·(K_M + S)/S, where Vi represents the initial reaction rate and S denotes the substrate concentration. All data correspond to the means ± standard error (SE) derived from at least three measurements.

2.6.2 Leaf extractable MDHAR activity

Enzyme assays were performed from plant leaves as previously described by the team (Noctor et al., 2016). The extraction buffer was prepared just before the experiment. 100-150 mg leaf samples were grinded in liquid nitrogen in a pre-chilled mortar using a pestle, and 50 mg insoluble polyvinylpyrrolidine (PVPP) was added, immediately followed by 1 mL of 50 mM MES/KOH pH 6 containing 1 mM Ascorbate, 40 mM KCl and 2 mM $CaCl_2$. After mixing thoroughly, the extract was centrifuged at 12,100 g. at 4 °C for 10 min. Then, the supernatant was carefully transferred into a new tube and centrifuged again for 10 min. The clarified extract was directly used for MDHAR activity measurements (see enzyme activity assay for recombinant proteins).

50 µL and 100 µL of leaf extract were used for testing NADH- and NADPH-dependent MDHAR activity, respectively. The enzyme assay mix was as for testing recombinant proteins activity except that the buffer was 50 mM HEPES pH 7.6. First, the activity was measured without AO, and then measured again after adding 0.8 units of AO to the cuvette. The decrease in absorbance at 340 nm was monitored for 1 min. The MDHAR activity is calculated on the basis of ΔA_{340} after AO – ΔA_{340} before AO.

Total protein concentrations in leaf extracts were measured by the Bradford method (Bradford, 1976). MDHAR activity in leaf extracts is expressed as nmol oxidized NAD(P)H mg^{-1} total protein min^{-1} and corresponds to: V_i (ΔA_{340}[0-0.1']) / $E_{NAD(P)H}$/protein quantity.

2.7 Arabidopsis plants expressing MDHAR2 fusion proteins with GFP

2.7.1 Validation of complementation lines at the protein level

Before my arrival in the lab, *mdar2* mutant plants transformed with GFP-MDHAR2 constructs (GFP fusion either at the N-terminus or at the C-terminus of MDHAR2) had been obtained and screened by PCR. I performed complementary western blot analyses to detect GFP-MDHAR2 fusion proteins in the leaf extracts from these plants using an anti-GFP antibody.

Leaf extracts were prepared as described for MDHAR activity tests from leaves, in TBS buffer supplemented with a protease inhibitor cocktail for plant cell and tissue extracts (diluted 100 times, Sigma-Aldrich). Leaf protein extract samples (10-50 µg, quantification by the Bradford method) were electrophoresed and immuno-detected (procedure as described for recombinant proteins) using an anti-GFP antibody (produced in rabbit, from Abcam, diluted 1:5,000). After over-night incubation at 4°C, and 3 washes in TBS-T, the PVDF membrane was exposed to a secondary anti-rabbit antibody conjugated to HRP (goat anti rabbit, from Abcam, diluted 1:10,000) for 2 hours at room temperature. After 3 washes in TBS-T, the ECL signal was developed using the ChemiDoc MP imaging system from Bio-Rad.

2.7.2 Subcellular localization of MDHAR2-GFP fusion proteins

12-day-old plants of the *cat2 mdar2*-MDHAR2 complemented lines were used to monitor the GFP signal observed by confocal microscopy. A Zeiss LSM 880 inverted confocal laser scanning microscope was used equipped with a 63x PLN APO oil-immersion objective. GFP was laser excited at 488-nm, and fluorescence was detected in the 490- to 560-nm window. Chlorophyll auto-fluorescence was used as a chloroplast marker, and monitored by excitation at 633 nm and detection in the 624 to 735 nm wavelength window.

2.8 Total Salicylic Acid (SA) assay by high-performance liquid chromatography (HPLC).

2.8.1 Leaf sample preparation

Leaf samples (*ca.* 150 mg fresh weight) were pulverized using a bead beater with 3-mm diameter steel beads in liquid nitrogen. For each sample, 1.5 mL of 90% methanol was added to initiate the extraction process. Following centrifugation at 12,100 g for 15 min at 4 °C, 1 mL of the supernatant was transferred into a new tube. Subsequently, 500 µL of 100% methanol was mixed with the residual sample to resuspend it, and then centrifuged at 12,100 g for 15 min at 4°C. The supernatant was combined with the initial extract, and then methanol was removed using a Mivac for 3 hours at 30 °C. The dried precipitate was dissolved in 600 µL of 3N HCl and incubated in a water bath at 80°C for 45 min. After addition of 1 mL diethyl ether and mixing (vortex 20 min), the ether (upper) phase was collected into a new tube. The remaining liquid was re-extracted by adding another 1 mL diethyl ether and the organic phase was taken and added to the first sample. Then, ether was allowed to evaporate at ambient temperature under a fume hood. Pellets were resuspended in 200 µL of a mix of 20 mM Na acetate (90 %) and Na acetonitryl (10 %) by vortexing. After a 10 min centrifugation at 12,100 g for 15 min, 100 µL of the supernatant was taken for SA assay.

2.8.2 SA assay by HPLC

Total SA assay was performed using an HPLC system from Waters (column: NovaPack C18, 4 µm, 3.9 X 150 mm; 717 plus autosampler; binary HPLC pump 1525; Multi-λ fluorescence detector 24575). The area of the peak eluting at 6-8 min were taken for calculation of total SA, based on the peak areas of authentic standards eluting at this point.

2.9 Glutathione and ascorbate assays

The analyses of the oxidized and reduced forms of ascorbate and glutathione were conducted as described by Noctor and Mhamdi (2022) using a plate-reader (Multiskan Spectrum, Thermo Labsystems), spectrometer for reading of absorbance values in a 96-well plate with automatic data recording.

Approximately 100 mg of leaf material was carefully ground in liquid nitrogen using a pestle in a mortar. After adding 1 mL of 0.2 mM HCl, the mixture was ground again. The homogenate was then centrifuged at 12,100 g for 10 min at 4°C. Subsequently, 500 µL of the supernatant was transferred into a new tube

and combined with 100 µL of 0.2 M NaH_2PO_4 (pH 5.6). The mixture was then adjusted to a pH of 5-6 (checked with a pH strip) using 0.2 M NaOH and used for the subsequent analyses ("neutralized" extract).

2.9.1 Glutathione assay

Total glutathione was measured directly in the neutralized extract, while for oxidized glutathione, samples were pre-incubated with 2-vinylpyridine (2-VPD) to remove reduced glutathione. In the total glutathione assay, GSH reduces the colourless chemical DTNB (5,5'-dithiobis-(2-nitrobenzoic acid)), and 2 GSH molecules are oxidized to GSSG. The reaction releases TNB^- which has a yellow colour (maximum absorbance at 412 nm). In the assay, GSSG is re-reduced to 2 GSH by glutathione reductase (GR) in an NADPH-dependent manner. The rate of the overall reaction is dependent on the concentration of glutathione because NADPH and GR are in excess in the assay. The reaction is started by adding GR (20-40 units) and shaking, and the initial rate of DTNB reduction is monitored at 412 nm for 2 min. Finally, GSH (reduced glutathione) quantity is calculated by: total glutathione – GSSG (oxidized glutathione).

2.9.2 Ascorbate assay

For the ascorbate assay, a UV-transparent plate must be used. Reduced ascorbate (ascorbate) is assayed directly in neutralized extracts at 265 nm (DHA has negligible absorbance at this wavelength).

Concurrently, "total" ascorbate (*i.e.* ascorbate + DHA) is assayed on samples treated with DTT, allowing DHA to be reduced to ascorbate. OD_{265nm} is measured before and after adding ascorbate oxidase (AO) to convert ascorbate to MDHA, and finally to DHA.

Ascorbate concentrations are calculated on the basis of :

OD_{265nm} reduced Asc = OD_{265nm} (without treatment) – OD_{265nm} (without treatment and after AO).

OD_{265nm} total Asc = OD_{265nm} (after DTT reduction and before AO) – OD_{265nm} (after DTT reduction and after AO).

An extinction coefficient of 14 mM^{-1} cm^{-1} was used for ascorbate at 265 nm.

2.10 Leaf lesion quantification

The ImageJ software was used to quantify the leaf lesion areas. The percentage of the leaf lesion area relative to the total rosette area was calculated for at least 10 plants.

2.11 Statistical analysis

Student's t-tests were conducted for statistical analyses. At least three separate and independent data sets were analyzed, under the assumption of equal variance between two samples and a two-tailed distribution. If not otherwise stated, a significant difference is denoted by a t-test with a *P*-value < 0.05.

CHAPTER 3 A STUDY OF MUTANTS FOR MONODEHYDROASCORBATE REDUCTASE IN OXIDATIVE STRESS CONDITIONS

This chapter is presented in the form of an article that will soon be submitted for publication:

Xu D, Trémulot L, Yang Z, Mhamdi A, Chatel-Innocenti G, Mathieu L, Espinasse C, Breusegem FV, Vanacker H, Issakidis-Bourguet E, Noctor G. Cytosolic MONODEHYDROASCORBATE REDUCTASE 2 promotes oxidative stress signaling in Arabidopsis.

CHAPTER 3 A STUDY OF MUTANTS FOR MONODEHYDROASCORBATE REDUCTASE IN OXIDATIVE STRESS CONDITIONS

Summary

Monodehydroascorbate reductase (MDHAR), an enzyme in the ascorbate-glutathione pathway, is encoded by five genes in Arabidopsis, including four that direct proteins to the cytosol and peroxisomes. The roles of these specific isoforms are poorly characterized.

T-DNA mutants for *MDAR* genes encoding cytosolic and peroxisomal isoforms were used to analyse the importance of each. To examine their roles in oxidative stress conditions, each mutant was crossed with a *cat2* line lacking the major leaf catalase.

Enzyme assays in *mdar* mutants and of recombinant MDHARs suggest that peroxisomal MDHAR1 and cytosolic MDHAR2 are major players in leaf NADH- and NADPH-dependent activities, respectively. All mutants showed a wild-type phenotype when grown in standard conditions. In the *cat2* background, loss of peroxisomal MDHAR functions decreased growth whereas loss of the cytosolic MDAR2 function had no effect on growth but annulled a large part of transcriptomic and phenotypic responses to oxidative stress. The effects of the *mdar2* mutation were associated with decreased salicylic acid accumulation and enhanced glutathione oxidation, and were reverted by complementation with the *MDAR2* sequence.

Together, the data show that the cytosolic MDHAR2 is dispensable in optimal growth conditions but essential to promote biotic defence responses triggered by oxidative stress.

Key words

Oxidative stress; antioxidants; ascorbate; glutathione; catalase; salicylic acid; pathogenesis-related (PR).

3.1 Introduction

Ascorbate is an essential compound in plants with several functions as an antioxidant and enzyme cofactor (Dowdle *et al*., 2007; Conklin *et al*., 2024). As an antioxidant, ascorbate reacts chemically with certain reactive oxygen species (ROS) and is a reductant for ascorbate peroxidase (APX; Conklin *et al*., 2024; Foyer & Kunert, 2024). APX is one of a battery of plant enzymes that counter excessive accumulation of H_2O_2 and avoid formation of its more reactive derivatives: others include various other types of peroxidases as well as catalase (Davletova *et al*., 2005; Mhamdi *et al*., 2010b).

Continued function of APX requires effective regeneration of ascorbate from its oxidized forms. The first oxidation product is monodehydroascorbate (MDHA), an unstable free radical that can be directly reduced back to ascorbate (Foyer & Kunert, 2024). A second fate is chemical dismutation, in which two MDHA molecules produce one molecule each of ascorbate and dehydroascorbate (DHA), a form that is both more oxidized and more stable than MDHA. While ascorbate and DHA can be readily quantified in tissue extracts, specialized equipment is required to detect MDHA and very little quantitative data are available. However, it has been reported that MDHA signals are enhanced in response to oxidative stress (Veljovic-Jovanovic *et al*., 1998) and kinetic modelling of the response to increased H_2O_2 concentrations suggests that MDHA will increase as ascorbate oxidation accelerates (Tuzet *et al*., 2019).

Reductases that can convert MDHA and DHA to ascorbate have been known for many years. While DHA reductase (DHAR) uses glutathione as reductant, MDHA reductase (MDHAR) is a flavoprotein that functions with NADH or NADPH as a co-factor (Foyer & Halliwell, 1977; Hossain & Asada, 1984, 1985; Hossain *et al*., 1984; Sano *et al*., 1995). Both enzymes are encoded by several genes in plants. Recent studies have examined the roles of specific DHAR isoforms using loss-of-function Arabidopsis mutants (Noshi *et al*., 2017; Rahantaniaina *et al*., 2017; Terai *et al*., 2020; Hamada *et al*., 2023), but less information is available for specific mutants for *MDAR*. Engineering altered expression of *MDAR* has been reported to influence both ascorbate contents and stress tolerance (El Airaj *et al*., 2013; Gest *et al*., 2013), but systematic comparisons of the roles of the different isoforms in response to oxidative stress are lacking.

In Arabidopsis, five *MDAR* genes encode enzymes located in various compartments. While *MDAR1* and *MDAR4* encode proteins associated with peroxisomes, *MDAR2* and *MDAR3* encode cytosolic enzymes (Lisenbee *et al*., 2005; Eastmond, 2007). A single gene, *MDAR5/6*, codes for proteins that are addressed to both mitochondria and chloroplasts (Obara *et al.*, 2002). As well as activities located in

these compartments, several other systems can also reduce MDHA to ascorbate. These include ferredoxin in the chloroplast, an MDHAR activity located at the plasma membrane, a tonoplast ascorbate-dependent type b cytochrome, and 12-oxo-phytodieonic acid reductase 3 (Miyake & Asada, 1994; Bérczi & Møller, 1998; Maynard *et al*., 2020; Gradagna *et al*., 2023).

Given the presence of these numerous MDHA-reducing systems, questions remain concerning the importance of each in given conditions. The peroxisome-associated MDHAR4 has been shown to be required for optimal post-germinative growth, probably linked to metabolism of H_2O_2 produced during metabolism of seed storage lipids (Eastmond, 2007). In contrast to this classical antioxidant function, the mitochondrial MDHAR6 has been implicated in sensitizing plants to the xenobiotic TNT, and evidence was presented that this occurs through catalysis of ROS production (Johnston *et al*., 2015). This last observation is a striking example of the possible pro-oxidant functions that so-called 'antioxidative' enzymes might exert in certain conditions (Noctor, 2015).

Loss-of-function mutants for the five Arabidopsis *MDAR* genes do not show a marked phenotype relative to the wild-type when grown in standard conditions (Tanaka *et al*., 2021). This is in line with many other studies of genes encoding antioxidative enzymes, and highlights the redundancy built in to the complex ROS-processing network. In the present report, we confirm these observations for *mdar* mutants grown in our conditions, but we also analyse the roles of MDHARs under conditions where increased H_2O_2 availability causes ascorbate metabolism to turn over more rapidly. For this, we introduced mutations for the peroxisomal and cytosolic isoforms into a catalase-deficient background (*cat2*; Yang *et al*., 2018). The interest of the *cat2* system is that increased H_2O_2 availability occurs through the photorespiratory pathway and can be sustained inside the cell, placing an increased load on antioxidative pathways and mimicking environmentally induced oxidative stress (Mhamdi *et al*., 2010a; Tuzet *et al*., 2019). Our findings reveal an important role for the cytosolic MDHAR2 in these conditions. Intriguingly, disabling the expression of this enzyme weakens rather than aggravates downstream responses triggered by the *cat2* mutation. This suggests that in addition to its antioxidant function, MDHAR2 can promote certain outcomes of oxidative stress.

3.2 Materials & Methods

3.2.1 Plant materials and growth

Arabidopsis mutants used in this study were in the Columbia genetic background, and all seeds were obtained from the Nottingham Arabidopsis Stock Centre (http://nasc.nott.ac.uk). Lines carrying T-DNA insertions in the *MDAR1*, *MDAR2*, *MDAR3*, and *MDAR4* genes were identified using insertion mutant information obtained from the SIGnAL Web site (http://signal.salk.edu). For further information, see Supporting Information Figure S3.1a. The *cat2* mutant was *cat2-1* (Queval *et al*., 2009). Double mutants were produced by crossing. After verification of heterozygotes in F1 plants by PCR, double homozygotes were identified similarly in the F2 generation (Figure S3.1b).

Seeds were firstly germinated in 0.5 MS medium containing 1% sucrose. After seven days, plants were transferred to soil and grown in a controlled-environment growth chamber in a 16 h photoperiod and an irradiance of 200 µmol. m^{-2} s^{-1} at leaf level, 20 °C/18 °C, 65 % humidity, and given nutrient solution twice per week. Unless otherwise stated, plants were sampled after three weeks growth. Samples were rapidly frozen in liquid nitrogen and stored at −80 °C until analysis. All data are means ± SE of at least three biological replicates obtained from different plants, and experiments were repeated at least twice.

3.2.2 Plasmid constructs and plant transformation

The full-length cDNA of Arabidopsis *MDAR2* was amplified on total cDNA from Col-0 and GFP and T35S sequences were amplified on the pH7FWG2 plasmid using the primers in Supporting Information Table S3.1. Then, the three fragments and pH7FWG2 plasmid opened with SpeI and XbaI restriction enzymes were assembled using the HiFi DNA Assembly Master Mix (New England BioLabs) according to the manufacturer's instructions. Two constructs were done, to obtain *MDAR2* fused to GFP in N-terminal or C-terminal, driven by the 35S promoter of the Cauliflower mosaic virus. Purified plasmids were analyzed and sequenced to confirm successful fusion constructs. Agrobacterium tumefaciens strain GV3101 pMP90 (Koncz & Schell, 1986) was transformed with confirmed binary vector constructs (Höfgen & Willmitzer, 1988) and used to transform developing floral tissues of *cat2 mdar2* by the floral dip method (Clough & Bent, 1998).

3.2.3 Recombinant protein production and purification

MDAR1 and *MDAR2* cDNA sequences were amplified from total cDNA from Col-0 with the primers in Supporting Information Table S3.1, and then cloned into the pGENI vector (Bohrer *et al*., 2012) opened with *Nco*I and *Xho*I restriction enzymes, using the HiFi DNA Assembly Master Mix (New England BioLabs). Recombinant protein production and purification were performed as described by Vanacker et al. (2018). Purity and molecular mass of the proteins were checked by SDS-PAGE with Coomassie blue staining. Protein concentrations were determined spectrophotometrically at 450 nm, corresponding to the flavin adenine nucleotide (FAD) absorption peak, using a molar extinction coefficient of 11.3 mM^{-1} cm^{-1} (Aliverti *et al*., 1999). The purified protein was stored at -80°C until use.

3.2.4 Transcriptomic analysis

For RNA sequencing, three biological replicates were used, each consisting of 100 mg leaf tissue. Samples were extracted using Spectrum™ Plant Total RNA Kit (SIGMA, Germany), and treated with DNase during RNA purification. Library preparation and sequencing were performed at the Nucleomics Core (VIB, Leuven, Belgium), using TruSeq Stranded mRNA Library Preparation Kit (Illumina). Samples were sequenced on IlluminaNextseq 500 (75-bp single-end reads), and reads were aligned to the Arabidopsis genome by STAR (v 2.5.2b) (Dobin *et al*., 2013) using the Araport11 annotation (Cheng *et al*., 2017). The number of reads per gene was quantified with the featureCounts function as implemented in the Subread package v 1.6.2 (Liao *et al*., 2014). Genes with less than 5 reads in at least three samples were excluded for further analysis. Differentially expressed genes (DEGs) determination was conducted using the DiCoExpress (Lambert *et al*., 2020) with FDR<0.01 and a |log2FC|>1 as threshold. Hierarchical clustering was performed on DEGs using the hclust function using “ward.D2” method with a distance matrix based on Pearson correlation coefficients (R Core Team, 2021). The heatmap was generated using ComplexHeatmap package v 2.12.1 (Gu *et al*., 2016). The Gene Ontology enrichment analysis for the 4 clusters was performed using clusterProfiler v 4.4.4 with a p-value<0.05 cutoff (Xu *et al*., 2024).

3.2.5 Subcellular localization and genetic complementation

Seedlings of the *cat2 mdar2* mutant were selected for stable transformation with GFP-MDAR2 or MDAR2-GFP. Transformed T1 seeds were germinated on agar and identified based on their resistance to hygromycin or screened using a Leica (Deerfield, IL) dissecting microscope equipped with a mercury lamp and epifluorescence filter set (Karimi et al., 2002). Resistant and PCR-positive transgenic plants

were transferred to a growth chamber and maintained up to the T2 generation, when segregation analysis was performed on complemented *cat2 mdar2* lines. Two independent complemented lines were selected and used for analysis. Confocal microscopy was performed as in Rahantaniaina et al. (2017). For immunoblotting, proteins from complementation lines were extracted using TBS 1x buffer with added protease inhibitor, as previously described, with 500 µL per extract. Protein quantification was performed using the Bradford assay. A TGX stain-free gel and PVDF membrane system were used. To detect the GFP-MDHAR2 fusion protein, the PVDF membrane was incubated in a primary anti-GFP antibody (rabbit, diluted 1:5000) from Abcam for over-night at 4°C, followed by a secondary anti-rabbit antibody (diluted 1:10000) incubation for two hours at room temperature.

3.2.6 Immunoprecipitation–mass spectrometry (IP-MS) analysis

IP-MS analysis of MDAR2-GFP lines was performed using biological triplicates as previously described (Wendrich *et al*., 2017). Briefly, around three grams of leaf material were ground in liquid nitrogen and homogenised in extraction buffer containing 50 mM Tris–HCl, pH 7.5, 0.15M NaCl, 1 protease inhibitor tablet/50 ml (Roche) and 1% (v/v) NP40. Protein extracts were sonicated, diluted to remove excess of NP40, and then centrifuged twice for 15 min at 41,657*g*. Extracts were incubated for 2 h with anti-GFP-coated microbeads (µMACS; Miltenyi), applied on the µColumns (µMACS; Miltenyi), washed and eluted with preheated ammonium bicarbonate buffer. To prepare samples for MS analysis, the 50 µL eluent was reduced with dithiothreitol, alkylated with iodoacetamide and digested with sequencing-grade Trypsin. The digested samples were purified using the Bond Elut OMIX tips (Agilent Technologies) and analysed by liquid chromatography–tandem mass spectrometry with a UltiMate™ 3000 RSLCnano System connected to LTQ Orbitrap Velos mass spectrometer (Thermo Fisher Scientific). The resulting raw data were analysed in label-free quantification mode using MaxQuant software (1.6.9.0) as reported by He *et al*. (2021). “ProteinGroups” file from MaxQuant was further used in an R-script to perform statistical analyses as described in Schippers *et al*. (2024). Due to the known subcellular localization of MDHAR2, annotated mitochondrial and plastidial proteins were omitted in this analysis. The candidate interacting proteins were filtered for an enrichment ratio >25 and an adjusted *p*-value<0.05. Biological process was assigned to each protein based on its annotation on Thalemine (https://bar.utoronto.ca/thalemine/; Pasha *et al*., 2020). The interaction networks were generated using Cytoscape 3.10.2 (Shannon *et al*., 2003) and the application "Autoannotate" (https://apps.cytoscape.org/apps/autoannotate).

3.2.7 Transcript quantification by RT-qPCR

Total RNA was extracted with the NucleoSpin RNA Plant and Fungi kit (Macherey-Nagel) following the manufacturer's instructions. RNA quality was determined by gel electrophoresis and concentration estimated using a nanodrop spectrophotometer at 260 nm. Reverse transcription and first-strand cDNA synthesis were performed using the ImProm-II™ Reverse Transcriptase (Promega). qPCR was performed according to Queval *et al*. (2009). Transcripts were quantified relative to those of *ACTIN2* and *PP2A* or *ACTIN2* and *UBIQUITIN*. Primer sequences are listed in Supporting Information Table S3.1.

3.2.8 Other analyses

Extractable enzyme activities were measured according to protocols detailed in Noctor *et al*. (2016). Oxidized and reduced forms of glutathione and ascorbate were measured by plate-reader assay as described by Queval & Noctor (2007). Total SA was measured according to the protocol of Chaouch *et al*. (2010). Percentage lesion area on rosette leaves was quantified using ImageJ software.

3.3 Results

3.3.1 Study of loss-of-function mutants under optimal and oxidized conditions

As a first step to exploring the roles of MDHAR isoforms in Arabidopsis, we characterised gene-specific mutants for the two cytosolic and two peroxisome-associated enzymes. Transcript abundance analysis showed that all four mutants were knockouts or severe knockdowns and that effects were specific to each gene (Figure 3.1a). However, with the exception of some delayed early growth in *mdar4* that could be overcome by germinating plants on medium containing sucrose (Eastmond, 2007), all plants showed a phenotype similar to wild-type, with little effect on rosette size (Figure S3.2). Enzyme assays revealed that total extractable leaf NADH-dependent MDHAR activity was substantially decreased in *mdar1* but not in *mdar2*, *mdar3*, or *mdar4* (Figure 3.1b). The NADPH-dependent activity was decreased in *mdar1* and *mdar2*, but unaffected in the other two lines (Figure 3.1b). None of the mutations had a detectable impact on leaf ascorbate or glutathione status, both of which remained largely reduced (Figure 3.1c,d). This suggests that, in standard conditions, where the ascorbate-glutathione pathway is turning over relatively slowly, none of the MDHAR isoforms are irreplaceable for growth and development.

Based on the activities observed in the mutants, MDHAR1 and MDHAR2 are the major players, albeit with different contributions to the NADH- and NADPH-dependent activities. To investigate this point further, the two enzymes were purified as recombinant proteins and their affinities for the two reductant cofactors were determined. Examples of kinetic curves are shown in Supporting Information Figure S3.3 and the data are summarized in Table 3.1. While both enzymes showed a greater predicted catalytic efficiency for NADH compared to NADPH, the difference was much less marked for MDHAR2. While K_{cat} was over 100-fold greater for NADH compared with NADPH in the case of MDHAR1, the difference was only 6-fold for MDHAR2 (Table 3.1).

Table 3.1. Kinetic constants for recombinant MDHAR1 and MDHAR2 with NADH or NADPH as cofactor.

	MDHAR1		MDHAR2	
	NADH	NADPH	NADH	NADPH
V_{max} (µmol.min^{-1}mg^{-1} prot)	3426 ± 82	1119 ± 59	2074 ± 211	906 ± 45
K_M (µM)	8.23 ± 0.71	217 ± 18	3.5 ± 0.34	9.49 ± 0.2
K_{cat} (V_{max}/K_M)	684	4	593	96

Data and standard errors are means of values obtained with three different curves (Figure S3.3). Similar results were obtained with different protein preparations.

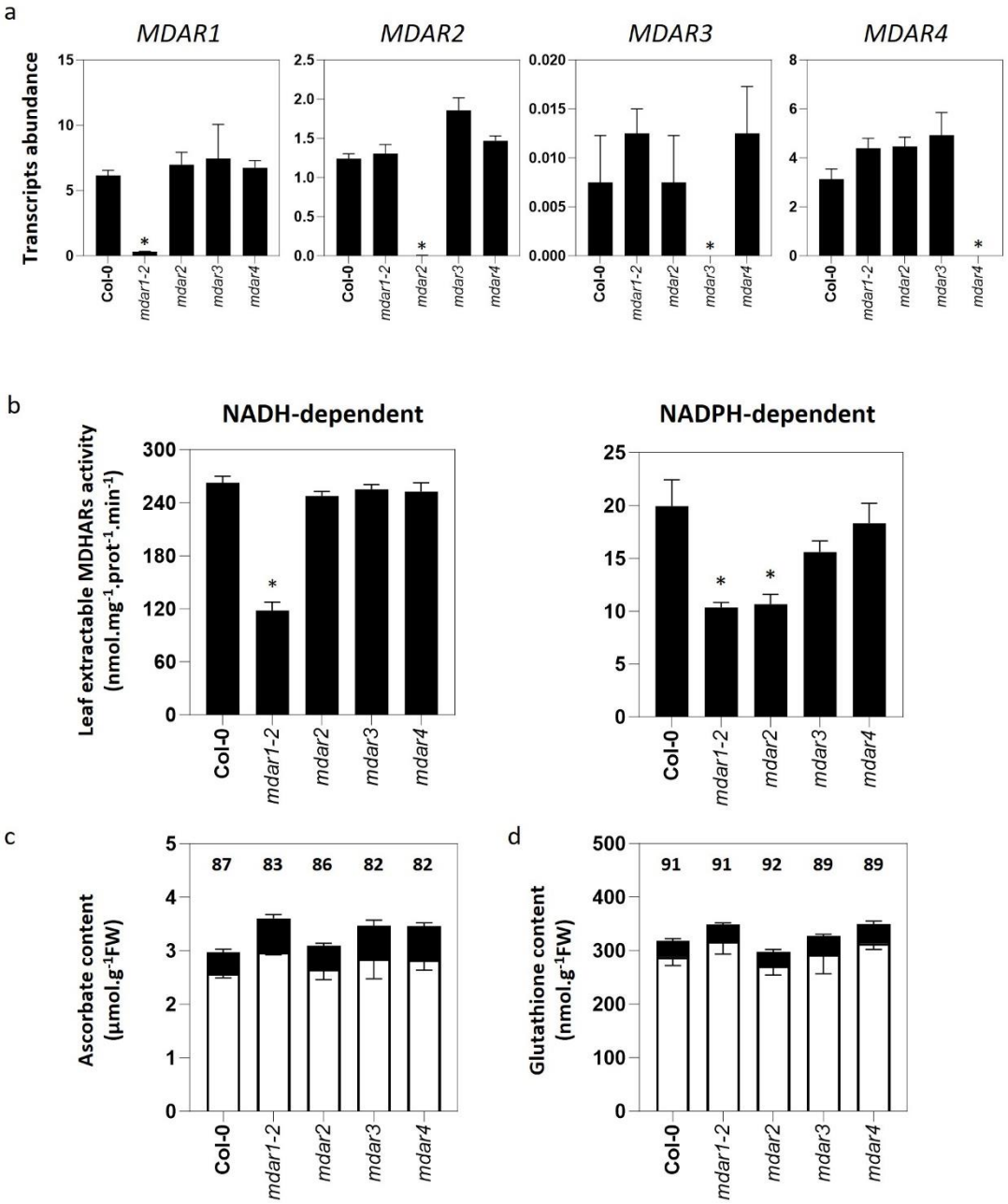

Figure 3.1. Effects of specific *mdar* mutations on expression, extractable activities, and contents of ascorbate and glutathione. a. qRT-PCR analysis of *MDAR* expression in the different lines, normalised to *ACTIN2* and *PP2A*. b. Effects of mutations on NADH and NADPH-dependent activities. c. Ascorbate contents. d. Glutathione contents. For c and d, numbers above the columns indicate percentage reduced (100 x reduced form/total content). Data are means ± SE of three biological replicates. Student's t-test, * Indicates significant differences compared to Col-0 at $P < 0.05$. FW: fresh weight. White bars: ASC or GSH, black bars: DHA or GSSG.

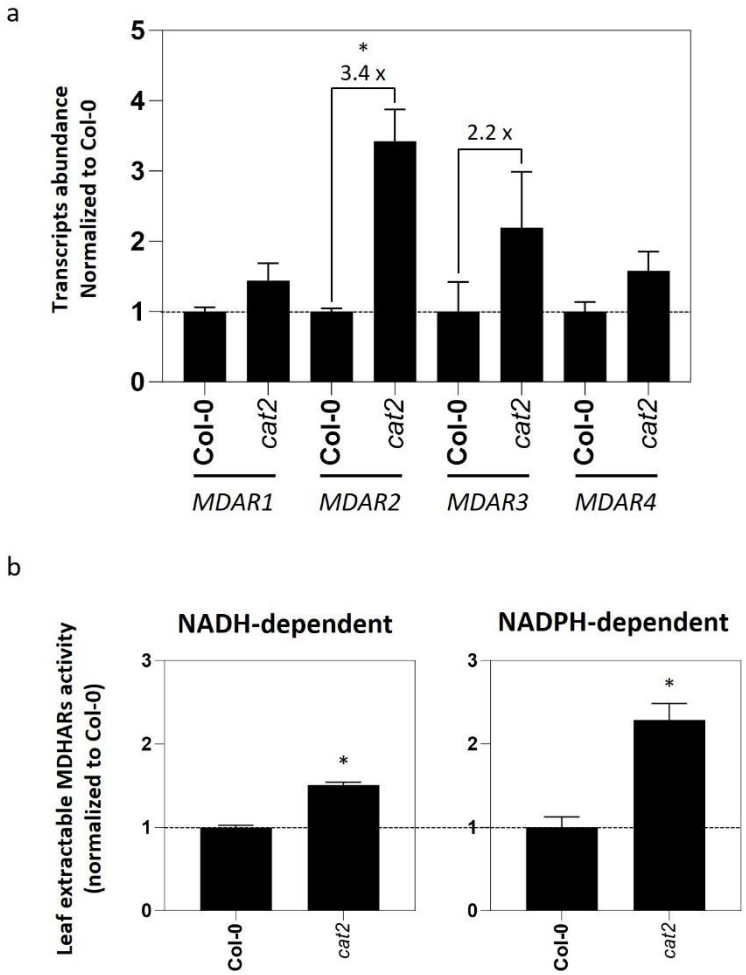

Figure 3.2. Response of *MDAR* expression and MDHAR activities to intracellular oxidative stress in *cat2*. a. Transcripts measured by qRT-PCR. Data were quantified relative to *ACTIN2* and *PP2A*, and then normalised to the Col-0 value. b. NADH- and NADPH-dependent MDHAR activities. Data are means ± SE of three biological replicates. Student's t-test, * Indicates significant difference compared to Col-0 at $P < 0.05$.

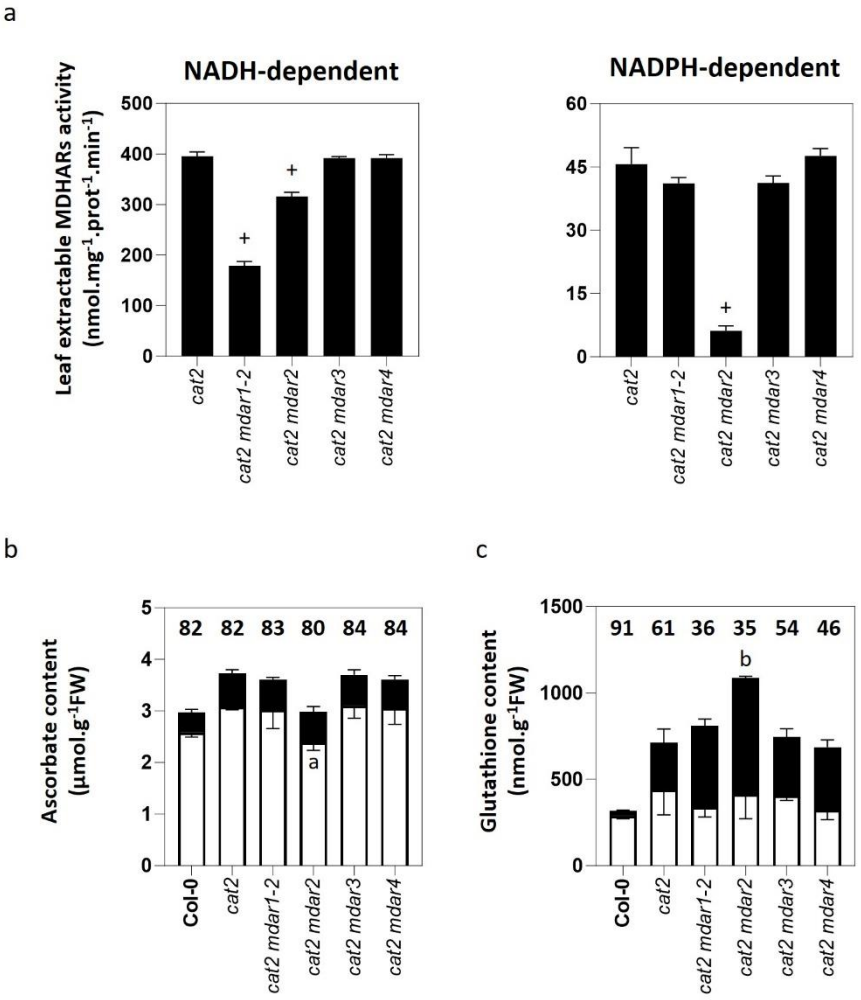

Figure 3.3. Effects of *mdar* mutations on MDHAR activities and contents of ascorbate and glutathione in the *cat2* background. a. NADH- and NADPH-dependent MDHAR activities. b. Ascorbate contents. c. Glutathione contents. Data are means ± SE of three biological replicates. [+]significant differences between double mutants and *cat2* at $P < 0.05$. Numbers above the columns indicate percentage reduced (100 x reduced form/total content). For b and c, white bars: ASC or GSH, black bars: DHA or GSSG. [a]Significant differences in reduced forms between double mutants and *cat2* at $P < 0.05$. [b]Significant differences in oxidized forms between double mutant and *cat2* at $P < 0.05$.

As a first step to testing whether any of the isoforms become functionally important when the ascorbate-glutathione pathway is more highly engaged, *MDAR* expression was compared in the wild-type, Col-0, and the oxidative stress line, *cat2*. Of the four transcripts, only the two cytosolic isoforms were induced by oxidative stress, with the strongest effects observed for *MDAR2* (Figure 3.2a), the more highly expressed of the two forms in leaves (compare *MDAR2* and *MDAR3* transcript levels in

Figure 3.1a). Induction of these two forms was accompanied by enhanced MDHAR in *cat2*, an effect that was stronger for the NADPH-dependent activity (Figure 3.2b).

3.3.2 Effect of *mdar* mutations on *cat2*-triggered salicylic acid (SA) pathway and oxidative stress

To examine the role of the different MDHARs in oxidative stress conditions more directly, each of the mutations was introduced into the *cat2* background to produce double mutants that lacked both most of the leaf catalase activity and one of the MDHAR isoforms. The mutations produced similar effects on the expression of the different *MDAR*s in the *cat2* background to those observed in the Col-0 background (Figure S3.4); ie, each mutation had a strong specific effect on the respective transcript without producing accompanying or compensatory effects on expression of the other *MDAR* genes. Neither *mdar3* nor *mdar4* affected the *cat2*-enhanced MDHAR activity. Most of the NADPH-dependent activity was removed by *mdar2* (Figure 3.3a) while the NADH-dependent activity was decreased in both *mdar1* and, to a lesser extent, *mdar2* (Figure 3.3a). Assays of ascorbate and glutathione in the *cat2* background revealed that *mdar2* produced significant effects on these antioxidant pools: while the effect on reduced ascorbate was slight (Figure 3.3b), a larger impact on glutathione was observed, with the *mdar2* mutation further increasing the accumulation of total and oxidized glutathione observed in *cat2* (Figure 3.3c).

The *cat2* mutation triggers two phenotypic effects. First, rosette growth is decreased compared to Col-0. Second, lesions that are similar to those observed in the hypersensitive response appear spontaneously on the leaves (Chaouch *et al*., 2010). Phenotypic analysis of growth in the double mutants revealed differential effects of the *mdar* mutations on these two effects: while the *cat2*-triggered decrease in growth was exacerbated in *cat2 mdar1* and *cat2 mdar4*, *cat2 mdar2* showed much fewer lesions than *cat2* and the other double mutants (Figure 3.4a,b). Since the *cat2* lesion phenotype is associated with, and dependent on, salicylic acid (SA) accumulation (Chaouch et al., 2010), this phytohormone was quantified, revealing (1) that the single *mdar2* mutants showed similarly low SA contents to those observed in the wild-type and (2) that the enhanced SA contents in *cat2* were largely abolished in *cat2 mdar2* (Figure 3.4c). Analyses of the expression of SA marker genes (*PR1*, *PR2*, *PR5*) and *ICS1*, encoding a key enzyme in SA synthesis, produced a similar pattern; ie, induction of the SA markers in *cat2* was compromised by the presence of the *mdar2* mutation but less so by loss of the other *MDAR* functions (Figure 3.4d).

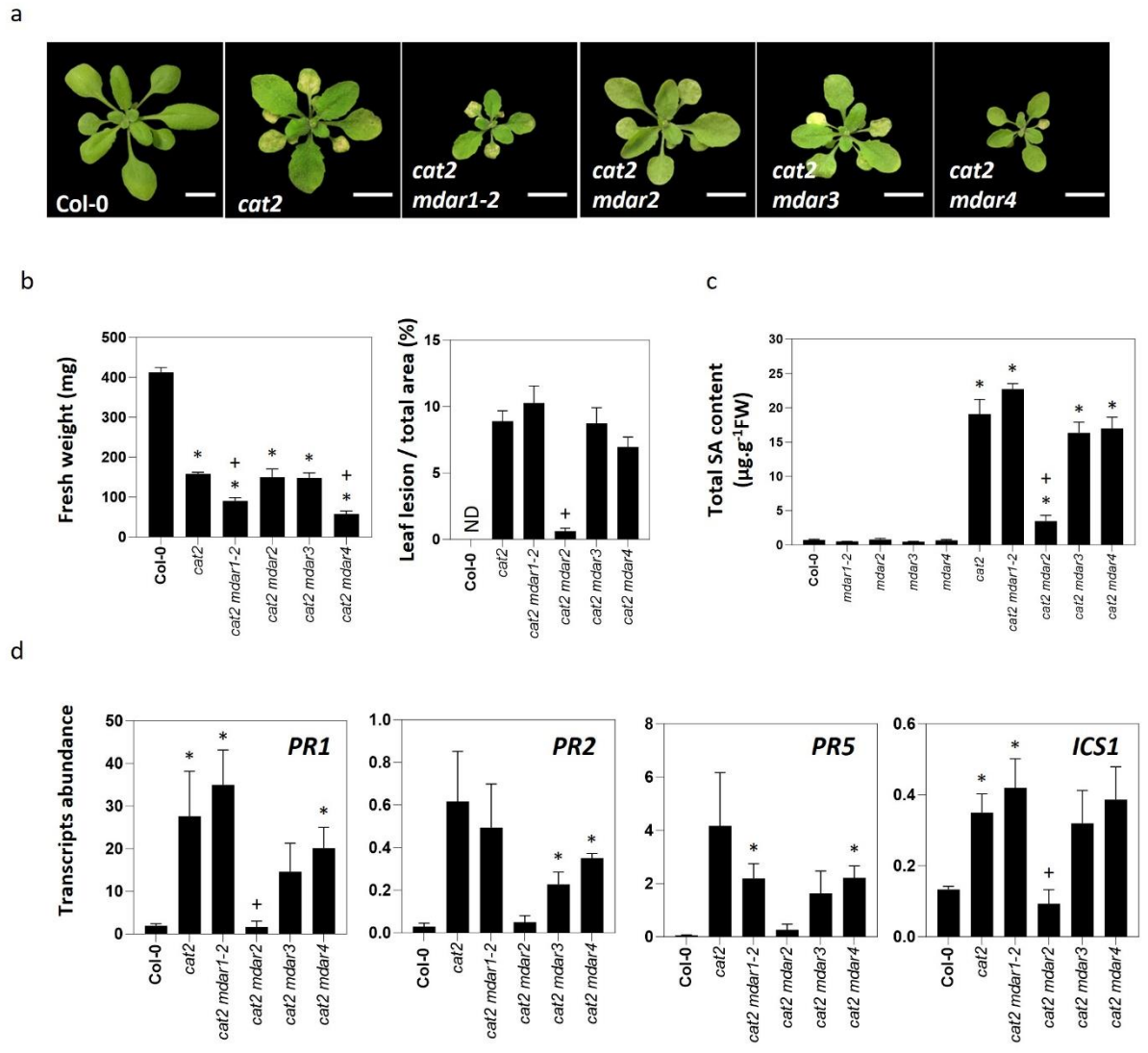

Figure 3.4. Effect of *mdar* mutations on the *cat2* phenotype and the SA pathway. a. Photographs of rosettes. b. Fresh weight and lesion quantification. Data are means ± SE of 10 plants. c. SA contents. d. *PR* gene expression, data were quantified relative to *ACTIN2* and *PP2A*. Data are means ± SE of three biological replicates. Student's t-test, *Significant difference compared to Col-0 at $P < 0.05$. $^{+}$Significant differences of double mutants compared with *cat2* at $P < 0.05$. Bars = 1 cm. ND: not detected.

The effects of the *mdar2* mutation on *cat2*-triggered SA signaling recall those reported in previous studies in which other components of the ascorbate-glutathione pathway were disabled, notably observations in a *cat2 dhar1 dhar2 dhar3* quadruple mutant, in which all three DHAR-encoding gene functions are lost (Rahantaniaina et al., 2017). Transcriptomic analysis was performed to investigate the effect of the *mdar2* mutation on *cat2* responses in more detail, and the *cat2 dhar1 dhar2 dhar3*

line was included for comparison (Figure 3.5). Approximately 1500 genes were differentially expressed between Col-0 and *cat2*. The transcriptomic impact of the *cat2* mutation was generally lessened by the presence of additional mutations in *MDAR2* or the three *DHARs* (Figure 3.5). The modulating effect of the additional mutations was particularly clear for genes that were induced in *cat2* compared to Col-0, with the clearest effects being observed in cluster 4 (Figure 3.5a, C4), which was enriched in genes involved in cell death, systemic acquired resistance, SA responses, and related processes. Analysis of the expression levels of the most strongly induced genes in *cat2* revealed that loss of function of *MDAR2* or the three DHARs produced a similar dampening effect on these genes (Figure 3.5b).

3.3.3 Study of *cat2 mdar2* MDHAR2 complemented lines to confirm the specific roles of MDHAR2

Together with the data in Figure 3.4, this expression analysis provides evidence that a functional MDHAR2 is required to mediate some of the downstream signaling responses triggered by oxidative stress in *cat2*. To confirm this point, we sought to increase MDHAR activity in the *cat2 mdar2* line by introducing the wild-type MDHAR2 linked to GFP in C- or N-terminal. Fluorescence analyses confirmed the cytosolic location of MDHAR2 (Figure 3.6a). Based on anti-GFP antibody tests and *MDAR2* transcript analyses, one line of each construct was chosen in which *MDAR2* expression was restored to at least the level observed in *cat2* (Figure 3.6b,c). In these lines, the NADH-dependent MDHAR activity was similar to or somewhat higher than in *cat2 mdar2* (Figure 3.6d, left). A clearer effect was seen on the NADPH-dependent activity, which was induced in *cat2*, undetectable in *cat2 mdar2*, and restored to the *cat2* level or above in the complemented lines (Figure 3.6d, right). While ascorbate contents were similar in all lines (Figure 3.6e), the increased MDHAR activity in the complemented lines reversed the very high glutathione contents and oxidation state observed in *cat2 mdar2*. Restoration of *MDAR2* expression caused glutathione contents and oxidation state to return to the *cat2* level or below (Figure 3.6f), effects that correlated with the extractable NADPH-dependent MDHAR activity (Figure 3.6d, right).

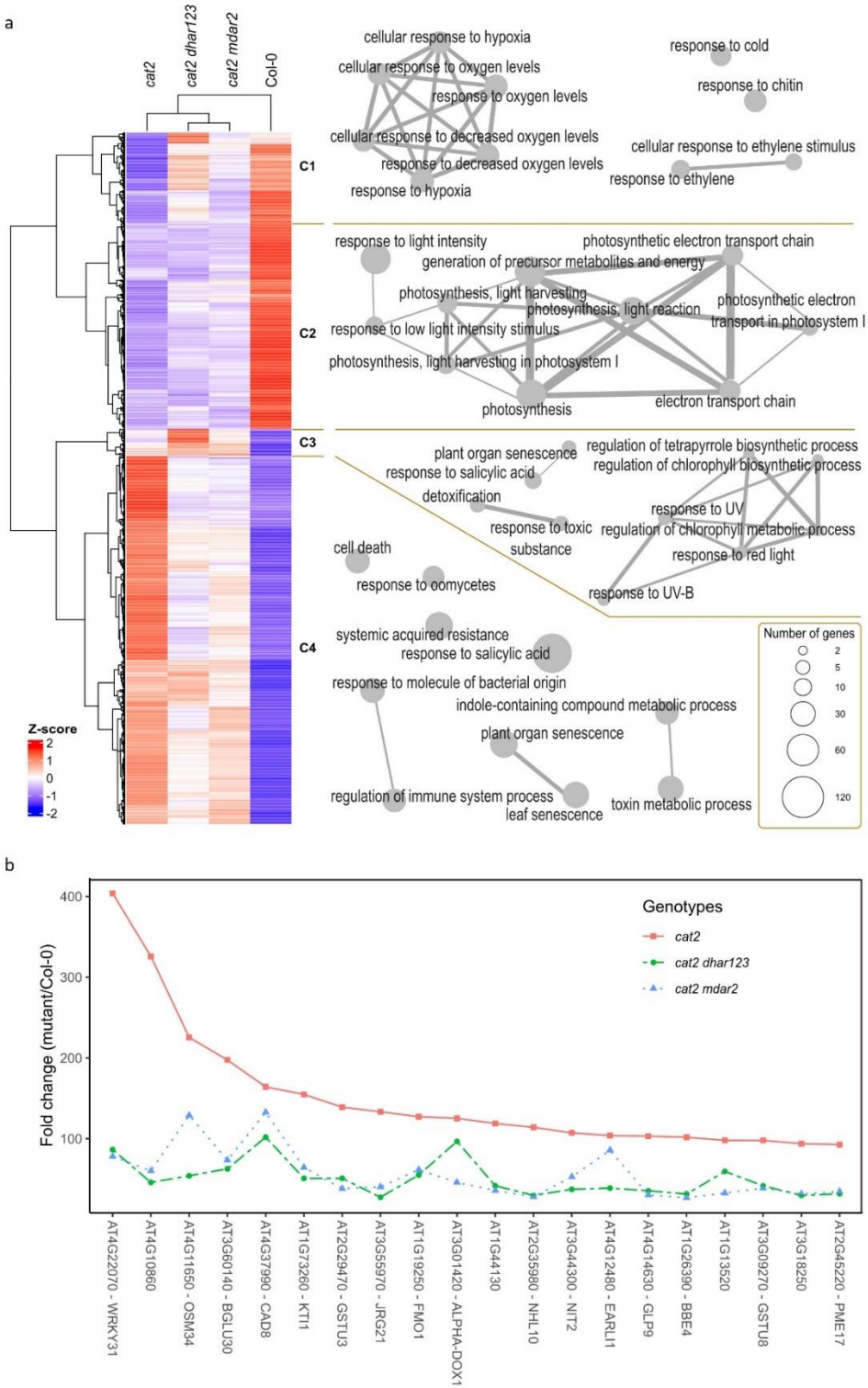

Figure 3.5. Transcriptomic analysis of *cat2*, *cat2 mdar2*, and *cat2 dhar1 dhar2 dhar3*. a. Heatmap showing normalized expression (Z-score of CPM) of the 1521 differentially expressed genes between Col-0 and *cat2* (FDR<0.01 & $|\log_2 FC|>1$). The top 10 of Biological Process GO enrichment for each of the 4 clusters is displayed on the right (p-adjust<0.05). The circle size corresponds to the number of DEGs responsible for the enrichment. A joining line indicates a link between GO terms. b. Effects of secondary mutations in ascorbate regeneration on the 20 genes with the highest fold change for *cat2* compared to Col-0. The fold change is calculated using mean CPM and Col-0 as reference.

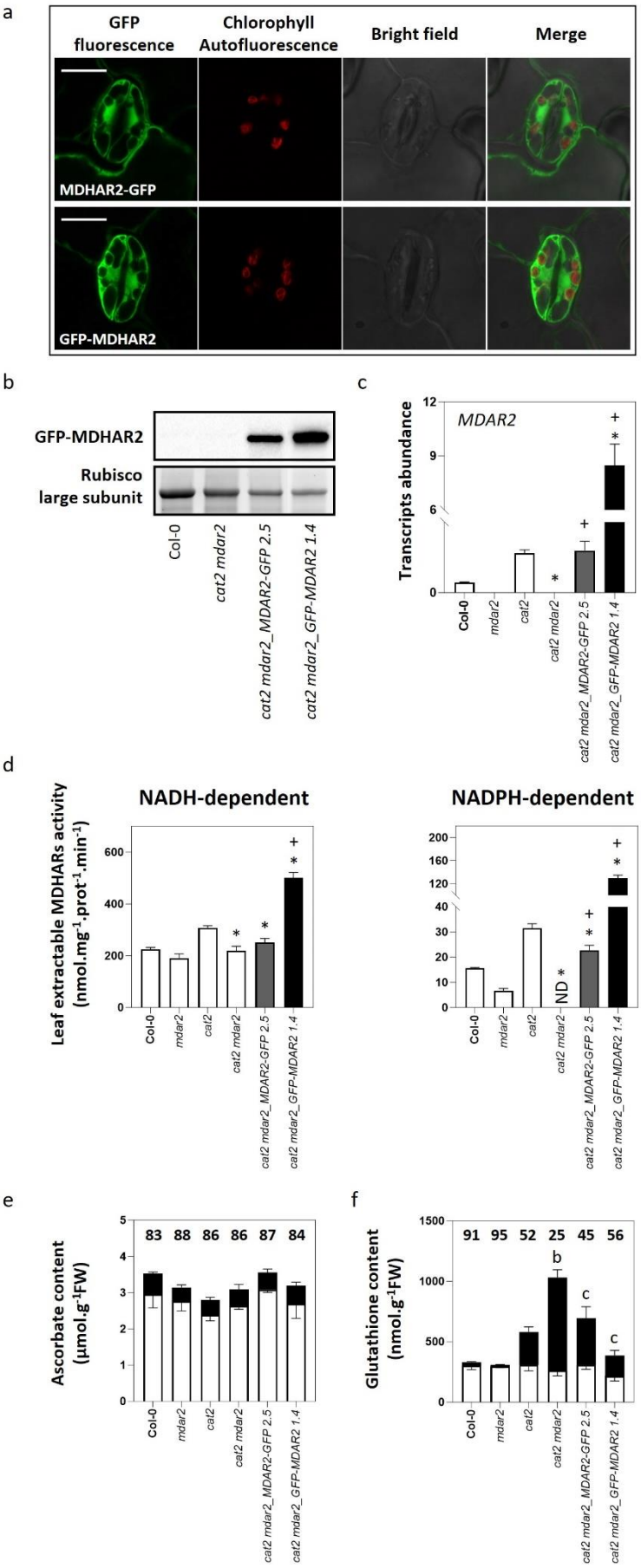
a
GFP fluorescence
Chlorophyll Autofluorescence
Bright field
Merge
MDHAR2-GFP
GFP-MDHAR2
b
GFP-MDHAR2
Rubisco large subunit
Col-0
cat2 mdar2
cat2 mdar2_MDAR2-GFP 2.5
cat2 mdar2_GFP-MDAR2 1.4
c
MDAR2
Transcripts abundance
d
NADH-dependent
NADPH-dependent
Leaf extractable MDHARs activity (nmol.mg-1.prot-1.min-1)
ND
e
Ascorbate content (µmol.g-1FW)
83 88 86 86 87 84
f
Glutathione content (nmol.g-1FW)
91 95 52 25 45 56
b
c
c

Figure 3.6. Complementation of *cat2 mdar2* with GFP-MDAR2. a. GFP analysis of subcellular localisation of MDHAR2. The bar indicates 10 µm. b. Verification of *MDAR2* expression in the complemented lines using an anti-GFP antibody. c. Verification of complemented *MDAR2* transcripts, data were quantified relative to *ACTIN2* and *Ubiquitin*. d. Effects on MDHAR activities. e. Effects on ascorbate contents. f. Effects on glutathione contents. Data are means ± SE of three biological replicates. *Significant difference compared to *cat2* at $P < 0.05$. $^{+}$Significant differences of complemented lines compared with *cat2 mdar2* at $P < 0.05$. For c and d, the white columns represent untransformed lines, the grey column represents the C-terminal transformed line, and the black column represents the N-terminal transformed line. ND: not detected. In e and f, ^{b} indicates significant differences of oxidized forms in the double mutant compared with *cat2* at $P < 0.05$ and ^{c} indicates significant differences in oxidized forms of MDHAR2 complemented lines compared with *cat2 mdar2* at $P < 0.05$.

In the two complemented lines, leaf lesions were also restored to the *cat2* level (Figure 3.7a,b). This effect was accompanied by increased SA contents (Figure 3.7c) and SA marker transcripts (Figure 3.7d). We also examined three genes associated with JA signaling: although effects were less clear compared to the SA pathway, *PFD1.2* and *VSP2* were both induced in *cat2*, much less in *cat2 mdar2*, and restored in the complemented lines (Figure 3.7e).

An anti-GFP pulldown strategy was implemented to identify proteins interacting with MDHAR2 fused to GFP, as described in Wendrich *et al*. (2017), in the *cat2 mdar2* mutant background. This analysis identified more than 100 proteins that could be grouped into different functional categories (Figure 3.8). Among potential interactants were proteins involved in regulating gene expression and in several areas of primary metabolism, including photorespiration and glycolysis (Figure 3.8). These proteins included glycolytic glyceraldehyde 3-phosphate dehydrogenase, NADP-malic enzyme 2 (NADP-ME2), and isocitrate dehydrogenase (NADP-ICDH), cytosolic enzymes involved in NADH or NADPH production. Other notable groups of potential interactants included other redox-related proteins and several proteins involved in biotic stress responses (Figure 3.8).

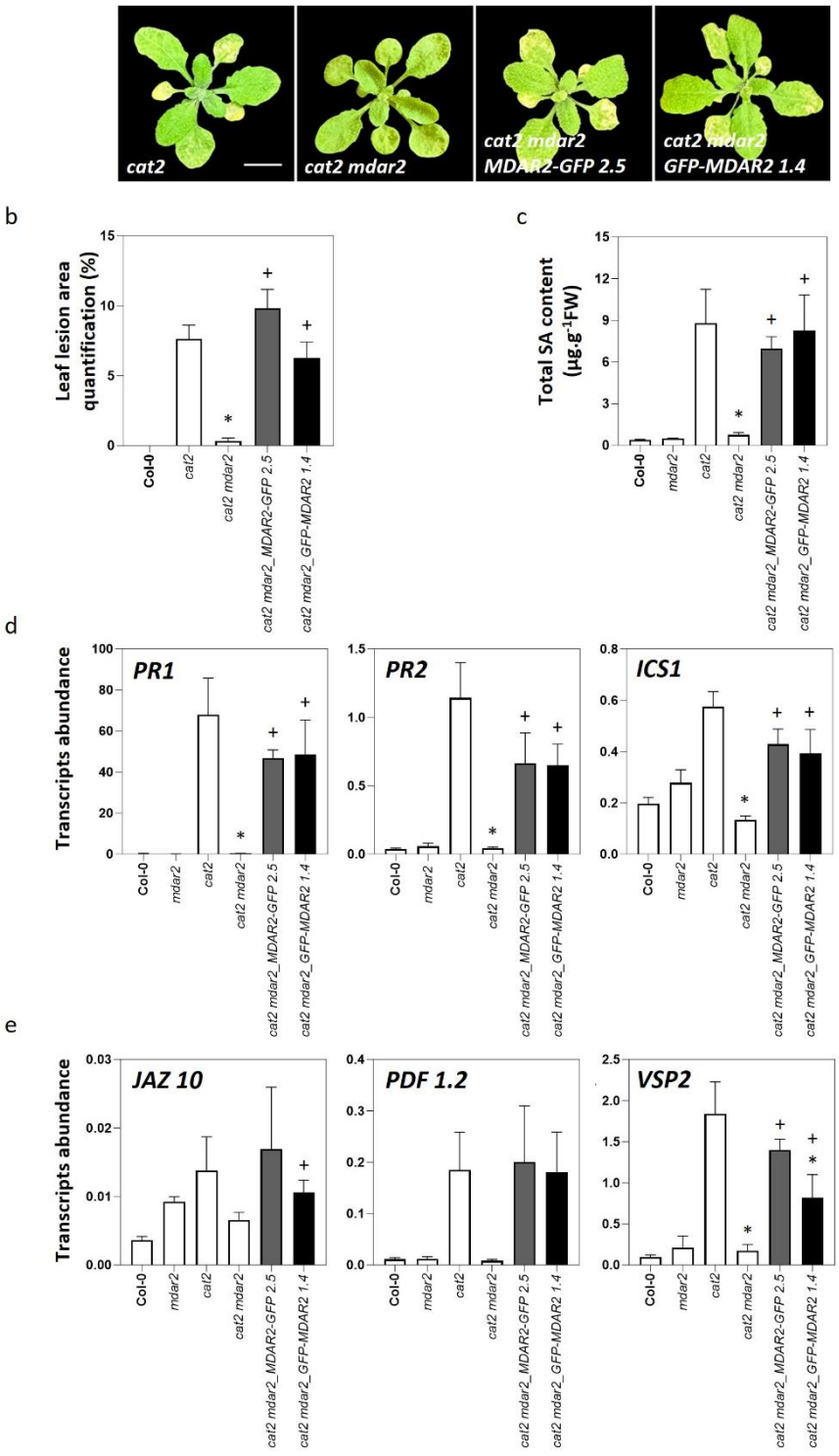

Figure 3.7. Complementation of *cat2 mdar2* with GFP-MDAR2 restores the *cat2* lesion phenotype and pathogenesis-related pathways. a. Phenotypes of complemented lines. b. Leaf lesion area quantification. c. SA contents. d. SA-related gene expression. e. JA-related gene expression. Data were quantified relative to *ACTIN2* and *Ubiquitin*. The white columns represent untransformed lines, the grey column represents the C-terminal transformed line, and the black column represents the N-terminal transformed line. *Significant difference compared to *cat2* at $P < 0.05$. $^{+}$Significant differences of complemented lines compared with *cat2 mdar2* at $P < 0.05$.

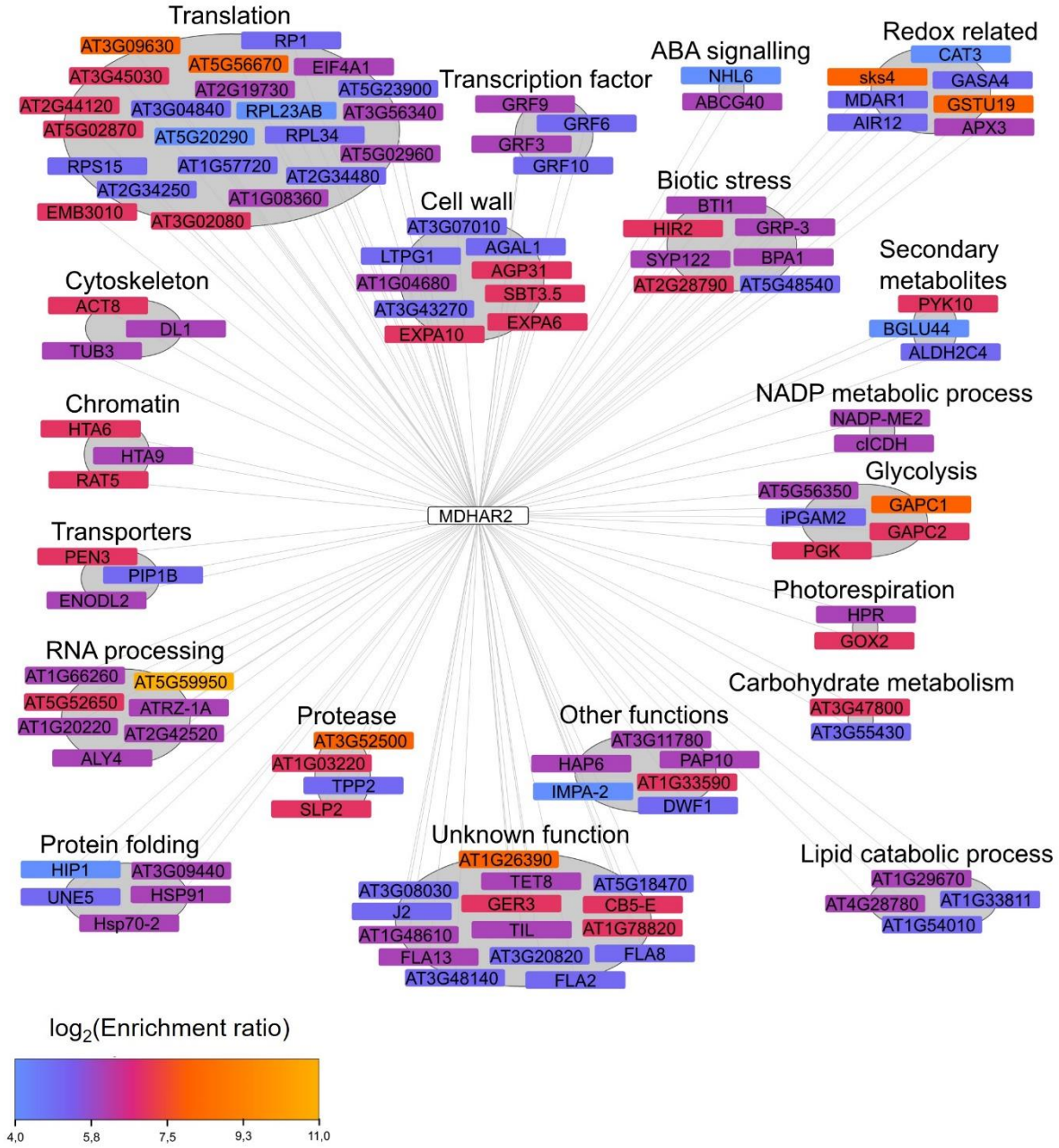

Figure 3.8. Overview of immunoprecipitation–mass spectrometry (IP-MS) search for protein interactants in *cat2 mdar2* MDAR2-GFP. The interactants shown have an enrichment ratio >25 and a p-value < 0.05. Proteins are grouped by biological processes. The box colour corresponds to the $\log_2$(enrichment ratio) with MDHAR2 protein.

3.4 Discussion

Our aim in this study was to assess the roles of specific MDHARs in optimal and oxidative stress conditions. Observations in single *mdar* mutants grown in our conditions are consistent with a previous report, notably in showing that none of the enzymes appears to be necessary for plant growth (Tanaka et al., 2021). However, when introduced into an oxidative stress background, the importance of certain MDHARs becomes more apparent. First, loss of the peroxisomal functions somewhat exacerbated the *cat2* dwarf phenotype. This is perhaps not surprising since the major role of CAT2 is to metabolise photorespiratory H_2O_2, which is predominantly produced in the peroxisomes (Yang et al., 2019). It is noteworthy, however, that the *mdar1* and *mdar4* mutations were not associated with altered ascorbate or glutathione status, either in the single mutants relative to Col-0 or in the double mutants relative to *cat2*. Only the *mdar2* mutation produced a significant effect on these pools (in *cat2 mdar2*) and it was this mutation that, in removing most of the leaf lesions triggered by catalase deficiency, produced the most interesting effect: rather than exacerbating transcriptomes and phenotype triggered by oxidative stress, loss of this secondary antioxidative function acted to oppose them. Below we discuss some of the conclusions that can be drawn from this study.

3.4.1 The cytosolic ascorbate-glutathione pathway is important in linking oxidative stress to phytohormone signaling

We previously reported that loss-of-function mutants for other cytosolic enzymes of the ascorbate-glutathione pathway (GR1, DHAR1, DHAR2) showed a wild-type phenotype but modulated the response to oxidative stress observed in response to catalase deficiency (Mhamdi *et al*., 2010b; Rahantaniaina *et al*., 2017). However, unequivocal conclusions on the importance of compartmentation were difficult to draw from these earlier analyses because GR1 is found in the peroxisomes as well as the cytosol (Kataya & Reumann, 2010) and it is not clear whether or not the peroxisomes contain DHAR. In the present study, we have been able to compare the importance of MDHARs located specifically in the two compartments in oxidative stress responses. Although loss of the peroxisomal *MDAR1* and *MDAR4* functions somewhat exacerbated the dwarf phenotype associated with the *cat2* mutation, it is the *mdar2* mutation that most influenced the *cat2* lesion phenotype, and this was associated with markedly decreased activation of the SA pathway. Thus, the cytosolic ascorbate-glutathione pathway appears to be a key player in transmission of oxidative stress signals that originate in other compartments. This is consistent with gene expression patterns in *cat2*, where the cytosolic but not the peroxisomal isoforms of MDHAR were up-regulated (Figure 3.2).

Although the results are not necessarily easy to compare, because of different growth conditions, an important role for the cytosol is consistent with previous reports on *apx1* mutants (Davletova *et al*., 2005; Vanderauwera *et al*., 2011). It should be noted that although CAT2 is mainly located in peroxisomes, the protein can also be located in other compartments, including the nucleus (Al-Hajaya *et al*., 2022), although the extent of ROS production in this compartment compared to the peroxisomes is unclear. It is likely that in the absence of CAT2, some H_2O_2 can move from these compartments into the cytosol, where it can be metabolised by APX, engaging downstream cytosolic enzymes such as MDHAR, DHAR, and GR (Mhamdi *et al*., 2010a).

3.4.2 Cytosolic MDHAR2 is the major contributor to NADPH-dependent activity in Arabidopsis leaves

In agreement with previous data (Tanaka *et al*., 2021), our analyses suggest that peroxisomal MDHAR1 and cytosolic MDHAR2 are major isoforms in Arabidopsis leaves. MDHAR activity can be supported by either NADH or NADPH, and insight into co-factor preference is important to situate the enzymes within their metabolic context. Both total extractable leaf MDHAR and recombinant MDHAR activities are higher with NADH. However, in addition to their differences in subcellular localization, the data show that MDHAR1 and MDHAR2 make different contributions to the activities with the two reductants (Figure 3.1, Figure 3.3, Table 3.1). The activity assays performed on recombinant proteins suggest that MDHAR1 will mainly use NADH *in vivo*, as the catalytic efficiency with NADPH is much lower. The preference of MDHAR2 is less clear. The K_M values for the two co-factors were much more similar than for MDHAR1 and well below the concentrations used in our standard assays of extractable leaf activity. This suggests that the *mdar2* mutation should have a similar effect on the NADH- and NADPH-dependent activities measured *in vitro*, at saturating co-factor concentrations. Our data are consistent with this: in the Col-0 background, the *mdar2* mutation decreased the extractable NADPH-dependent activity by about 10 $nmol.mg^{-1}prot.min^{-1}$, which corresponds to about 50% of the total activity with this co-factor (Figure 3.1b). Against the background of the much higher total activities of NADH-dependent activity, a decrease of this magnitude is harder to detect (in fact, slight but statistically insignificant decreases in NADH-dependent activity of this order can be observed in *mdar2*; Figure 3.1b). In the *cat2* background, where *MDAR2* is induced at both the transcript level and the total extractable activities are increased, the *mdar2* mutation affects both extractable activities, decreasing the NADPH-dependent activity by about 40 $nmol.mg^{-1}prot.min^{-1}$ and the NADH-dependent activity by a similar or greater value (Figure 3.3). Again, the higher total extractable activity of NADH-dependent activity makes the proportional impact of the *mdar2* mutation on the NADPH-dependent

activity more evident (Figure 3.3). A key point for placing these observations in their physiological context is that NADH concentrations in the cytosol, where MDHAR2 is located, are thought to be very low (at or below 1 µM; Heineke et al., 1991). This means that the extractable activities measured at 250 µM are likely to be markedly over-estimating the cytosolic NADH-dependent activity *in vivo*. If so, the enhanced engagement of the ascorbate-glutathione pathway in *cat2* might draw mainly on cytosolic NADPH, to support MDHAR2 and also the cytosolic GR previously shown to be important in oxidative stress responses in this context (Mhamdi *et al*., 2010b). The refinement of fluorescent probes that can measure concentrations of these cofactors *in situ* could throw further light on this question.

Observations from the GFP pulldown experiments suggest that interactions with other proteins might also be part of the biological functions of MDHAR2. In addition to proteins whose functional connections to MDHAR2 remain to be elucidated, several enzymes were identified that are linked in terms of antioxidant or other redox function. Notably, cytosolic enzymes involved in glycolysis (PGK, GAPC) or NADPH production (NADP-ME2, cICDH) were found to bind to MDHAR2 (Figure 3.8). The importance of NADP-isocitrate dehydrogenase and NADP-malic enzyme 2 functions have previously been examined in the *cat2* background (Mhamdi *et al*., 2010c; Li *et al*., 2013) and the latter enzyme has been implicated in with pathogenesis-related responses (Voll *et al*., 2012). Further, loss of *nadp-icdh* function in *cat2* slightly modulates biotic stress responses triggered by oxidative stress (Mhamdi *et al*., 2010c), although much less strongly than the *mdar2* mutation.

Since the pulldown experiments were performed in the complemented *cat2 mdar2* double mutant, it is possible that some of the interactions might be dependent on strong expression triggered by oxidative stress, and therefore become particularly important in this condition. However, a search of the RNA seq data for the genes corresponding to the potential interactants did not reveal any clear pattern, with some transcripts being down-regulated in *cat2* and others unchanged or up-regulated. In any case, the presence of several interactants involved in biotic stress responses underscores the potential role of MDHAR2 in linking oxidative stress management to the activation of pathogenesis-related responses.

3.4.3 Decreased MDHAR capacity affects glutathione but not ascorbate status during oxidative stress

It is striking that none of the mutations produced marked effects on the ascorbate pool and redox status, at least as measured globally in leaf extracts. The only significant effect was in *cat2 mdar2*, in

which a modest decrease in ascorbate was sometimes but not consistently observed (Figure 3.3b, Figure 3.6e). Maintenance of the ascorbate pool, even during the combined absence of CAT2 and MDHAR2, probably reflects the numerous pathways by which this molecule can be regenerated from both MDHA and DHA in plants, as well as the relatively positive redox potential of ascorbate compared to more powerful reductants such as glutathione, NAD(P)H, glutaredoxins, and thioredoxins (Foyer & Noctor, 2016).

In contrast to the stability of the ascorbate pool, a consistent and specific effect of *MDAR2* expression level and activity on glutathione was observed (Figure 3.3c, Figure 3.6f). This is probably explainable by two effects. First, MDHAR capacity is inversely correlated with the formation of DHA, the main driver for glutathione oxidation (Rahantaniaina *et al*., 2017; Tuzet *et al*., 2019), and so decreased MDHAR activity is predicted to accelerate DHA formation, driving faster oxidation of GSH and accumulation of GSSG (Figure 3.9). Second, a substantial part of the GSSG that accumulates in *cat2* is located in the vacuole, where it is protected from immediate re-reduction (Queval *et al*., 2011).

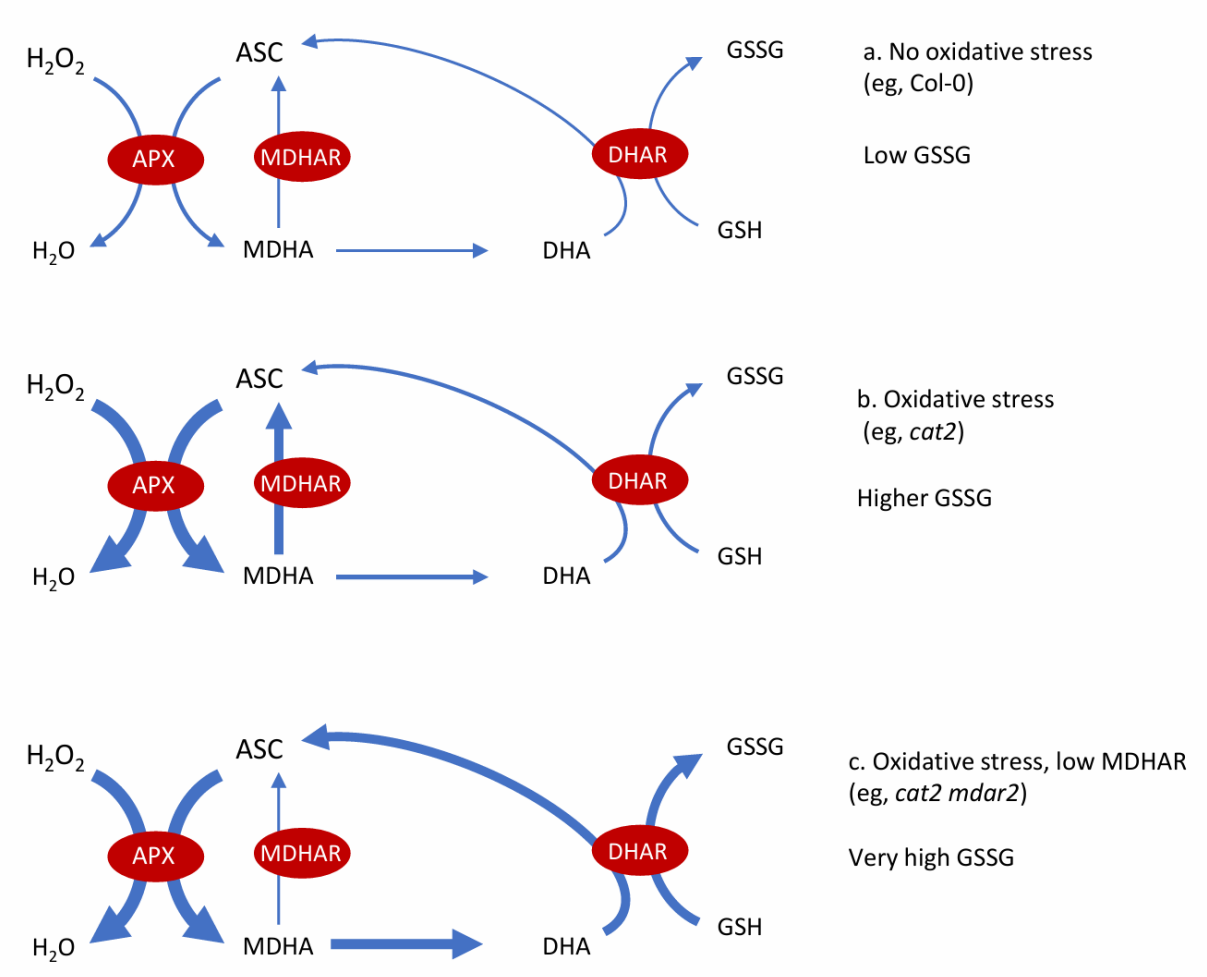

Figure 3.9. Impact of oxidative stress and MDHAR capacity on measured glutathione status. In conditions where H_2O_2 can be largely removed by catalase (a), flux through the ascorbate and glutathione pools is low and glutathione remains highly reduced. When catalase is decreased (b), flux through the ascorbate pool is increased, causing accelerated formation of both MDHA and DHA, with the latter engaging the glutathione pool, leading to GSSG accumulation. When flux is high and MDHAR is decreased (c), conversion of MDHA to DHA is increased compared to b and the glutathione pool is further engaged, leading to even higher GSSG accumulation. Note that the pathway is shown in simplified form and that reactions are not shown stoichiometrically.

3.4.4 Possible mechanisms to explain the influence of MDHAR2

While other pathways exist in plants, catalase and the ascorbate-glutathione pathway can be considered as important H_2O_2-processing systems acting in parallel. Given this, perhaps the most striking of our observations is that loss of cytosolic *MDAR2* function does not exacerbate *cat2* phenotypes but instead partly reverts them. This is not the first observation of this type. In both tobacco and Arabidopsis, decreasing APX and catalase expression produced phenotypes that were less severe than in plants lacking only one of the enzymes (Rizhsky et al., 2002; Vanderauwera et al., 2011). While differences in experimental protocols and growth regimes make it difficult to compare our studies with these previous ones, some of the mechanisms could be common. In Arabidopsis lines doubly deficient in catalase and APX, an ameliorated phenotype was associated with induction of a DNA repair pathway that was not activated in plants lacking only one of the enzymes (Vanderauwera et al., 2011). Hence, we queried our transcriptomics data for the response of genes involved in such DNA repair pathways. However, they provide little evidence that this can explain the effect of *mdar2* on *cat2*-triggered responses in the growth conditions of moderate irradiance we have used here.

What is the nature of the MDHAR-related signal that seems to be important to link oxidative stress to downstream signaling? One possibility is that it involves altered status of glutathione, an influential player in pathogenesis-related responses (Noctor *et al*., 2024). Based on the overlapping impacts of the *dhar* and *mdar* mutations on pathways related to biotic stress (Figure 3.5), a simple role for glutathione status seems unlikely: whereas *dhar* mutations antagonize both *cat2*-triggered glutathione oxidation and SA accumulation (Rahantaniana *et al*., 2017), the *mdar2* mutation antagonizes SA accumulation but promotes glutathione oxidation (Figures 3.3c, 3.4c, 3.6f and 3.7c). Nevertheless, we cannot exclude that altered glutathione status affects the GSNO/GSNO reductase system, which plays a role in oxidative stress responses in *cat2* (Zhang *et al*., 2020). A further possibility is that MDHAR2 acts to catalyse ROS production in a secondary reaction, similar to the mitochondrial MDHAR5, which promotes sensitivity to certain xenobiotics in this way (Johnston *et al*., 2015). Based on available knowledge, this could require a sensitizing redox-cycling metabolite, with which MDHAR2 would interact, to accumulate during oxidative stress. In this connection, it should be noted that we have previously used different techniques to attempt to quantify ROS, including H_2O_2, in *cat2* and derived lines. However, signals were consistently found to be variable and not greatly different from the wild-type, even under conditions in which *cat2* plants are clearly undergoing oxidative stress (Queval *et al*., 2008; Mhamdi *et al*., 2010b; Yang *et al*., 2019). Similarly, we have invested effort in developing lines expressing roGFP and similar probes, but gene silencing in mutant backgrounds and

the difficulty of measuring signals in the mesophyll cells of mature leaves have prevented progress with these measurements.

Finally, given the similarity of the effects of the *mdar2* and *dhar* mutations on oxidative stress-triggered responses (Figure 3.5), one other hypothesis is that accumulation of oxidized forms of ascorbate in the cytosol might interlink with key regulators in phytohormone or other signaling pathways. Ascorbate-deficient mutants show some spontaneous activation of SA-related pathogenesis-related pathways (Pastori *et al*., 2003; Pavet *et al*., 2005) and attention has been drawn to the potential importance of ascorbate oxidase (which produces MDHA) in influencing defence and phytohormone signaling (Pignocci *et al*., 2006). Such observations are often interpreted in terms of the roles of ascorbate as a redox buffer or indirect effects on ROS contents. However, plants with decreased ascorbate might be expected to have lower MDHA and DHA (by adjustment of the equilibrium between ascorbate, DHA, and MDHA). Similarly, loss of DHAR function might also boost MDHA concentrations as a secondary effect. If either of the two oxidized forms of ascorbate is capable of binding to signal transduction proteins to interfere with biotic stress responses, such interactions might explain some of our observations in this work and those previously reported in other plants with alterations in ascorbate contents or metabolism. While this notion remains entirely hypothetical, such effects would add greater subtlety to the influence of the ascorbate-glutathione pathway on cellular function: cell signaling could be impacted not only by the capacity of the pathway to remove ROS themselves but also by ROS-mediated effects on the concentrations of pathway intermediates.

Acknowledgments

Dongdong Xu and Zheng Yang were supported by PhD grants from the China Scholarship Council. Lug Trémulot is supported by a PhD grant from the Université Paris Saclay and MESRI (Ministère de l'Enseignement Supérieur, de la Recherche, et de l'Innovation), France. The GN laboratory received financial support from the French Agence Nationale de la Recherche HIPATH project (ANR-17-CE20-0025) and the Institut Universitaire de France (IUF). The FVB laboratory is supported in part by the Research Foundation Flanders (FWO) (The Excellence of Science [EOS] Research project 869 30829584), and NUCLEOX (grant number G007723N).

Author contributions

D.X., Z.Y., G.C-I. produced, characterized and analysed the mutants and transgenic lines. L.T., A.M., L.M. and F.V.B. contributed analysis of transcriptomics and proteomics data. G.N. H.V. and E.I-B. conceived the project, supervised experimental work, and interpreted data. Together with input from co-authors, G.N. wrote the manuscript.

Supplemental Data

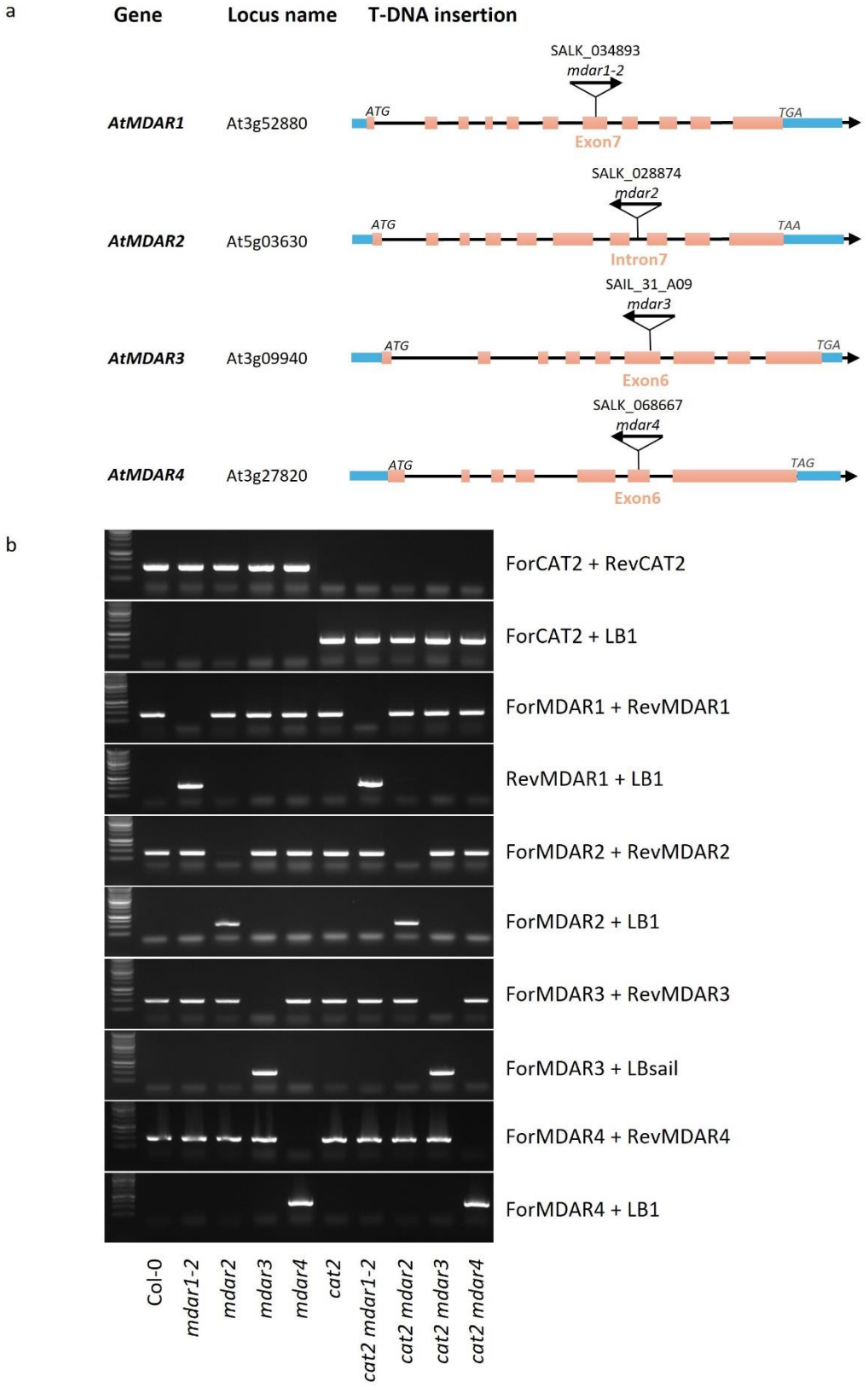

Supporting Information Figure S3.1. Gene maps and genotyping of *mdar* mutants.

Supporting Information Figure S3.2. Photographs of *mdar* mutants and rosette fresh weights

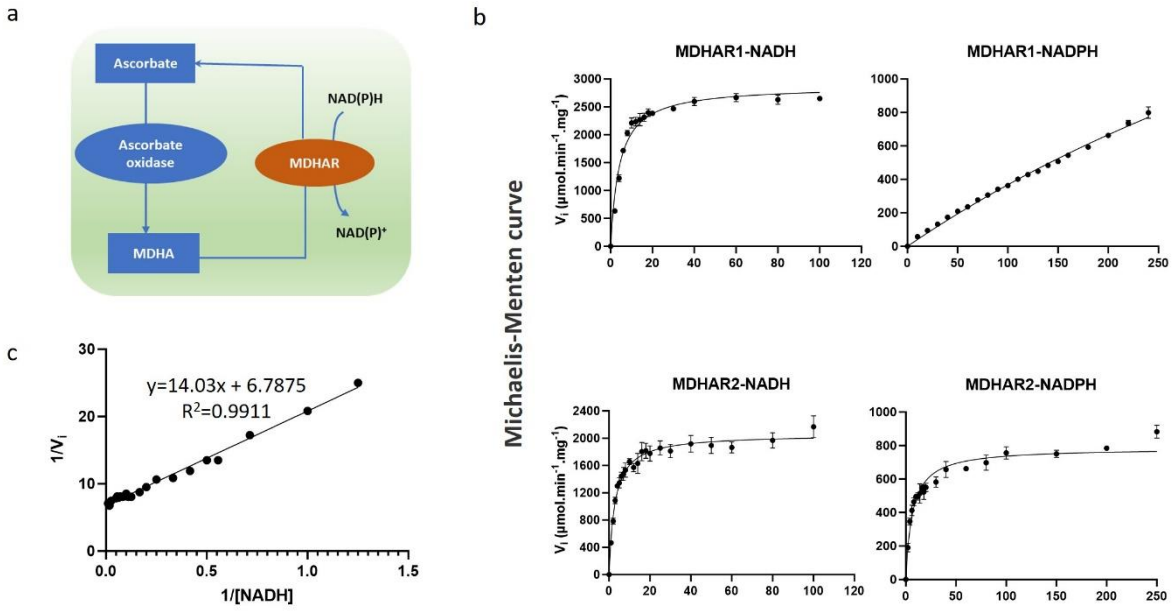

Supporting Information Figure S3.3. Kinetic curves for MDHAR activity of recombinant proteins.

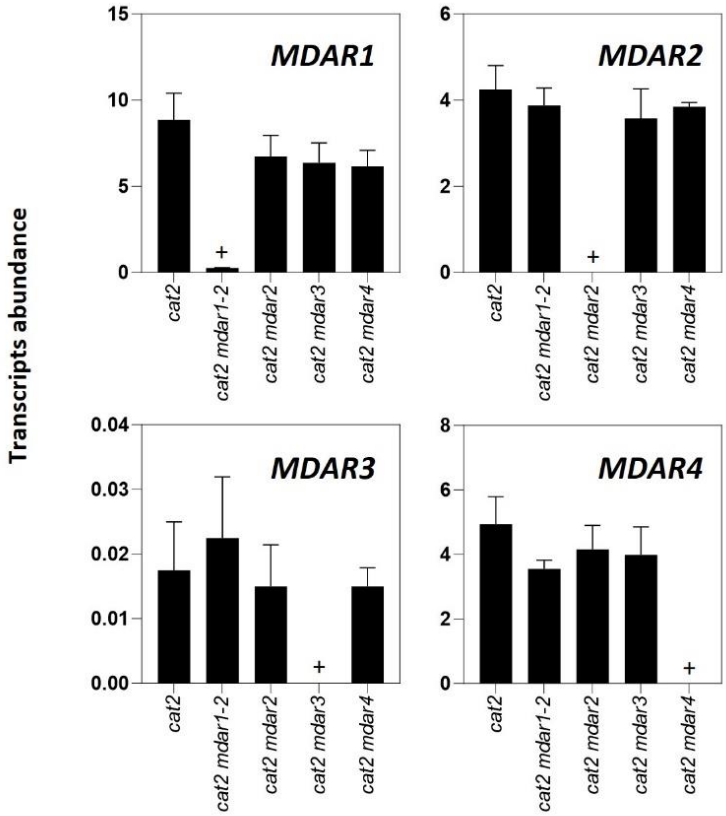

Supporting Information Figure S3.4. Analysis of expression of *MDAR* genes in the *cat2* background.

Supporting Information Table S3.1. List of gene primers.

Oligonucleotide	**Sequence**	**Technique**
ForCAT2	5’-CCCAGAGGTACCTCTTCTTCTCCCATG-3’	Genotyping
RevCAT2	5’-TCAGGGAACTTCATCCCATCGC-3’	Genotyping
ForMDAR1_2	5’-TGTTGGCGGAGGTTACATTG-3’	Genotyping
RevMDAR1_2	5’-TCGTCAAACGAAACCAAACC-3’	Genotyping
ForMDAR2	5’-TGGTTTATCCAGAACCTTGG-3’	Genotyping
RevMDAR2	5’-GTCTACCACCGACACCCACT-3’	Genotyping
ForMDAR3	5’-TTGCAACCGGTTCTACTGTG-3’	Genotyping
RevMDAR3	5’-TTGATTCCCTTGTTGGCATAG-3’	Genotyping
ForMDAR4	5’-CTTGTCACATTTGGCTCGTG-3’	Genotyping
RevMDAR4	5’-CCAGACATTTTTCGAGTTGAATC-3’	Genotyping
NewLB1	5’-TGGACCGCTTGCTGCAACTCT-3’	Genotyping
LBSail	5’-GAAATGGATAAATAGCCTTGCTTCC-3’	Genotyping
ForACTIN2	5’-CTGTACGGTAACATTGTGCTCAG-3’	RT-qPCR
RevACTIN2	5’-CCGATCCAGACACTGTACTTCC-3’	RT-qPCR
ForUbiquitin	5’-CTGTTCACGGAACCCAATTC-3’	RT-qPCR
RevUbiquitin	5’-GGAAAAAGGTCTGACCGACA-3’	RT-qPCR
ForPP2A	5’-TAACGTGGCCAAAATGATGC-3’	RT-qPCR
RevPP2A	5’-GTTCTCCACAACCGCTTGGT-3’	RT-qPCR
ForCAT2	5’-TGCTGGAAACTACCCTGAATGG-3’	RT-qPCR
RevCAT2	5’-TCAACACCATACGTCCAACAGG-3’	RT-qPCR
ForMDAR1	5’-ATCTGAGTGAAACACAACCACC-3’	RT-qPCR
RevMDAR1	5’-GGGTTTCCTCTGCCGTAGAC-3’	RT-qPCR
ForMDAR2	5’-CGAGCACAACCTTCTGTTGAG-3’	RT-qPCR
RevMDAR2	5’-GCCACTCTGAACTCAAAGCTC-3’	RT-qPCR
ForMDAR3	5’-CGGTTTCTTAGGGCTTGAGAT-3’	RT-qPCR
RevMDAR3	5’-TTGATTCCCTTGTTGGCATAG-3’	RT-qPCR
ForMDAR4	5’-GAGACGCCGTAGATGGTGAG-3’	RT-qPCR
RevMDAR4	5’-CCCACCAATGCTACAAACAAC-3’	RT-qPCR
ForPR1	5’-AGGCTAACTACAACTACGCTGCG-3’	RT-qPCR
RevPR1	5’-GCTTCTCGTTCACATAATTCCCAC-3’	RT-qPCR
ForPR2	5’-TCAAGGAGCTTAGCCTCACC-3’	RT-qPCR
RevPR2	5’-CGCCTAGCATCCCGTAGC-3’	RT-qPCR
ForPR5	5’-GCCCTACCACCGTCTGG-3’	RT-qPCR
RevPR5	5’-CGGGAAGCACCTGGAGTC-3’	RT-qPCR
ForICS1	5’-TTGGTGGCGAGGAGAGTG-3’	RT-qPCR
RevICS1	5’-CTTCCAGCTACTATCCCTGTCC-3’	RT-qPCR

ForPDF1.2	5’-CCAAACATGGATCATGCAAC-3’	RT-qPCR
RevPDF1.2	5’-CACACGATTTAGCACCAAAGA-3’	RT-qPCR
ForJAZ10	5’-CATCGGCTAAATCTCGTTCG-3’	RT-qPCR
RevJAZ10	5’-CGGTACTAGACCTGGCGAGA-3’	RT-qPCR
ForVSP2	5’-TACGACTCCAAAACCGTGTG-3’	RT-qPCR
RevVSP2	5’-GACGGTGTCGTTCTTTAGGG-3’	RT-qPCR
ForMDAR2(GFP)	5’-CAAATGGAGAGGTCACTGAGGT-3’	RT-qPCR
RevMDAR2(GFP)	5’-GTGGTTTGAAGACTGATGGGTTC-3’	RT-qPCR

Oligonucleotide sequences used in Plasmid *pGENI-MDAR* cloning

Oligonucleotide	**Sequence (Uppercase=gene-specific primer)**	
For pGENI_MDAR1	5’-actttaagaaggagatataccatggATGGCGGAGAAGAGCTTTAAG-3’	cloning
Rev pGENI_MDAR1	5’-tagcgctagcgctagcgctctcagaGATCTTAGCTGCGAAGGAAATTCC-3’	cloning
For pGENI_MDAR2	5’-actttaagaaggagatataccATGGCAGAAGAAAAGAGCTTCAAG-3’	cloning
Rev pGENI_MDAR2	5’-tagcgctagcgctagcgctctcagaTATATTTGTGGCGAAGGAAAGGC-3’	cloning

Oligonucleotide sequences used in Plasmid *pH7FWG2* cloning

Oligonucleotide	**Sequence (Uppercase=gene-specific primer)**	
For pH7FWG2-Egfp	5’-tctagtcgacctgcaggcggccgcactaGTGATATCAATGGTGAGCAAGGG-3’	cloning
Rev MDAR2-Egfp	5’-tttcttctgccatCTTGTACAGCTCGTCCATGC-3’	cloning
For EgfP-MDAR2	5’-cgagctgtacaagATGGCAGAAGAAAAGAGCTTCAAG-3’	cloning
Rev T35S-MDAR2	5’-agcatggccgcggTTATATATTTGTGGCGAAGGAAAGGC-3’	cloning
For MDAR2-T35S	5’-cacaaatatataaCCGCGGCCATGCTAGAGTC-3’	cloning
Rev pH7FWG2-T35S	5’-ctagAATTCGAGGGTACCCGGG-3’	cloning
For pH7FWG2-MDAR2	5’-tctagtcagcctgcaggcggccgcactagtATGGCAGAAGAAAAGAGCTTCAAC-3’	cloning
Rev Egfp+T35S-MDAR2	5’-ccattgatatcacTATATTTGTGGCGAAGGAAAGGC-3’	cloning
For MDAR2-Egfp+T35S	5’-cgccacaaatataGTGATATCAATGGTGAGCAAGGG-3’	cloning
Rev pH7FWG2-Egfp+T35S	5’-ctagAATTCGAGGGTACCCGGG-3’	cloning

CHAPTER 4 PRODUCING DOUBLE-DEFICIENT MUTANTS FOR PEROXISOMAL MONODEHYDROASCORBATE REDUCTASES

CHAPTER 4 PRODUCING DOUBLE-DEFICIENT MUTANTS FOR PEROXISOMAL MONODEHYDROASCORBATE REDUCTASES

Summary

In Arabidopsis, MDHAR1 and MDHAR4 are targeted to peroxisomes due to the presence of a C-terminal peroxisomal targeting signal (PTS) in MDHAR1 and a PTS-like transmembrane domain in MDHAR4. In this Chapter, the focus was on generating double and triple mutants involving *mdar1*, *mdar4* and *cat2*. The primary goal was to explore whether the peroxisomes need at least one functional MDHAR.

Previous work in the laboratory had failed to obtain *mdar1 mdar4* double mutants but had obtained a *cat2 mdar1 mdar4* triple mutant. This surprising observation led to a hypothesis that the oxidative stress *cat2* background might facilitate the recovery of the *mdar1 mdar4* mutant combination. To attempt to test this idea, a large-scale genotyping of descendants of *mdar1* crossed with *mdar4* was performed in this study, both in the backgrounds of *CAT2* (WT for this gene) and *cat2* (loss-of-function for this gene). This involved crossing *mdar1* with *mdar4* or *cat2 mdar1* with *cat2 mdar4*. Two mutant alleles of differing strength were available for *MDAR1* (*mdar1-2* and *mdar1-3*), and both were used in these experiments.

Whereas the *mdar1-2* allele appears to be a knockout, the *mdar1-3* shows a somewhat weaker effect on *MDAR1* transcripts and is therefore a knockdown. Based on segregation ratios of F2 plants from crosses of *mdar1-2* or *mdar1-3* with *mdar4*, it appears that strong genetic linkage is occurring to prevent recovery of the *mdar1-2 mdar4* double mutant in F2, but that this phenomenon is weaker in the case of the *mdar1-3 mdar4* combination. Analysis of F3 progeny of F2 sesqui-mutants points to negative selection against the *mdar1-2 mdar4* double mutant in some contexts but not others. Overall, it is concluded that genetic linkage and, possibly, selection complicate the production of lines that are severely lacking in peroxisomal MDHAR.

4.1 Introduction

As outlined in Chapter 1, MDHAR1 and MDHAR4 are located in the peroxisomes. Single mutants do not exhibit distinct phenotypes, although growth on sugar is required to favour early development of *mdar4* mutants (Chapter 3). Indeed, previous studies suggest that MDHAR4 is involved in ascorbate recycling in the peroxisomes (Lisenbee et al., 2005) and that loss of *MDAR4* function affected seed oil hydrolysis and seedling development, indicating that MDHAR4-dependent ascorbate recycling is required during peroxisomal β-oxidation of fatty acids, which produces H_2O_2 during germination and early post-germinative growth (Eastmond, 2007). Apart from this requirement, *mdar4* mutants show a wild-type phenotype. As noted in Chapter 3, a wild-type phenotype is also observed in *mdar1*, despite the substantial contribution of MDHAR1 to the extractable leaf activity. However, *mdar1* and *mdar4* have some impact on the *cat2* phenotype, which is thought to be caused by decreased capacity to deal with H_2O_2 that is mostly produced in the peroxisomes (Chapter 3). Nevertheless, the effects of loss of *MDAR1* and *MDAR4* functions are relatively minor, even in oxidative stress conditions.

These observations raise the questions of (1) genetic redundancy between *MDAR1* and *MDAR4* and (2) the nature of the functional interactions between these genes and *CAT2*. Hence, we sought to investigate the effect of simultaneously removing both peroxisomal isoforms of MDHAR. As reported in Chapter 3, although the *mdar2* mutation does not by itself greatly affect growth or performance when plants are cultivated in optimal conditions, it does antagonise rather than promote responses to oxidative stress. These observations are an example of the sometimes unpredictable effects of associating mutations for enzymes involved in the antioxidative system, and suggest that further work is required to elucidate the complexity of the interactions between different pathways.

As a further possible indication of unexpected interactions between antioxidant systems, a previous observation in the laboratory suggested that a triple *cat2 mdar1-2 mdar4* mutant could be obtained by crossing *cat2 mdar1-2* and *cat2 mdar4*. In contrast, no double *mdar1-2 mdar4* was obtained after crossing *mdar1-2* and *mdar4*. One aim of this work was to validate this preliminary observation, which seems surprising given that the *mdar1 mdar4* combination might be predicted to be more deleterious in plants that are also catalase-deficient. Attempts were made to construct and analyze double or triple *(cat2) mdar1 mdar4* mutants, with the initial aim of establishing the functional impact of loss of the two peroxisomal isoforms. As it became clear that the *mdar1-2 mdar4* combination was difficult to obtain, genotyping studies were performed on a larger scale to attempt to identify plants with this genotype and/or identify the causes underlying the difficulty.

4.2 Materials and methods

4.2.1 Plant material

Lines carrying T-DNA insertions in the *MDAR* genes were obtained from the SIGnAL Web site (http://signal.salk.edu/). The *cat2*, *mdar1-2* and *mdar4* mutants were the same as those described in the previous chapter but a second allelic mutant for *MDAR1* was also used in this part of the work (*mdar1-3*; SAIL_720_H04). Gene maps for the T-DNA insertions in the three *mdar* lines are shown in Figure 4.1. Cross-fertilization of two single mutants was performed under a loop to ensure that the stigma was not contaminated with its own pollen and that all pollen was removed. The *mdar1* and *mdar4* mutants were crossed to produce the *mdar1 mdar4* double mutants and the *cat2 mdar1* and *cat2 mdar4* lines were crossed to generate the triple *cat2 mdar1 mdar4* mutants.

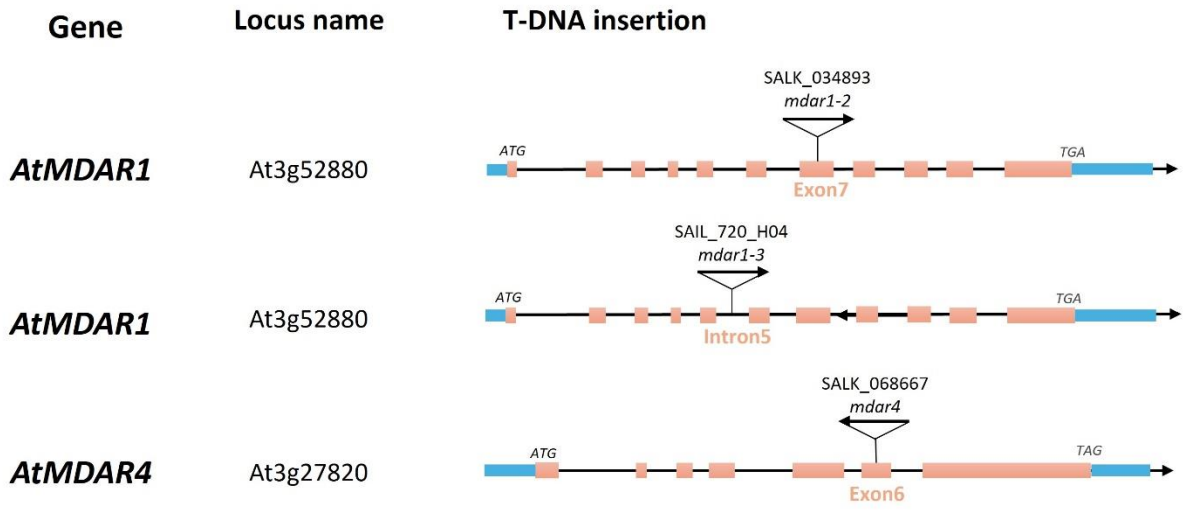

Figure 4.1. Gene maps of the *mdar* mutants used in this chapter.

4.2.2 Growth, sampling, and analysis

The Arabidopsis seeds were sown in 1/2 Murashige and Skoog solid medium (basal salt mixture; M0221; Duchefa) in 12cm x 12cm plates with the addition of 1% sucrose. Fourteen-day-old seedlings were transferred to soil culture under a 16-hour light/8-hour dark photoperiod. Young Arabidopsis leaves were carefully sampled and frozen in -20°C for future analysis. DNA extraction was performed as described in Chapter 2. PCR reactions were carried out in a 96-well PCR plate. Specific oligonucleotides were designed for each target gene. Both wild-type and mutant were tested.

To detect the presence of T-DNA insertions, pairs of oligonucleotides were designed with one primer specific to the wild-type gene and the other primer targeting the T-DNA insertion (Table 4.1).

Table 4.1. Oligonucleotides used in this study

		Oligonucleotide	
Genotype	**Expected size**	**Forward**	**Reverse**
CAT2 wild-type	507	ForCAT2	RevCAT2
CAT2 mutant	388	NewLB1	RevCAT2
MDAR1_2 wild-type	413	ForMDAR1-2	RevMDAR1-2
MDAR1_2 mutant	457	NewLB1	RevMDAR1-2
MDAR1_3 wild-type	316	ForMDAR1-3	RevMDAR1-3
MDAR1_3 mutant	225	LBSail	RevMDAR1-3
MDAR4 wild-type	498	ForMDAR4	RevMDAR4
MDAR4 mutant	185	ForMDAR4	NewLB1

Oligonucleotide sequence list

N°	**Oligonucleotide**	**Sequence**
1	ForCAT2	5’-CCCAGAGGTACCTCTTCTTCTCCCATG-3’
2	RevCAT2	5’-TCAGGGAACTTCATCCCATCGC-3’
3	ForMDAR1_2	5’-TGTTGGCGGAGGTTACATTG-3’
4	RevMDAR1_2	5’-TCGTCAAACGAAACCAAACC-3’
5	ForMDAR1_3	5’-GACTTCCAGGTTTCCATTGC-3’
6	RevMDAR1_3	5’-GAAGACATCCCCAGTTGCAC-3’
7	ForMDAR4	5’-CTTGTCACATTTGGCTCGTG-3’
8	RevMDAR4	5’-CCAGACATTTTTCGAGTTGAATC-3’
9	NewLB1	5’-TGGACCGCTTGCTGCAACTCT-3’
10	LBSail	5’-GAAATGGATAAATAGCCTTGCTTCC-3’

Specific hybridization conditions, along with elongation times and temperatures, were optimized for each primer pair. Multiple primer pairs were utilized to identify both double and triple mutants and to test the T-DNA inserts at various genomic locations. The PCR products were then analyzed with gel electrophoresis. A negative result in the wild-type test and a positive result in the mutant test confirmed the presence of the mutation at the targeted locus (Figure 4.2).

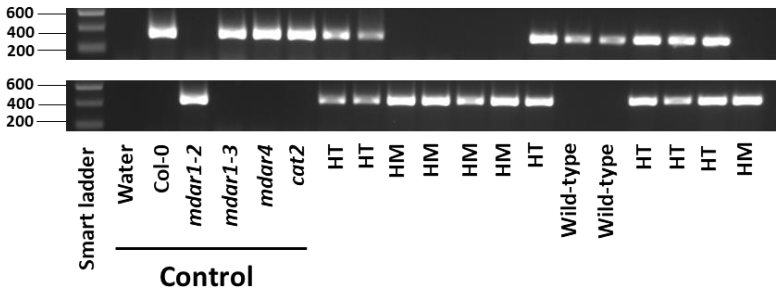

Figure 4.2. An example for the gel electrophoresis of PCR products for T-DNA mutants. Genotyping for the *mdar1-2* mutant line is shown as an example. DNA from water, Col-0, *mdar1-2*, *mdar1-3*, *mdar4*, and *cat2* mutants were used as controls. The top gel shows analysis using primers detecting the wild-type *MDAR1* allele, whereas the bottom gel shows products of reactions with one primer derived from the native gene sequence and the other from the T-DNA insertion site (sequences detailed in Table 4.1). Signals present in both gels indicate a heterozygous genotype. Signals appearing exclusively in top gel indicate a wild-type genotype, while signals detected only in the bottom gel suggest a homozygous mutant genotype. HT: heterozygous, HM: homozygous.

Analysis of transcript abundance by RT-qPCR was performed as described in Chapter 2.

4.3 Results

According to preliminary work in the laboratory, the *cat2 mdar1-2 mdar4* mutant had already been obtained before I arrived, but attempts to produce the double *mdar1-2 mdar4* mutant did not yield positive results. Hence the question was why an *mdar1 mdar4* double mutant could not be obtained if it was possible to obtain this combination in the *cat2* background. It was essential to establish whether this result was due to chance or whether there was some positive selective effect linked to oxidative stress that is occurring at the functional or genetic levels. An important issue is that *MDAR1* and *MDAR4* are both located on chromosome 3, suggesting that significant genetic linkage effect might be operating to limit the crossing-over that is required to produce a new combination of alleles on the same sister chromosome. If so, it is possible that a positive selection of oxidative stress (in the *cat2* genetic background) might be partly or wholly operating on the frequency of recombination, explaining why we can obtain *cat2 mdar1 mdar4* but not *mdar1 mdar4*. To test this hypothesis, it is necessary to have rigorous statistical data from genotyping.

As used here, the terms 'Col-0 background' or 'wild-type background' refer to plants that are homozygous for the wild-type *CAT2* allele (denoted *CAT2 CAT2* in figures and tables) and that have a full complement of catalase. By contrast, the term '*cat2* background' denotes plants that are homozygous mutant at this locus (denoted *cat2 cat2* in figures and tables), corresponding to the catalase-deficient *cat2* line described in the previous chapter. The initial aim was to find a double *mdar1 mdar4* mutant combination in both backgrounds, in order to enable an analysis of the functional interplay between the encoded proteins.

4.3.1 *MDAR* expression analysis in the different parent mutants

Previous work in the laboratory, which managed to obtain a *cat2 mdar1-2 mdar4* triple mutant (*cat2* background) but not the *mdar1-2 mdar4* double mutant (Col-0 background), used the only *MDAR1* mutant line available at the time (*mdar1-2*). Since that work was done, a second T-DNA mutant allele has been obtained (*mdar1-3*; Table 4.1). Therefore, even though only one line was available for *MDAR4*, I wished to establish whether similar results would be obtained with the *mdar1-3* allele as the previously used *mdar1-2*. As a first step, RT-qPCR analysis was performed to characterize the effects of the *mdar1-2* and *mdar1-3* mutations on *MDAR1* transcript levels. For *mdar1-2* and *mdar4*, the results confirm those shown in the previous chapter in revealing very low levels of transcripts of *MDAR1* and *MDAR4,* respectively, in these two lines (Figure 4.3). In contrast, *MDAR1* transcripts were somewhat more abundant in *mdar1-3* than in *mdar1-2* (Figure 4.3). These results suggest that the single mutant

lines *mdar4* and *mdar1-2* are knockouts, with very low transcript levels for the affected gene, while *mdar1-3* can be considered a knockdown mutant. This is a potentially important point in the interpretation of genotyping experiments.

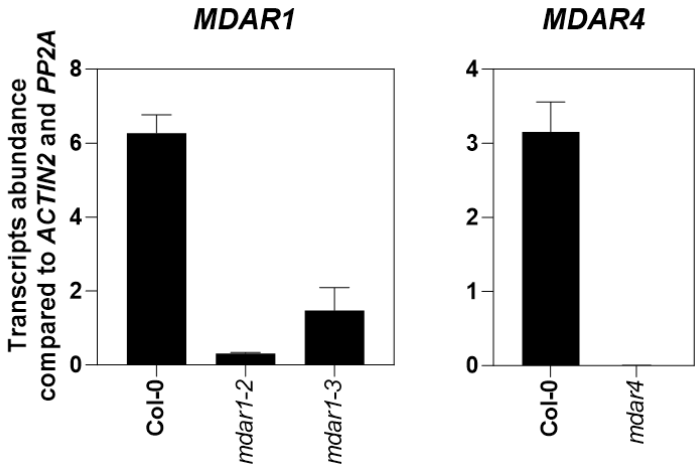

Figure 4.3. Transcript abundance of *MDAR1* and *MDAR4*. The left panel shows a comparison of *MDAR1* transcripts in Col-0 and the *mdar1-2* and *mdar1-3* mutants, while the right panel shows a comparison of *MDAR4* transcripts in Col-0 and the *mdar4* mutant.

4.3.2 Production of the *mdar1-3 mdar4* double mutant and the *cat2 mdar1-3 mdar4* triple mutant

Given that previous laboratory attempts to produce *mdar1-2 mdar4* had not been successful, I initially focused on screening for *mdar1-3* (knockdown allele for *mdar1*) *mdar4* double mutants from the progeny of F1 *mdar1-3 mdar4* double heterozygotes, work conducted in both the Col-0 and *cat2* genetic backgrounds. The aim was to examine whether a double *mdar1 mdar4* mutant could be found with a less severe *MDAR1* allele (Figure 4.3). First, a homozygous *mdar1-3* mutant was crossed with a homozygous *mdar4* plant to obtain *MDAR1 mdar1-3 MDAR4 mdar4* double heterozygotes in F1, and about fifty F2 plants resulting from self-fertilization of a double heterozygote were genotyped. This analysis showed that, similar to previous results of the laboratory with *mdar1-2* and *mdar4*, *mdar1-3 mdar4* double mutants could not be found within the F2 generation (Table 4.2). However, the sample size was too small to exclude an effect of chance, since only 3-4 double mutant plants were expected from the 55 plants analyzed (1/16, if segregation followed Mendelian laws). Indeed, segregation of F1 double heterozygotes to the double wild-type in F2 only yielded two plants (Table 4.2, top row), showing that a more detailed analysis would be required to be able to exclude effects that might be purely due to chance.

Table 4.2. F2 gene segregation after self-fertilization of double heterozygous progeny in the Col-0 background (homozygous wild-type at the *CAT2* locus).

F1 genotype:
CAT2 CAT2 MDAR1 mdar1-3 MDAR4 mdar4

Genotype (gene segregation)	Number of plants	Percentage	Expected number	Expected percentage
CAT2 CAT2 MDAR1 MDAR1 MDAR4 MDAR4	2	3.64%	3.4	6.25%
CAT2 CAT2 MDAR1 MDAR1 MDAR4 mdar4	4	7.27%	6.9	12.5%
CAT2 CAT2 MDAR1 MDAR1 mdar4 mdar4	2	3.64%	3.4	6.25%
CAT2 CAT2 MDAR1 mdar1-3 MDAR4 MDAR4	12	21.82%	6.9	12.5%
CAT2 CAT2 MDAR1 mdar1-3 MDAR4 mdar4	15	27.27%	13.8	25%
CAT2 CAT2 MDAR1 mdar1-3 mdar4 mdar4	6	10.91%	6.9	12.5%
CAT2 CAT2 mdar1-3 mdar1-3 MDAR4 MDAR4	7	12.73%	3.4	6.25%
CAT2 CAT2 mdar1-3 mdar1-3 MDAR4 mdar4	7	12.73%	6.9	12.5%
CAT2 CAT2 mdar1-3 mdar1-3 mdar4 mdar4	0	0%	3.4	6.25%
Total	55	100.00%	55	100%

For this more detailed analysis, the progeny of a *CAT2 CAT2 mdar1-3 mdar1-3 MDAR4 mdar4* plant were genotyped. This sesqui-mutant F2 parent plant was homozygous for the *mdar1-3* mutation but heterozygous for *mdar4*. As the *mdar1-3* mutation is already homozygous in the parent plant, no linkage effect should affect assortment in the progeny and, if there is no effect of selection, *MDAR4 mdar4* should segregate as 1:2:1 between wild-type, heterozygote, and mutant homozygote at this locus. As Table 4.3 shows, the double homozygous mutant was obtained, and observed segregation ratios were close to those expected, albeit with a slightly higher than expected proportion of plants that were wild-type for *MDAR4*.

Table 4.3. F3 gene segregation after self-fertilization of sesqui-mutant progeny in the Col-0 background (homozygous wild-type at the *CAT2* locus).

F2 genotype:
CAT2 CAT2 mdar1-3 mdar1-3 MDAR4 mdar4

Genotype (gene segregation)	Number of plants	Percentage	Expected number	Expected percentage
CAT2 CAT2 mdar1-3 mdar1-3 MDAR4 MDAR4	27	28.72%	23.5	25%
CAT2 CAT2 mdar1-3 mdar1-3 MDAR4 mdar4	46	48.94%	47	50%
CAT2 CAT2 mdar1-3 mdar1-3 mdar4 mdar4	21	22.34%	23.5	25%
Total	94	100%	94	100%

Next, the same genotyping analyses were performed in the *cat2* background; ie, *cat2 mdar1-3* was crossed with *cat2 mdar4* to obtain *cat2 cat2 MDAR1 mdar1-3 MDAR4 mdar4* F1 individuals, and individuals of these plants were then allowed to self-fertilise to produce 88 F2 progeny that were genotyped (Table 4.4). Subsequently, an F2 sesqui-mutant was allowed to self-fertilize, and F3 plants were genotyped to establish segregation ratios more closely (Table 4.5). This analysis revealed that it was possible to obtain triple homozygous *cat2 mdar1-3 mdar4* plants in F2, with numbers being very close to those expected (5/88).

Table 4.4. F2 gene segregation after self-fertilization of double heterozygous progeny in the *cat2* background (homozygous mutant at the *CAT2* locus).

F1 genotype:
cat2 cat2 MDAR1 mdar1-3 MDAR4 mdar4

Genotype (gene segregation)	Number of plants	Percentage	Expected number	Expected percentage
cat2 cat2 MDAR1 MDAR1 MDAR4 MDAR4	2	2.27%	5.5	6.25%
cat2 cat2 MDAR1 MDAR1 MDAR4 mdar4	10	11.36%	11	12.5%
cat2 cat2 MDAR1 MDAR1 mdar4 mdar4	10	11.36%	5.5	6.25%
cat2 cat2 MDAR1 mdar1-3 MDAR4 MDAR4	6	6.82%	11	12.5%
cat2 cat2 MDAR1 mdar1-3 MDAR4 mdar4	23	26.14%	22	25%
cat2 cat2 MDAR1 mdar1-3 mdar4 mdar4	12	13.64%	11	12.5%
cat2 cat2 mdar1-3 mdar1-3 MDAR4 MDAR4	10	11.36%	5.5	6.25%
cat2 cat2 mdar1-3 mdar1-3 MDAR4 mdar4	10	11.36%	11	12.5%
cat2 cat2 mdar1-3 mdar1-3 mdar4 mdar4	5	5.68%	5.5	6.25%
Total	88	100.00%	88	100%

Analysis of 96 F3 progeny produced from a sesqui-mutant confirmed that it was indeed possible to produce the triple homozygote mutant. As in F2 (Table 4.4), this more robust statistical analysis showed that segregation ratios were close to those expected (Table 4.5).

Table 4.5. F3 gene segregation after self-fertilization of sesqui-mutant progeny in the *cat2* background (homozygous mutant at the *CAT2* locus).

F2 genotype:
cat2 cat2 MDAR1 mdar1-3 mdar4 mdar4

Genotype (gene segregation)	Number of plants	Percentage	Expected number	Expected percentage
cat2 cat2 MDAR1 MDAR1 mdar4 mdar4	21	21.88%	24	25%
cat2 cat2 MDAR1 mdar1-3 mdar4 mdar4	52	54.17%	48	50%
cat2 cat2 mdar1-3 mdar1-3 mdar4 mdar4	23	23.96%	24	25%
Total	96	100%	96	100%

Overall, the results show that it is possible to obtain the *mdar1-3 mdar4* combination in a genetic background with high or low catalase activity. These data provide little evidence of selection against this combination in either genetic background. However, the *mdar1-3* allele has a weaker effect on *MDAR1* transcripts than *mdar1-2* (Figure 4.3). Hence, selection against the *mdar1-2 mdar4* combination cannot be discounted on the basis of these results alone. Similarly, the above studies of

gene segregation in F2 (Tables 4.2 and 4.4) are not extensive enough to establish whether genetic linkage between the loci is an influential factor. A series of larger scale genotyping experiments was therefore conducted, with the dual aims of (1) finally obtaining a double *mdar1-2 mdar4* knockout mutant for functional analysis; and (2) understanding the genetic or functional factors that make this mutant so difficult to obtain.

4.3.3 Large-scale genotyping method for *mdar1-2 mdar4* alleles in the Col-0 and *cat2* backgrounds

To allow for any possible gametophyte-specific effects, crossing of *mdar1-2* and *mdar4* single mutants was carried out with either mutant as female or male parent in both the Col-0 and *cat2* backgrounds. In a first step, the pollen of *mdar1-2* was transferred to the stigma of a *mdar4* plant. After verification of double heterozygotes in F1, plants were allowed to mature and then self-fertilize to produce F2 progeny on which a segregation analysis could be performed (Figure 4.4). From more than 250 F2 plants, the following genotypic distribution was obtained: approximately 40% were homozygous for a mutation at one of the loci (*MDAR1 MDAR1 mdar4 mdar4* and *mdar1-2 mdar1-2 MDAR4 MDAR4*), and about 53% were double heterozygotes (*MDAR1 mdar1-2 MDAR4 mdar4*). These results substantially exceeded the expected Mendelian ratios (Table 4.6). In contrast, the genotypes *MDAR1 mdar1-2 MDAR4 MDAR4* and *MDAR1 mdar1-2 mdar4 mdar4*, which are heterozygous at the *MDAR1* locus and homozygous for *MDAR4* wild-type or the *mdar4* mutant, only occurred at a frequency of 2-3%, much lower than the expected 12.5% based on independent assortment. Concerning the double homozygote mutant, no plant was identified with this genotype (Table 4.6, expected number of plants from a simple Mendelian segregation = 16). Similarly, however, no plant was obtained that was homozygous for the wild-type alleles at the two loci, which are predicted to be equal in frequency to the double mutant (Table 4.6).

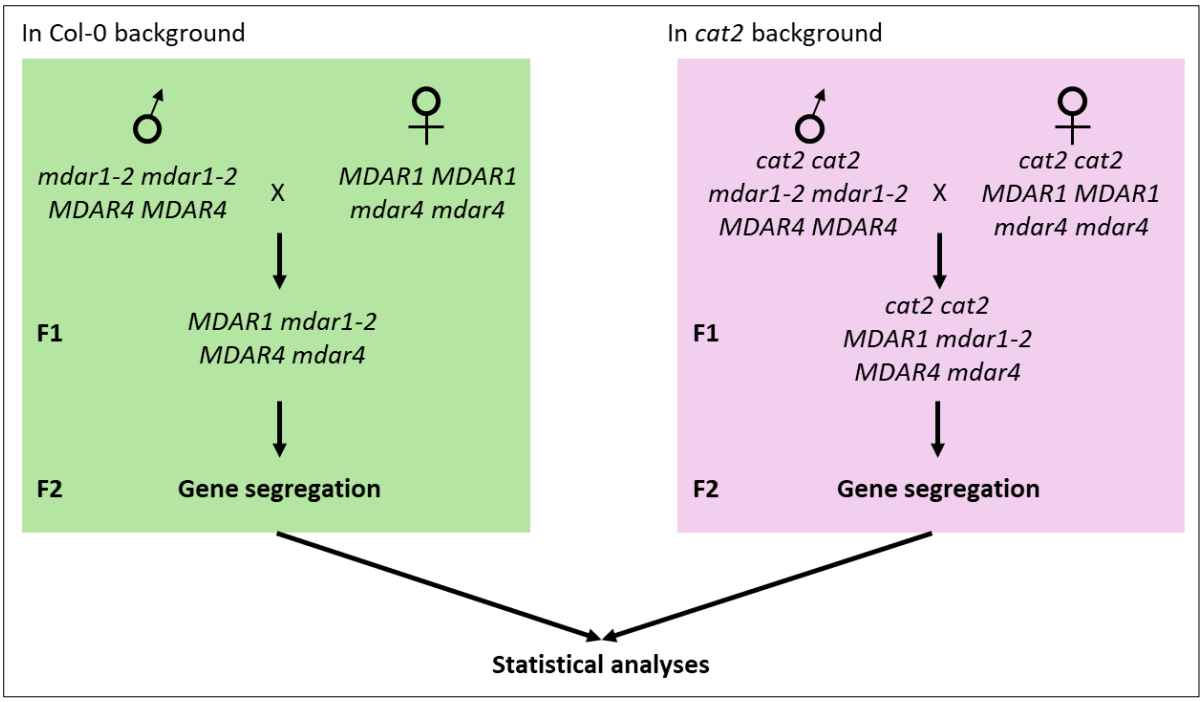

Figure 4.4. Crossing of *mdar1-2* and *mdar4* single mutant. The *mdar4* stigma was fertilized with *mdar1-2* pollen in either Col-0 or *cat2* backgrounds.

Table 4.6. F2 gene segregation after crossing of *mdar1-2* (male) and *mdar4* (female) in the Col-0 background.

F1 genotype:
CAT2 CAT2 MDAR1 mdar1-2 MDAR4 mdar4

Genotype (gene segregation)	Number of plants	Percentage	Expected number	Expected percentage
CAT2 CAT2 MDAR1 MDAR1 MDAR4 MDAR4	0	0%	16	6.25%
CAT2 CAT2 MDAR1 MDAR1 MDAR4 mdar4	0	0%	32	12.5%
CAT2 CAT2 MDAR1 MDAR1 mdar4 mdar4	49	19.1%	16	6.25%
CAT2 CAT2 MDAR1 mdar1-2 MDAR4 MDAR4	6	2.3%	32	12.5%
CAT2 CAT2 MDAR1 mdar1-2 MDAR4 mdar4	137	53.3%	64	25%
CAT2 CAT2 MDAR1 mdar1-2 mdar4 mdar4	8	3.1%	32	12.5%
CAT2 CAT2 mdar1-2 mdar1-2 MDAR4 MDAR4	57	22.2%	16	6.25%
CAT2 CAT2 mdar1-2 mdar1-2 MDAR4 mdar4	0	0%	32	12.5%
CAT2 CAT2 mdar1-2 mdar1-2 mdar4 mdar4	0	0%	16	6.25%
Total	257	100%	257	100%

The same approach was employed in the *cat2* background: the pollen of *cat2 mdar1-2* was transferred to the stigma of a *cat2 mdar4* plant. After verification of double heterozygotes in F1, more than 250 plants were genotyped in F2. This analysis produced similar results to those obtained in the Col-0 background; ie, no double mutants or double wild-type plants were obtained and double heterozygotes and the two single *mdar* mutants were over-represented in F2, together accounting for about 90% of all individuals (Table 4.7).

Table 4.7. F2 gene segregation after crossing of *mdar1-2* (male) and *mdar4* (female) in the *cat2* background.

F1 genotype:

cat2 cat2 MDAR1 mdar1-2 MDAR4 mdar4

Genotype (gene segregation)	Number of plants	Percentage	Expected number	Expected percentage
cat2 cat2 MDAR1 MDAR1 MDAR4 MDAR4	0	0%	16	6.25%
cat2 cat2 MDAR1 MDAR1 MDAR4 mdar4	0	0%	32	12.5%
cat2 cat2 MDAR1 MDAR1 mdar4 mdar4	50	19.5%	16	6.25%
cat2 cat2 MDAR1 mdar1-2 MDAR4 MDAR4	10	3.9%	32	12.5%
cat2 cat2 MDAR1 mdar1-2 MDAR4 mdar4	129	50.4%	64	25%
cat2 cat2 MDAR1 mdar1-2 mdar4 mdar4	12	4.7%	32	12.5%
cat2 cat2 mdar1-2 mdar1-2 MDAR4 MDAR4	55	21.5%	16	6.25%
cat2 cat2 mdar1-2 mdar1-2 MDAR4 mdar4	0	0%	32	12.5%
cat2 cat2 mdar1-2 mdar1-2 mdar4 mdar4	0	0%	16	6.25%
Total	256	100%	256	100%

In a second approach, *mdar1-2* was used as female parent with pollen from *mdar4* (Figure 4.5).

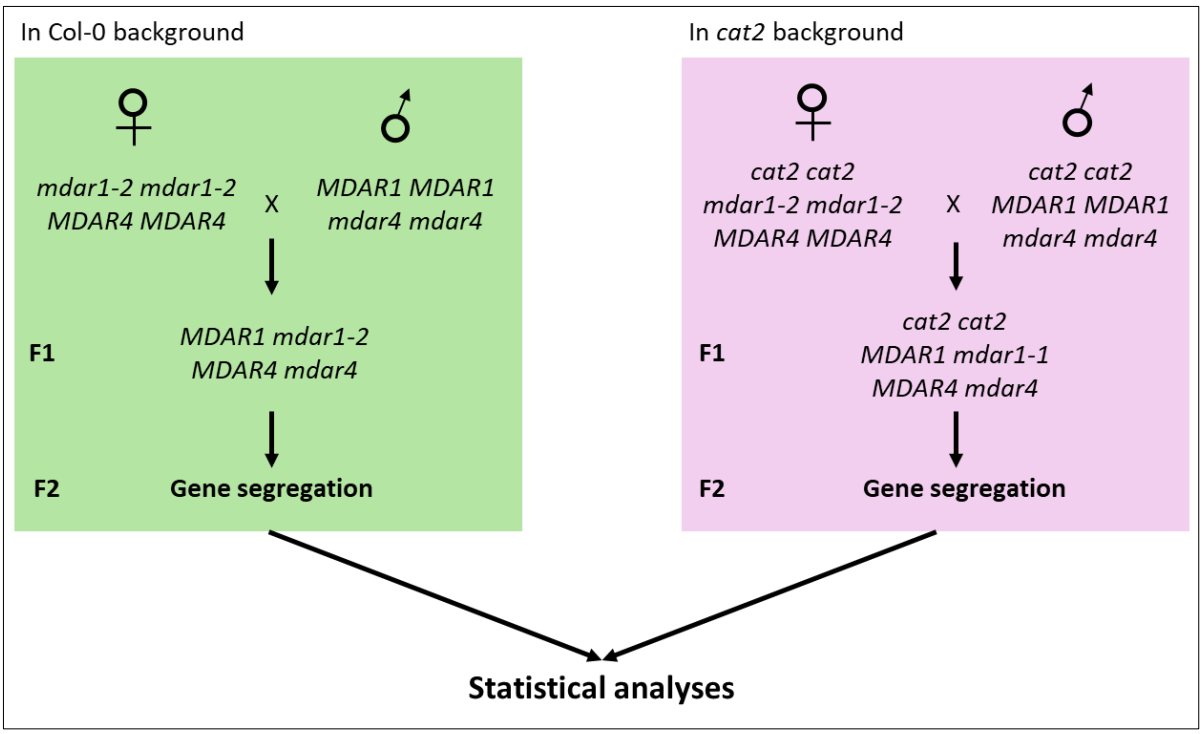

Figure 4.5. Crossing of *mdar1-2* and *mdar4* single mutants with *mdar1-2* as female parent. The *mdar1-2* stigma was fertilized with *mdar4* pollen in either Col-0 or *cat2* backgrounds.

As shown in Tables 4.8 and 4.9, the results were similar to those obtained in Tables 4.6 and 4.7: the predominant genotypes were *MDAR1 MDAR1 mdar4 mdar4*, *MDAR1 mdar1-2 MDAR4 mdar4*, and *mdar1-2 mdar1-2 MDAR4 MDAR4*, with frequencies of 15%, 56%, and 24% respectively. Two infrequent genotypes, *MDAR1 mdar1-2 MDAR4 MDAR4* and *MDAR1 mdar1-2 mdar4 mdar4*, were observed at rates of about 4% and 1% respectively (Table 4.8). In the *cat2* background, similar results were obtained. In this set of experiments, double mutants and double wild-type genotypes were also not observed (Table 4.9).

Table 4.8. F2 gene segregation after crossing of *mdar1-2* (female) and *mdar4* (male) in the Col-0 background

F1 genotype:
CAT2 CAT2 MDAR1 mdar1-2 MDAR4 mdar4

Genotype (gene segregation)	Number of plants	Percentage	Expected number	Expected percentage
CAT2 CAT2 MDAR1 MDAR1 MDAR4 MDAR4	0	0%	16	6.25%
CAT2 CAT2 MDAR1 MDAR1 MDAR4 mdar4	0	0%	32	12.5%
CAT2 CAT2 MDAR1 MDAR1 mdar4 mdar4	39	15.4%	16	6.25%
CAT2 CAT2 MDAR1 mdar1-2 MDAR4 MDAR4	9	3.5%	32	12.5%
CAT2 CAT2 MDAR1 mdar1-2 MDAR4 mdar4	141	55.5%	64	25%
CAT2 CAT2 MDAR1 mdar1-2 mdar4 mdar4	3	1.2%	32	12.5%
CAT2 CAT2 mdar1-2 mdar1-2 MDAR4 MDAR4	62	24.4%	16	6.25%
CAT2 CAT2 mdar1-2 mdar1-2 MDAR4 mdar4	0	0%	32	12.5%
CAT2 CAT2 mdar1-2 mdar1-2 mdar4 mdar4	0	0%	16	6.25%
Total	254	100%	254	100%

Table 4.9. F2 gene segregation after crossing of *mdar1-2* (female) and *mdar4* (male) in the *cat2* background

F1 genotype*:*
cat2 cat2 MDAR1 mdar1-2 MDAR4 mdar4

Genotype (gene segregation)	Number of plants	Percentage	Expected number	Expected percentage
cat2 cat2 MDAR1 MDAR1 MDAR4 MDAR4	0	0%	15	6.25%
cat2 cat2 MDAR1 MDAR1 MDAR4 mdar4	0	0%	30	12.5%
cat2 cat2 MDAR1 MDAR1 mdar4 mdar4	51	21.1%	15	6.25%
cat2 cat2 MDAR1 mdar1-2 MDAR4 MDAR4	6	2.5%	30	12.5%
cat2 cat2 MDAR1 mdar1-2 MDAR4 mdar4	126	52.1%	61	25%
cat2 cat2 MDAR1 mdar1-2 mdar4 mdar4	4	1.7%	30	12.5%
cat2 cat2 mdar1-2 mdar1-2 MDAR4 MDAR4	55	22.7%	15	6.25%
cat2 cat2 mdar1-2 mdar1-2 MDAR4 mdar4	0	0%	30	12.5%
cat2 cat2 mdar1-2 mdar1-2 mdar4 mdar4	0	0%	15	6.25%
Total	242	100%	242	100%

Thus, crosses performed with either mutant as male or female parent followed by analysis of approximately 250 F2 progeny have not allowed us to obtain the double *mdar1-2 mdar4* combination in Col-0 or *cat2* backgrounds. However, the strong departure of segregation ratios from expected

Mendelian values, including the failure to observe double wild-type genotypes in F2, points to significant genetic linkage rather than selection as the cause of the failure to obtain the mutants. To examine this point further, F2 sesqui-mutants were chosen for self-fertilization to examine if double mutants could be found in F3 in either Col-0 or *cat2* backgrounds.

4.3.4 Statistical analysis in F3 progeny

Despite the large-scale nature of the analysis, no plants that were homozygous for *mdar1-2* and heterozygous for *mdar4* could be obtained, whether the *cat2* mutation was also present or not (Tables 4.6-4.9; second genotype from bottom). In contrast, plants that were heterozygous for *mdar1-2* and homozygous for *mdar4* were obtained, at a low frequency, in both Col-0 and *cat2* backgrounds (Tables 4.6-4.9; fourth genotype row from bottom). I sought to establish whether double mutants could be found in the progeny of F2 plants with this genotype. To maximize this possibility, approximately 180 F3 plants were genotyped.

In the F3 generation, gene segregation at the *MDAR1* locus can result in three possible genotypes: *MDAR1 MDAR1 mdar4 mdar4*, *MDAR1 mdar1-2 mdar4 mdar4*, and *mdar1-2 mdar1-2 mdar4 mdar4*. According to Mendel's laws, the expected ratio of these three genotypes is 1:2:1, with the expected percentage of double mutants being 25%. From 180 plants, 45 double mutants are predicted if no other factors, such as selection or linkage, are operating.

As shown in Table 4.10, the observed outcomes did not align with those predicted from Mendelian genetics in the Col-0 background. In the F3 generation, no double mutants were identified. Instead, at the *MDAR1* locus, there was a stronger tendency to obtain the homozygous wild-type combination (*MDAR1 MDAR1 mdar4 mdar4*) rather than the homozygous mutant. Specifically, 56 plants (29.6%) were of the genotype *CAT2 CAT2 MDAR1 MDAR1 mdar4 mdar4* while 133 plants (70.4%) were of the genotype *CAT2 CAT2 MDAR1 mdar1-2 mdar4 mdar4* (Table 4.10). In the *cat2* background, similar results were obtained: again, the double homozygous *mdar1-2 mdar4* combination could not be found (Table 4.11).

Table 4.10. Gene segregation in F3 of an F2 sesqui-mutant produced from F0 *mdar1-2* (female) and *mdar4* (male) in the Col-0 background

F2 genotype:
CAT2 CAT2 MDAR1 mdar1-2 mdar4 mdar4

Genotype (gene segregation)	Number of plants	Percentage	Expected number	Expected percentage
CAT2 CAT2 MDAR1 MDAR1 mdar4 mdar4	56	29.6%	47.25	25%
CAT2 CAT2 MDAR1 mdar1-2 mdar4 mdar4	133	70.4%	94.5	50%
CAT2 CAT2 mdar1-2 mdar1-2 mdar4 mdar4	0	0%	47.25	25%
Total	189	100%	189	100%

Table 4.11. Gene segregation in F3 of an F2 sesqui-mutant produced from F0 *mdar1-2* (female) and *mdar4* (male) in the *cat2* background

F2 genotype*:*
cat2 cat2 MDAR1 mdar1-2 mdar4 mdar4

Genotype (gene segregation)	Number of plants	Percentage	Expected number	Expected percentage
cat2 cat2 MDAR1 MDAR1 mdar4 mdar4	55	31.4%	43.75	25%
cat2 cat2 MDAR1 mdar1-2 mdar4 mdar4	120	68.6%	87.5	50%
cat2 cat2 mdar1-2 mdar1-2 mdar4 mdar4	0	0%	43.75	25%
Total	175	100%	175	100%

4.4 Discussion

As described in Chapter 3, single *mdar1* and *mdar4* knockouts for the peroxisomal MDHAR isoforms show a phenotype that is similar to the wild-type. The initial aim of the work described in this chapter was to seek to generate a double knockout mutant for the two genes, in order to test the functional significance of peroxisomal MDHAR activity and possible redundancy between the two genes. Within this context, I have been able to show that it is possible to obtain a double *mdar1-3 mdar4* mutant. This observation demonstrates that, at least in some contexts, linkage between the *MDAR1* and *MDAR4* loci is not an insurmountable obstacle to obtaining double mutants. It also suggests that Arabidopsis can survive without a large part of the peroxisomal MDHAR. However, within the time available, it was not possible to perform wider scale segregation analyses on this combination in order to quantify the effects of linkage. Neither was time available to conduct functional analyses of the *mdar1-3 mdar4* double mutant. Instead, the major focus was placed on attempting to explain why previous crosses in the laboratory had been able to obtain a triple *cat2 mdar1-2 mdar4* plant but not a double *mdar1-2 mdar4* plant, when one might expect the latter would be easier to obtain than the former. It should be noted that the analyses performed prior to my arrival were goal-orientated and did not involve attempts to quantify segregation: rather, the aim was simply to generate the double and triple mutants for functional study. Because of the potential interest of the observation in terms of interactions between catalase and peroxisomal MDHAR, I performed several large-scale genotyping experiments after new crossings of the *mdar1-2* and *mdar4* mutants.

Based on the data presented in Tables 4.6 to 4.9, there is a stark difference between the observed and expected genotype ratios in F2. Such distorted ratios may result from selection (effects of mutations on survival) or genetic linkage. For example, genotypes *MDAR1 mdar1-2 MDAR4 MDAR4* and *MDAR1 mdar1-2 mdar4 mdar4*, which are heterozygous at the *MDAR1* locus and homozygous for *MDAR4*, occurred at frequencies of 2.3-3.9% and 1.2-4.7%, respectively (Tables 4.6-4.9). These results are far below the expected Mendelian ratio of 12.5%, but it is difficult to explain them in terms of negative selection since genotypes with three mutant alleles (*MDAR1 mdar1-2 mdar4 mdar4*) and a single mutant allele (*MDAR1 mdar1-2 MDAR4 MDAR4*) both had lower than expected frequencies. Similarly, the double mutant homozygote was not the only genotype absent from the F2: the double homozygote wild-type as well as *mdar1-2 mdar1-2 MDAR4 mdar4* and *MDAR1-2 MDAR1-2 MDAR4 mdar4* were also absent from the approximately 250 plants genotyped in the four experiments (Tables 4.6-4.9). Overall, there is a strong tendency to maintenance of the double heterozygote or reversion to the single mutant in F2.

a

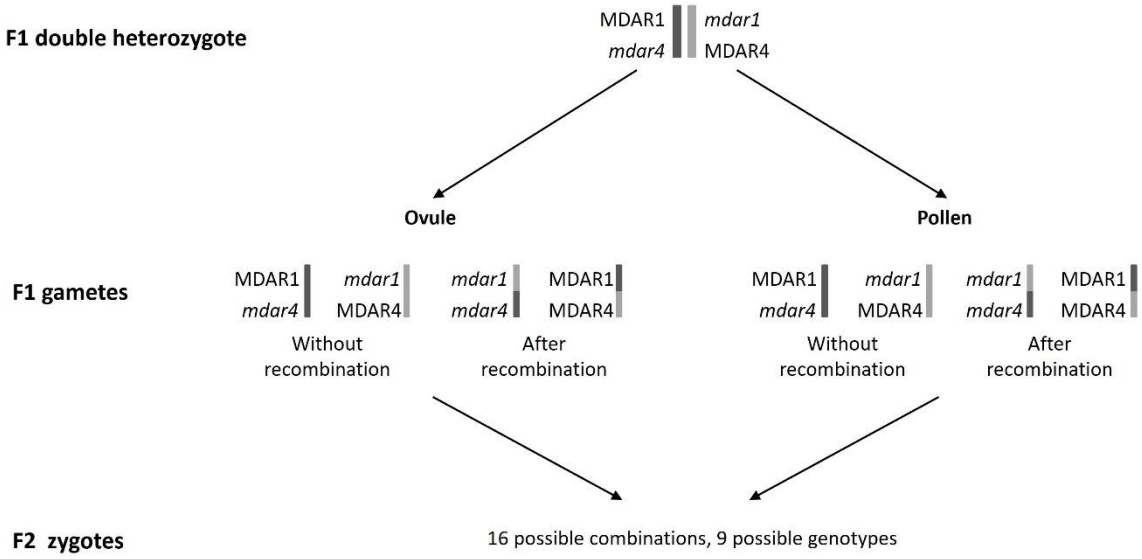

b

Ovule \ Pollen	MDAR1 / mdar4	mdar1 / MDAR4	mdar1 / mdar4	MDAR1 / MDAR4
MDAR1 / mdar4	MDAR1 MDAR1 / mdar4 mdar4 (1)	MDAR1 mdar1 / mdar4 MDAR4 (2)	MDAR1 mdar1 / mdar4 mdar4 (3)	MDAR1 MDAR1 / mdar4 MDAR4 * (4)
mdar1 / MDAR4	mdar1 MDAR1 / MDAR4 mdar4 (5)	mdar1 mdar1 / MDAR4 MDAR4 (6)	mdar1 mdar1 / MDAR4 mdar4 * (7)	mdar1 MDAR1 / MDAR4 MDAR4 (8)
mdar1 / mdar4	mdar1 MDAR1 / mdar4 mdar4 (9)	mdar1 mdar1 / mdar4 MDAR4 * (10)	mdar1 mdar1 / mdar4 mdar4 * (11)	mdar1 MDAR1 / mdar4 MDAR4 (12)
MDAR1 / MDAR4	MDAR1 MDAR1 / MDAR4 mdar4 * (13)	MDAR1 mdar1 / MDAR4 MDAR4 (14)	MDAR1 mdar1 / MDAR4 mdar4 (15)	MDAR1 MDAR1 / MDAR4 MDAR4 * (16)

Figure 4.6. Scheme for the gene recombination and segregation following crosses between *mdar1* and *mdar4* mutants. a. The potential gametes produced by the *MDAR1 mdar1 MDAR4 mdar4* F1 double heterozygotes and their combinations in the F2 generation. b. Summary of the genotypes for all combinations in the F2 generation. In this figure, *mdar1* specifically refers to *mdar1-2*. The combinations with a blue background represent gametes where neither chromosome has undergone recombination. The combinations with a green background represent gametes where one chromosome has undergone recombination. The combinations with a pink background represent gametes where both chromosomes have undergone recombination. *Genotype that was not obtained.

Figure 4.6 schematizes the possible genotypes following a cross between *mdar1-2* and *mdar4* parents. In the F2 generation, according to Mendelian laws, nine possible genotypes are predicted. Within some

of these genotypes, different chromosomal structures can be present (Figure 4.6). For example, 4/16 possible combinations will generate the same double heterozygote as the F1 parent. These are cases 2 and 5, which involve no crossing over, and 12 and 15, which would require crossing over between the two loci during meiosis in both parents; ie, two recombination events (Figure 4.6b). As noted above, the results in Table 4.6-4.9 reveal that only five of the nine genotypes were observed.

Based on the observations, it is hypothesized that during these experiments, the *MDAR1* and *MDAR4* loci showed quite close genetic linkage, leading to a severe distortion of ratios from those predicted by Mendel's laws of independent assortment and segregation. This is perhaps surprising since, although they are found on the same chromosome, the two loci are not very close together. However, recombination frequency is known to vary between different regions so that it is not possible to predict genetic distance from physical distance (Singer et al., 2006). It is important to note that production of double homozygous mutants (and double wild-type homozygotes) from an F1 plant that is heterozygous for two loci on the same chromosome requires crossing over during meiosis in both the female and male parents (Figure 4.6).

Very large-scale genetic analyses in Arabidopsis show that the recombination rate is low compared to other organisms such as yeast, mice, or humans: most individual plants carry only one or two crossing-over events per chromosome, meaning that large non-recombined sections are inherited from each parent (Salomé et al., 2012). Hence, it may be that a greater number of F2 individuals would have to be analyzed to obtain those genetic combinations that we failed to find, including the double mutant. It should be noted that the three genotypes that were consistently over-represented in all four experiments (together accounting for about 90% of plants instead of the predicted 37.5%) were those that result from no recombination events (single homozygous mutants and double heterozygotes: Figure 4.6b, blue squares). By contrast, two of the four genotypes we failed to find in F2 (the double homozygous mutant and double wild-type; cases 11 and 16) require recombination in both parents (Figure 4.6b, pink squares). The other possibilities that would result from a single recombination event in each of the parents (cases 12 and 15) are double heterozygotes (Figure 6B). Since our genotyping analyses cannot distinguish these cases from the double heterozygotes in cases 2 and 5, it is likely that the approximately 50% of F2 plants that had this genotype were simply among those in which no recombination had occurred in either parent (Figure 4.6b).

Simple genetic linkage cannot explain all the observations. First, although no double homozygous mutant was obtained by crossing *mdar1-3* and *mdar4* (Table 4.2), a triple homozygous mutant was obtained in F2 after crossing *cat2 mdar1-3* and *cat2 mdar4* (Table 4.4). Sample sizes were smaller in

these experiments than in those shown in Tables 4.6-4.9, making it difficult to draw any conclusions on the frequencies of specific genotypes, particularly those such as the *mdar1-3 mdar4* double homozygote combination, which are expected at low frequency. However, a comparison of the F2 data for the analyses with *mdar1-3* (Tables 4.2 and 4.4) and *mdar1-2* (Tables 4.6-4.9) reveals that segregation ratios were much less distorted in the former case. This suggests an additional factor is affecting the ratios. One possibility is selection against the stronger allele, *mdar1-2*. This notion seems to be supported by the failure to identify the *mdar1-2 mdar4* double homozygote in the F3 progeny of an F2 sesqui-mutant (Tables 4.10 and 4.11). In this case, linkage cannot be an explanation, since the two mutant alleles (*mdar1-2* and *mdar4*) are already associated on one of the homologs of chromosome 3 in the F2 parent. Hence, it is possible that the two mutations cannot be transmitted through the gametes or that double homozygosity causes early death of any diploid F3 plants. As discussed below, however, this explanation does not seem consistent with results I produced towards the end of this work.

The data shown in Tables 4.10 and 4.11 were obtained using an *MDAR1 mdar1-2 mdar4 mdar4* sesqui-mutant, in which the mutation was homozygous at the *MDAR4* locus. It was not possible to use *mdar1-2 mdar1-2 MDAR4 mdar4,* with the mutation homozygous at the *MDAR1* locus, because no such combination was identified in F2 in any of my experiments (Tables 4.6-4.9). However, it should be noted that an *mdar1-2 mdar1-2 MDAR4 mdar4* combination had been identified earlier in the *cat2* background, and I undertook to analyze the progeny of this plant to confirm that it was indeed possible to obtain a triple *cat2 mdar1-2 mdar4* mutant, as previously found in the laboratory. In contrast to results shown in Tables 4.10 and 4.11, my analysis confirmed that it was indeed possible to obtain a triple *cat2 mdar1-2 mdar4* homozygote by self-fertilization and that, moreover, the frequency was quite close to 25%, as expected for Mendelian segregation at a single locus (Table 4.12). This result therefore argues against strong negative selection linked to the *mdar1-2 mdar4* combination, at least in the *cat2* background. To date, we have not been able to identify the *mdar1-2 mdar1-2 MDAR4 mdar4* combination in F2 in the Col-0 background. Thus, it is not possible to use such a plant to analyze possible effects of decreased catalase on the probability of finding *mdar1-2 mdar4* double mutants.

Table 4.12. Gene segregation analysis in the progeny of *cat2 cat2 mdar1 mdar1-2 MDAR4 mdar4*

Parent genotype:

cat2 cat2 mdar1 mdar1-2 MDAR4 mdar4

Genotype (gene segregation)	Number of plant	Percentage	Expected number	Expected percentage
cat2 cat2 mdar1-2 mdar1-2 MDAR4 MDAR4	52	31.14%	41.75	25%
cat2 cat2 mdar1-2 mdar1-2 MDAR4 mdar4	80	47.9%	83.5	50%
cat2 cat2 mdar1-2 mdar1-2 mdar4 mdar4	35	20.96%	41.75	25%
Total	167	100%	167	100%

In summary, despite considerable effort, it was not possible within the time available to complete this study to arrive at definitive conclusions on what is happening during the crosses between *mdar1* and *mdar4* lines. Linkage is certainly one factor that can affect segregation frequencies and seems to be important in the case of the *mdar1-2* mutation. Selection might be occurring, but further experiments, perhaps on even larger scale, would be required to assess its strength. It is possible that both the strength of selection and the frequency of recombination might be affected by some of the mutations studied here, leading to results that are difficult to explain by the application of general principles. Based on some of the observations, we can tentatively hypothesize that the additional presence of the *cat2* mutation favors recovery of *mdar1 mdar4* double mutants, but further work would be required to test this idea more fully.

CHAPTER 5 GENERAL CONCLUSIONS AND PERSPECTIVES

The plant H_2O_2 processing system has been extensively studied, with catalase and the ascorbate-glutathione pathway thought to play pivotal roles in maintaining cellular redox balance. However, the specific roles of certain proteins within this system remain underexplored. MDHAR participates in the system by reducing MDHA to ascorbate in an NAD(P)H-dependent reaction, thus contributing to the maintenance of the cellular redox state. The overall focus of this work was to throw new light on the importance of MDHAR within the H_2O_2 processing system in Arabidopsis.

Catalase, a primary enzyme responsible for scavenging excess H_2O_2, plays a crucial role in protecting plants from oxidative stress. When catalase capacity is decreased in the *cat2* mutant, there is an increased reliance on the ascorbate-glutathione pathway (Mhamdi et al., 2010a,b). Further, loss of *CAT2* function triggers the salicylic acid (SA) synthesis pathway under conditions that are optimal for growth of catalase-replete plants, resulting in leaf lesions and a notable decrease in the fresh weight of Arabidopsis rosettes. Consequently, my thesis work also investigated whether the loss of MDHAR functions in the context of CAT deficiency, could influence the phenotype and underlying mechanisms associated with *cat2* mutants.

Since the single *mdar* mutants do not display distinct phenotypes under optimal conditions, we hypothesized that functional redundancy may occur between MDHAR1 and MDHAR4 in peroxisomes. To explore this, we investigated whether the simultaneous presence of mutations for the peroxisomal *MDAR1* and *MDAR4* genes would result in a distinct phenotype in Arabidopsis. Unfortunately, it was not possible to obtain such plants, and the genetic analysis I performed has to date been unable to establish why.

5.1 Conclusions

5.1.1 MDHAR1 and MDHAR2 are the major contributors to NADH and NADPH-dependent activities, respectively

In this study, we observed that the recombinant MDHAR2 was able to utilize both NADH and NADPH as cofactors. It is noteworthy that like MDHAR1, MDHAR2 has a higher efficiency using NADH compared to NADPH. This suggests that it will reach near-maximal activity at a concentration of 250 µM when NADPH is used as a cofactor, which is significantly more efficient compared to peroxisomal MDHAR1 (Table 3.1; Figure S3.3). In light of this, and considering the studies that assessed the extractable activity of MDHAR, it is evident that the NADPH-dependent activity is largely influenced by the expression levels of the *MDAR2* gene.

The high catalytic efficiency of MDHAR1 with NADH, particularly in its role as a peroxisomal isoform, suggests that it plays a significant role in antioxidant defence within the peroxisomes. This is because a high catalytic efficiency indicates that the enzyme can effectively reduce MDHA to ascorbate, which is an important antioxidant molecule. As peroxisomes are sites of ROS production due to processes like fatty acid β-oxidation (Eastmond, 2007; Kunau et al., 1995), photorespiration (Foyer & Noctor, 2000) and the glyoxylate cycle (Corpas et al., 2001; Foyer et al., 2009; Sandalio et al., 2013), the presence of MDHAR1 can help to mitigate oxidative stress by replenishing the pool of ascorbate, thus maintaining the redox balance within the organelle.

In interpreting the results on the co-factor preference, it is necessary to distinguish between three types of activity that might provide very different information: (1) activity of the purified recombinant protein, which can define the kinetic characteristics of an individual enzyme; (2) activity in tissue extracts of specific mutants, which can estimate the contribution of a given isoform to the overall activity measured *in vitro*; (3) the real *in vivo* activity, which in the cases of enzymes such as MDHAR is very difficult to measure. We cannot easily extrapolate from recombinant enzyme activity to co-factor preference *in planta*, because information on NADH and NADPH concentrations are fragmentary and they might be very different from each other (Heineke et al., 1991; Lim et al., 2020; Smith et al., 2021). However, information from the recombinant protein data can be used to inform the interpretation of the measurements in leaf extracts. For example, we can compare the K_M values obtained for the recombinant protein (3.5 and 9.5 µM for NADH and NADPH, respectively, for MDHAR2; Table 3.1) to the co-factor concentrations used in the standard MDHAR assays of tissue extracts, which were 250 µM for both NADH or NADPH. At these concentrations, the low K_M values of MDHAR2 should mean the enzyme shows a fairly similar activity with the two co-factors. Data shown in Chapter 3 are consistent with this: the *mdar2* mutation decreased the extractable NADPH-dependent activity by about 10 $nmol.mg^{-1}prot.min^{-1}$, which corresponds to about 50% of the total activity with this co-factor, in the Col-0 background (Figure 3.1b). As discussed in Chapter 3, a decrease of 10 $nmol.mg^{-1}prot.min^{-1}$ is hard to detect against the background of the much higher total activities of NADH-dependent activity (Figure 3.1b). In the *cat2* background, where *MDAR2* is induced at the transcript level and the total extractable activities are increased, the *mdar2* mutation has a greater effect and decreases both extractable activities significantly (Figure 3.3). Nevertheless, the *mdar2* mutation has a greater proportional effect on the NADPH-dependent activity because the total extractable activity of NADH-dependent activity is much higher (Figure 3.3a). To infer effects on *in vivo* activities, it is necessary to know the co-factor concentrations in the cytosol, where MDHAR2 is located. Relevant data are as yet scarce, but it is thought that NADH is very low (at or below 1µM; Heineke et al., 1991). If so, the

extractable activities measured at 250 µM would be over-estimating the cytosolic NADH-dependent activity *in vivo*. Further work, notably with *in vivo* probes that are able to quantify NADH and NADPH concentrations in various compartments, might help to throw further light on this question.

5.1.2 Specific MDHAR isoforms play roles in response to oxidative stress

As reported in Chapter 3, from the results in Col-0 background, it is evident that the expression levels of *MDAR1* and *MDAR4*, which are localized in peroxisomes, are comparable, while the expression of *MDAR2* and *MDAR3*, which are cytosolic, differ by nearly two orders of magnitude. This differential gene expression suggests that, in contrast to MDHAR2, MDHAR3 may not play a particularly important role in many Arabidopsis leaf cells. This hypothesis has been confirmed by our research.

Under optimal conditions, none of the MDHARs seem to play an irreplaceable role. However, a key concept in oxidative stress research is that antioxidant enzymes become particularly important in stress conditions, when ROS production is increased. Hence, we chose to introduce the *mdar* mutations into the *cat2* background to test their functions in oxidative stress environment. This initiative allowed us to observe two effects of loss of specific MDHAR function. First, loss of peroxisomal MDHAR functions in the *cat2* background causes some decrease in rosette fresh weight. While this is understandable, given the location of CAT2 primarily in the peroxisomes, its relationship to increased oxidative stress is not clear. Indeed, at the developmental stage our measurements were performed, little evidence was obtained that *MDAR4* contributes greatly to total extractable activity, either with NADH or NADPH (Figure 3.1b and 3.3a). Further work is required to analyse the processes underlying these observations.

The second effect was that the *mdar2* mutation strongly inhibited *cat2*-induced leaf lesion formation (Figure 3.4a). As this effect was relevant to certain observations previously reported by the laboratory for other factors involved in the ascorbate-glutathione pathway (Mhamdi et al., 2010a; Rahantaniaina et al., 2017), it turned out to be a major focus of the present work. Through additional studies analysing SA content, as well as the expression of pathogenesis-related genes and *ICS1* which is involved in SA biosynthesis pathway, we observed that MDHAR2 plays an influential role in the *cat2*-triggered SA pathway; ie, its absence in *cat2 mdar2* annuls a large part of the up-regulation of the SA and related pathways by oxidative stress. Even though the *cat2*-triggered accumulation of SA is suppressed in the *cat2 mdar2* mutant, the deficiency of MDHAR2 increases glutathione oxidation, indicating a complex interaction between oxidative stress regulation and the SA pathway in the *cat2 mdar2* mutant.

Analysis of the *cat2 mdar2*-MDHAR2 complemented lines confirmed the essential role of MDHAR2 in maintaining the glutathione redox state, and linking oxidative stress to the activation of pathogenesis-related pathways. As well as the SA pathway, we observed that *MDAR2* expression was correlated with the expression of JA markers (*PDF1.2*, *VSP2*). This recalls observations in GR-deficient plants (*cat2 gr1*; Mhamdi et al., 2010a), as well as lines deficient in glutathione itself (*cat2 cad2*; Han et al., 2013a,b). In both *cat2 gr1* and *cat2 cad2*, oxidative stress-triggered induction of both SA and JA markers is antagonised. This perhaps points to some role for alterations in glutathione in mediating the effects of *MDAR2*. However, this hypothesis does not fit well with other data, as discussed in the next section.

5.1.3 The cytosolic ascorbate-glutathione pathway is important in linking oxidative stress to downstream responses

Several previous studies have introduced secondary mutations into the *cat2* background and reported their effects on the phytohormone-related signaling that can be triggered by oxidative stress. One relevant example is DHAR, which is closely related to MDHAR in the ascorbate-glutathione pathway. As previously reported, *cat2* requires at least two DHAR gene mutations to suppress leaf lesion formation (Rahantaniaina et al., 2017). No single *dhar* mutant exhibits effects as pronounced as the *mdar2* single mutant reported here. As noted above, MDHAR2 makes a major contribution to NADPH-dependent activity in both the Col-0 and *cat2* background, while *MDAR3*, also encoding a cytosolic isoform, seems to contribute little to leaf activity in either genetic context (Figure 3.1 and 3.3). Moreover, SA and glutathione assays in the *cat2 mdar2*-MDHAR2 complemented lines confirmed that MDHAR2 plays a critical role in the cytosol, particularly in the *cat2*-triggered SA pathway and in maintaining the glutathione redox state.

While loss of DHAR and MDHAR functions can decrease the response to oxidative stress, neither has strong effects on leaf ascorbate pools, presumably reflecting the redundancy of different ascorbate-regenerating systems. In terms of glutathione, opposing effects of the two types of mutation are observed. In *cat2 dhar* mutants, much of the *cat2*-triggered oxidation is abolished (Rahantaniaina et al., 2017). Since DHAR uses GSH as a reductant, this observation suggests that most of the glutathione oxidation is DHAR-dependent. In view of this, the opposite effect (ie, an increase in GSSG relative to *cat2*) observed in the *cat2 mdar2* mutant might be partly due to enhanced accumulation of H_2O_2 but is also explainable in terms of increased conversion of MDHA to DHA, leading to enhanced oxidation of GSH to GSSG (Figure 3.9). Thus, MDHAR2 plays a critical role in maintaining glutathione in its reduced form, while DHAR isoforms, in contrast, promote the oxidation of GSH. Despite this, both *dhar* and *mdar2* mutations decrease SA content in the *cat2* background (Rahantaniaina et al., 2017; Chapter

3). From the observation that both *dhar* and *mdar2* mutations suppress the *cat2*-triggered SA pathway but result in opposite effects on the glutathione redox state, it seems the relationship between the induction of the SA pathway by H_2O_2 and glutathione redox state is not a straightforward causal connection.

Other studies have also reported effects of different mutations on the *cat2* phenotype. Like *mdar2*, the *gsnor1* mutation suppresses the leaf lesions observed in *cat2* (Zhang et al., 2020). When GSNOR is knocked out in the *cat2* background, the reduced activity of GSNOR leads to elevated levels of *S*-nitrosoglutathione (GSNO), an important player in protein *S*-nitrosylation. Increased NO signals counteract the effects of excess H_2O_2 by modulating redox signaling and alleviating oxidative stress, thereby preventing the formation of leaf lesions. Also, loss-of-function mutants for cytosolic glutathione reductase (*gr1*) mitigate leaf lesions triggered by CAT2 deficiency (Mhamdi et al., 2010b). Other ongoing work within the laboratory also highlights the importance of cytosolic redox factors in mediating signaling triggered by oxidative stress.

5.1.4 Interplay between MDHAR2 and CAT2

The *cat2* mutant exhibits significant transcriptional reprogramming in response to oxidative stress, particularly in processes related to photosynthesis, senescence, immunity, and cell death. Both the *mdar2* single and the *dhar1 dhar2 dhar3* triple mutant appear to mitigate some of these effects induced in *cat2*, restoring certain aspects closer to those observed in Col-0 (Figure3.5). This suggests that these ascorbate-regenerating enzymes may regulate these biological processes and hence play a role in acclimation to adverse conditions.

When *CAT2* is mutated, resulting in oxidative stress, MDHAR2 interacts with proteins involved in a broad range of biological processes (Figure 3.8). It is clear from the transcriptomic data that the *cat2* mutation has a widespread impact on various pathways, particularly those related to biotic stress responses and phytohormone signaling processes, and that part of this influence is mediated by MDHAR2 (ie, decreased in *cat2 mdar2* compared to *cat2*). Therefore, one hypothesis is that the leaf lesion formation and associated gene expression patterns observed in the *cat2* mutant may be due to the interaction of MDHAR2 with one or more specific proteins identified in the interactome work. A model of MDHAR2-dependent protein interactions in leaf lesion formation in the *cat2* background is shown in Figure 5.1.

Overall, the transcriptomic and interactome analyses suggest that MDHAR2 engages in a complex functional or physical interplay with other proteins, highlighting the complex role of this enzyme in oxidative stress and, possibly, pathogen defence. The interactome data might imply that MDHAR2 is involved in a multifaceted network of interactions that modulate the plant response to oxidative stress, possibly by affecting protein complexes crucial for maintaining redox homeostasis and regulating the SA pathway (Figure 5.1).

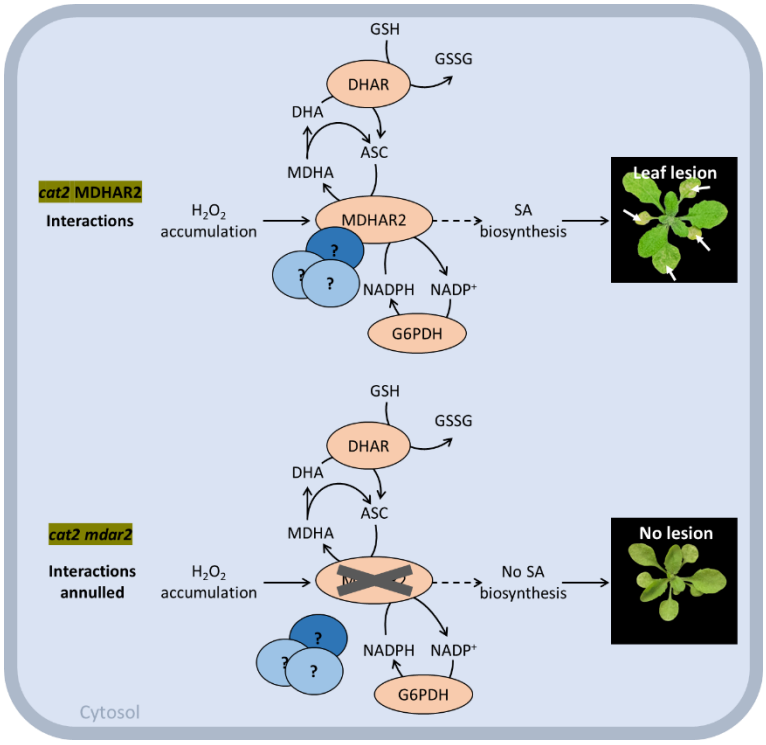

Figure 5.1. Model of MDHAR2-dependent protein interactions in leaf lesion formation in the *cat2* background.

5.1.5 Double *mdar* mutant production

The *mdar1-3 mdar4* double mutant has been successfully generated during this work. Similarly, the laboratory had previously succeeded in generating a viable double *mdar2 mdar3* mutant, in which both cytosolic isoforms are knocked out. However, attempts to obtain the double peroxisomal *mdar1-2 mdar4* knockout have been unsuccessful, even though I confirmed a previous laboratory observation that a triple *cat2 mdar1-2 mdar4* mutant can be obtained. Although we cannot rule out a positive effect of the *cat2* mutation on the probability of obtaining the *mdar1 mdar4* combination, it is clear that tight linkage can be observed between the *MDAR1* and *MDAR4* loci. Hence, it is possible that the

successful production of *cat2 mdar1-2 mdar4* but not *mdar1-2 mdar4* can be ascribed to chance. However, one conclusion from the work reported in Chapter 4 is that any linkage that is observed seems to be genotype-dependent, since it was observed to be strong in attempts to associate the *mdar1-2* and *mdar4* alleles but less so during the production of the *mdar1-3 mdar4* double mutant. One possibility is that genetic rearrangement has occurred in these lines, or is occurring during the crosses. As it is, and despite the investment of effort in the genetic analyses, we have not been able to distinguish the causes of the difficulties in obtaining the *mdar1-2 mdar4* double mutant within this work.

5.2 Perspectives

My study raises several perspectives for future research. Notably, questions arise regarding whether the differences in lesion formation, suppression of the SA pathway, and glutathione oxidation observed in *cat2 mdar2* compared to *cat2* are due to the interaction between MDHAR2 and its associated proteins in *cat2* background. Furthermore, the possibility of other pathways being involved in these effects warrants further investigation. Some of the perspectives coming out of this thesis are described below.

5.2.1 Short-term perspectives

Several experiments appear interesting in the light of the findings highlighted in this work. Some of these were envisaged within the timescale of the thesis. Although this turned out not to be possible, some of the experiments are relatively simple and might be envisaged in the near future.

5.2.1.1 Effects of antioxidative enzyme deficiency on H_2O_2 levels

One question that remains unresolved is that of leaf H_2O_2 contents in our different systems. This has been an issue for several years, given that the laboratory has extensively used the *cat2* mutant as a model oxidative stress system. Despite the obvious signs of oxidative stress in this line, it has not been possible to demonstrate a sustained, marked increase in leaf contents of this key oxidant. Possible reasons for this include technical issues that have been previously discussed (Queval et al., 2008; Noctor et al., 2016) as well as the presence of reductant-based antioxidant systems that are able to replace catalase in keeping concentrations of this molecule at low levels. Indeed, the present work adds further evidence that reductant-based systems are strongly induced to stabilise tissue redox state in response to catalase deficiency. Nevertheless, it is likely that H_2O_2 increases to some extent when antioxidative enzymes are removed, at least locally and/or transiently, and genetically encoded sensors

would seem ideal to analyse this issue. Despite the keen interest elicited by these systems, their use is far from trivial, especially in the mesophyll cells of mature leaves, which is our main focus of interest. Further, introducing these genetically encoded sensors into lines already carrying T-DNA sequences often leads to gene silencing, an issue that becomes increasingly problematic in double or triple mutants. Nevertheless, given the interest of these systems to report on relative changes in H_2O_2 concentrations, we are still endeavouring to introduce them into several of our different lines.

5.2.1.2 Roles of different MDHARs in responses to other stresses

Although the main objective of this work was to establish the roles of specific *MDAR* genes in optimal and oxidative stress conditions, it would be interesting to test their importance in other challenging conditions. These could include exposing the mutants to cold, heavy metals, or atmospheric pollution, all conditions in which oxidative stress is known to be involved. Given the observed impact of the *mdar2* mutation on oxidative stress-triggered defence phytohormone pathways, we could envisage to test the response of this (and other *mdar*) mutants to pathogens, for example, bacteria and fungi that are known to elicit the SA and JA pathways in plants.

5.2.1.3 Exploring the potential role of oxidized forms of ascorbate

One of the hypotheses generated by the work in Chapter 3 is that oxidized forms of ascorbate could have some role in signaling, particularly in oxidative stress conditions. Less attention has focused on this possibility compared to the keen interest in the roles of oxidized glutathione forms, such as GSSG and, particularly, GSNO. This is probably because biochemical mechanisms are less apparent. The idea therefore remains entirely hypothetical. Nevertheless, it could be tested by treating leaves with oxidized forms of ascorbate to explore whether this elicits any increase in marker genes for phytohormone signaling pathways. Potentially, it is possible to treat leaves directly with DHA, which is commercially available. In the case of MDHA, it would be necessary to generate this unstable form. One possibility is to treat plants with ascorbate oxidase, which converts ascorbate to MDHA in a ROS-independent manner (Pignocci et al., 2006).

5.2.1.4 The role of the fifth *MDAR* gene in oxidative stress

While this work has focused on the four genes encoding cytosolic and peroxisomal MDHARs, a fifth gene (*MDAR5/6*) encodes a protein that is dual-addressed to the chloroplast (MDHAR6) and mitochondrion (MDHAR5). At the outset of this work, the aim was to include this gene in the analysis, but mutant lines that were unambiguously knockouts could not be characterized. Nevertheless, the

availability of such lines would enable us to add to the information reported here. It is noteworthy that a significant part of the extractable NADH-dependent MDHAR activity cannot be easily accounted for by the four genes we have analysed here (Figure 3.1) and it is possible that this residual activity is due to *MDAR5/6*. Further, loss of the mitochondrial MDHAR5 function has been reported to enhance tolerance to certain xenobiotics (Johnston et al., 2015) while the chloroplast MDHAR6 is regulated by TRX (Vanacker et al., 2018). It would therefore be interesting to test the functional significance of this gene in an oxidative stress background.

5.2.1.5 A wider analysis of metabolism

Part of this work involved a transcriptomic analysis of *cat2 mdar2* (Chapter 3). It could be interesting to complement these data by a metabolite profiling analysis. This could involve a non-specific analysis by gas chromatography-mass spectrometry (GC-MS), for which several datasets have been produced for *cat2* and other mutants (Noctor et al., 2015). Given that several enzymes involved in cytosolic NADH and NADPH production were identified as potential MDHAR2 interactants (GAPC, NADP-ME2, c-ICDH), GC-MS analysis could shed some light on the response of compounds such as sugars, organic acids, and amino acids in the different lines. These metabolite data could be complemented by analysing the activities of key enzymes involved in respiratory pathways as well as ATP/ADP and NAD(P)H/NAD(P)$^+$ ratios. This could allow an assessment of the link between oxidative stress and glycolysis and related pathways, particularly related to MDHAR and GR, the two enzymes of the ascorbate-glutathione pathway that require NAD(P)H.

5.2.2 Longer-term perspectives

Several approaches are envisageable to continue the analysis of pathways involved in the response to oxidative stress. In particular, it would be interesting to generate confirmatory data on the protein interactants identified in Chapter 3. In the longer term, forward genetics approaches based on mutagenesis could be used, although this is a time-consuming project and is already being employed by other laboratories at the international context.

5.2.2.1 Yeast two-hybrid (Y2H) system for verifying the interactions of MDHAR2 and the candidate proteins

To verify the significance of MDHAR2 interactions with other proteins, several techniques could be employed. One example is a yeast two-hybrid (Y2H) screening system (Joung et al., 2000). Y2H is a molecular biology technique used to detect protein-protein interactions (PPIs) by testing for physical

interactions, such as binding, between two proteins or between a protein and a DNA molecule. Through Y2H, we can confirm the specific interactions or binding between MDHAR2 and the candidate proteins. The goal is to identify proteins that interact with MDHAR2 and contribute to leaf cell death in the *cat2* mutant, and subsequently explore whether these proteins are involved in other signalling pathways. However, this hypothesis assumes that the interaction between MDHAR2 and its interactants leads to leaf lesions in the *cat2* background. The exact role of these interactants in the reprogramming process in *cat2* remains to be further explored.

5.2.2.2 Forward genetics screens for other lesion suppressors in *cat2*

The work reported in this thesis adds *mdar2* to a group of mutants that have been shown to suppress lesions in *cat2*. As well as a mutant for isochorismate synthase 1 (ICS1, involved in SA synthesis), these include mutants for other enzymes of the ascorbate-glutathione pathway or associated redox factors (Chaouch et al., 2010; Mhamdi et al., 2010a; Rahantaniaina et al., 2017; Zhang et al., 2020). Uncovering the detailed mechanism of the links between redox factors and leaf lesion formation in *cat2* is a challenging endeavour. One approach is to perform a secondary forward genetics screen in *cat2* after chemical mutagenesis. Ethyl methane sulfonate (EMS), a widely used chemical mutagen, functions as an alkylating agent that leads to chemical modifications of nucleotides and induces mutations in the genome (Chen et al., 2023; Sega, 1984; Fu et al., 2012). The extent of mutations is dose-dependent, and a well-established protocol has been used to produce several populations of mutants in our laboratory.

To search for genes involved in linking oxidative stress to the formation of leaf lesions and the activation of the salicylic acid (SA) pathway, screening could be conducted on a population of *cat2* plants generated from seeds treated with an appropriate dose of EMS. The plants that show annulled leaf lesion formation would be candidates, and whole-genome sequencing would be performed to identify the genes that are affected. It would be particularly interesting to determine whether there are mutations in the genes encoding the proteins shown in the protein interactome shown in Figure 3.8.

5.2.2.3 Functional relationship between MDHAR2 and various pathways

From the MDHAR2-GFP pull-down experiments in the *cat2 mdar2* background, interactions with several proteins were observed (Chapter 3). These included proteins involved in the regulation of oxidative stress, phytohormone function, and respiratory metabolism. The list of proteins can be considered as a group of candidates whose interactions with MDHAR2 at the functional level could be

tested using mutants or overexpressors. Once their interactions with MDHAR2 are better characterized, it could be possible to choose proteins worthy of further study. Given the number of potential candidates, proteins would have to be selected based on the criteria such as the interaction strength and available knowledge. One possibility is to focus on the NAD(P)H-producing pathways mentioned above in section 5.2.1.5. Another is the ABA signaling pathway, since two interactants were observed, including ABCG40 (Figure 3.8). Indeed, ABA and SA are known to interact both synergistically and antagonistically, with ABA promoting SA accumulation under certain stress conditions and SA inhibiting ABA signaling by interfering with ABA receptor components, maintaining a balance in stress responses (Chen et al., 2020; Parwez et al., 2022). By investigating the role of MDHAR2 in the ABA signaling pathway, we can further our understanding of the *cat2*-triggered SA pathway. Experiments that could be performed include treating *cat2*, *mdar2*, *abcg40* single mutants, and *cat2 mdar2*, *cat2 abcg40* double mutants with ABA and analysing the extent of known ABA-triggered responses, such as growth inhibition and stomatal closure rates. The expression of ABA marker genes (e.g., *RD29A*, *RAB18* and *DREB2A*) could also be used to verify the interplay between MDHAR2 and ABCG40 in ABA responses.

REFERENCES

Al-Hajaya, Karpinska B, Foyer CH, Baker A (2022) Nuclear and peroxisomal targeting of catalase. Plant Cell Environ **45**: 1096-1108

Aliverti A, Curti B, Vanoni MA (1999) Identifying and quantitating FAD and FMN in simple and in iron-sulfur-containing flavoproteins. Methods Mol Biol **131**: 9-23

Alonso JM, Hirayama T, Roman G, Nourizadeh S, Ecker JR (1999) EIN2, a bifunctional transducer of ethylene and stress responses in Arabidopsis. Science **284**: 2148-2152

Alonso JM, Stepanova AN, Leisse TJ, Kim CJ, Chen H, Shinn P, Stevenson DK, Zimmerman J, Barajas P, Cheuk R (2003) Genome-wide insertional mutagenesis of *Arabidopsis thaliana*. Science **301**: 653-657

Alonso-Blanco C, Aarts MGM, Bentsink L, Keurentjes JJB, Reymond M, Vreugdenhil D, Koornneef M (2009) What has natural variation taught us about plant development, physiology, and adaptation? Plant Cell **21**: 1877-1896

Anas M, Liao F, Verma KK, Sarwar MA, Mahmood A, Chen ZL, Li Q, Zeng XP, Liu Y, Li YR (2020) Fate of nitrogen in agriculture and environment: agronomic, eco-physiological and molecular approaches to improve nitrogen use efficiency. Biol Res **53**: 47

Andrés CMC, Pérez de la Lastra JM, Andrés Juan C, Plou FJ, Pérez-Lebeña E (2023) Superoxide anion chemistry-its role at the core of the innate immunity. Int J Mol Sci **24**: 1841

Antoniw JF, White RF (1980) The effects of aspirin and polyacrylic acid on soluble leaf proteins and resistance to virus infection in five cultivars of tobacco. J Phytopathol **98**: 331-341

Apel K, Hirt H (2004) REACTIVE OXYGEN SPECIES: metabolism, oxidative stress, and signal transduction. Annu Rev Plant Biol **55**: 373-399

Arnér ES, Holmgren A (2000) Physiological functions of thioredoxin and thioredoxin reductase. Eur J Biochem **267**: 6102-6109

Asada K (1992) Ascorbate peroxidase – a hydrogen peroxide-scavenging enzyme in plants. Physiol Plant **85**: 235-241

Asada K (2006) Production and scavenging of reactive oxygen species in chloroplasts and their functions. Physiol Plant **141**: 391-396

Attacha S, Solbach D, Bela K, Moseler A, Wagner S, Schwarzländer M, Aller I, Müller SJ, Meyer AJ (2017) Glutathione peroxidase-like enzymes cover five distinct cell compartments and membrane surfaces in *Arabidopsis thaliana*. Plant Cell Environ **40**: 1281-1295

Awad J, Stotz HU, Fekete A, Krischke M, Engert C, Havaux M, Berger S, Mueller MJ (2015) 2 cysteine peroxiredoxins and thylakoid ascorbate peroxidase create a water-water cycle that is essential to protect the photosynthetic apparatus under high light stress conditions. Plant Physiol **167**: 1592-1603

Bai J, Cederbaum AI (2001) Mitochondrial catalase and oxidative injury. Biol Signals Recept **10**: 189-199

Bashandy T, Guilleminot J, Vernoux T, Caparros-Ruiz D, Ljung K, Meyer Y, Reichheld JP (2010) Interplay between the NADP-linked thioredoxin and glutathione systems in Arabidopsis auxin signaling. Plant Cell **22**: 376-391

Belenky P, Bogan KL, Brenner C (2007) NAD^+ metabolism in health and disease. Trends Biochem Sci **32**: 12-19

Bérczi A, Møller IM (1998) NADH-monodehydroascorbate oxidoreductase is one of the redox enzymes in spinach leaf plasma membranes. Plant Physiol **116**: 1029-1036

Bienert GP, Møller AL, Kristiansen KA, Schulz A, Møller IM, Schjoerring JK, Jahn TP (2007) Specific aquaporins facilitate the diffusion of hydrogen peroxide across membranes. J Biol Chem **282**: 1183-1192

Bohrer AS, Massot V, Innocenti G, Reichheld JP, Issakidis-Bourguet E, Vanacker H (2012) New insights into the reduction systems of plastidial thioredoxins point out the unique properties of thioredoxin z from Arabidopsis. J Exp Bot **63**: 6315-6323

Borraccino G, Dipierro S, Arrigoni O (1986) Purification and properties of ascorbate free-radical reductase from potato tubers. Planta **167**: 521-526

Boutros T, Chevet E, Metrakos P (2008) Mitogen-activated protein (MAP) kinase/MAP kinase phosphatase regulation: roles in cell growth, death, and cancer. Pharmacol Rev **60**: 261-310

Bradford, MM (1976) A rapid and sensitive method for the quantitation of microgram quantities of protein utilizing the principle of protein-dye binding. Anal Biochem **72**:248-254

Brown LA, Baker A (2008) Shuttles and cycles: transport of proteins into the peroxisome matrix (Review). Mol Membr Biol **25**: 363-375

Bueso E, Alejandro S, Carbonell P, Perez-Amador MA, Fayos J, Bellés JM, Rodriguez PL, Serrano R (2007) The lithium tolerance of the Arabidopsis *cat2* mutant reveals a cross-talk between oxidative stress and ethylene. Plant J **52**: 1052-1065

Cadenas E, Boveris A, Ragan CI, Stoppani AOM (1977) Production of superoxide radicals and hydrogen peroxide by NADH-ubiquinone reductase and ubiquinol-cytochrome *c* reductase from beef-heart mitochondria. Arch Biochem Biophys **180**: 248-257

Cairns NG, Pasternak M, Wachter A, Cobbett CS, Meyer AJ (2006) Maturation of Arabidopsis seeds is dependent on glutathione biosynthesis within the embryo. Plant Physiol **141**: 446-455

Cardona T, Shao S, Nixon PJ (2018) Enhancing photosynthesis in plants: the light reactions. Essays Biochem **62**: 85-94

Caverzan A, Passaia G, Barcellos Rosa S, Ribeiro CW, Lazzarotto F, Margis-Pinheiro M (2012) Plant responses to stresses: Role of ascorbate peroxidase in the antioxidant protection. Genet Mol Biol **35**: 1011-1019

Chai J, Liu J, Zhou J, Xing D (2014) Mitogen-activated protein kinase 6 regulates *NPR1* gene expression and activation during leaf senescence induced by salicylic acid. J Exp Bot **65**: 6513-6528

Chandel NS, McClintock DS, Feliciano CE, Wood TM, Melendez JA, Rodriguez AM, Schumacker PT (2000) Reactive oxygen species generated at mitochondrial complex III stabilize hypoxia-inducible factor-1α during hypoxia: a mechanism of O_2 sensing. J Biol Chem **275**: 25130-25138

Chaouch S, Queval G, Vanderauwera S, Mhamdi A, Vandorpe M, Langlois-Meurinne M, van Breusegem F, Saindrenan P, Noctor G (2010) Peroxisomal hydrogen peroxide is coupled to biotic defense responses by ISOCHORISMATE SYNTHASE1 in a daylength-related manner. Plant Physiol **153**: 1692-1705

Cheeseman JM (2007) Hydrogen peroxide and plant stress: a challenging relationship. Plant Stress **1**: 4-15

Chelikani P, Fita I, Loewen PC (2004) Diversity of structures and properties among catalases. Cell Mol Life Sci **61**: 192-208

Chen K, Li GJ, Bressan RA, Song CP, Zhu JK, Zhao Y (2020) Abscisic acid dynamics, signaling, and functions in plants. J Integr Plant Biol **62**: 25-54

Chen L, Duan L, Sun M, Yang Z, Li H, Hu K, Yang H, Liu L (2023) Current trends and insights on EMS mutagenesis application to studies on plant abiotic stress tolerance and development. Front Plant Sci **13**: 1052569

Chen Z, Gallie DR (2004) The ascorbic acid redox state controls guard cell signaling and stomatal movement. Plant Cell **16**: 1143-1162

Cheng CY, Krishnakumar V, Chan AP, Thibaud-Nissen F, Schobel S, Town CD (2017) Araport11: a complete reannotation of the *Arabidopsis thaliana* reference genome. Plant J **89**: 789-804

Chew O, Whelan J, Millar AH (2003) Molecular definition of the ascorbate-glutathione cycle in Arabidopsis mitochondria reveals dual targeting of antioxidant defenses in plants. J Biol Chem **278**: 46869-46877

Chung JS, Zhu JK, Bressan RA, Hasegawa PM, Shi H (2008) Reactive oxygen species mediate Na^+-induced *SOS1* mRNA stability in Arabidopsis. Plant J **53**: 554-565

Clough SJ, Bent AF (1998) Floral dip: A simplified method for *Agrobacterium*-mediated transformation of *Arabidopsis thaliana*. Plant J **16**: 735-743

Conklin PL, Foyer CH, Hancock RD, Ishikawa T, Smirnoff N (2024) Ascorbate acid metabolism and functions. J Exp Bot **75**: 2599-2603

Corpas FJ, Barroso JB, del Río LA (2001) Role for peroxisomes as a source of reactive oxygen species and nitric oxide signal molecules in plant cells. Trends Plant Sci **6**: 145-150

Corpas FJ, Barroso JB, Sandalio LM, Distefano S, Palma JM, Lupiáñez JA, Del Río LA (1998) A dehydrogenase-mediated recycling system of NADPH in plant peroxisomes. Biochem J **330**:777-784

Crantz AA, Brummell DA, Bennett AB (1995) Ascorbate free radical reductase mRNA levels are induced by wounding. Plant Physiol **108**: 411-418

D'Autréaux B, Toledano MB (2007) ROS as signalling molecules: mechanisms that generate specificity in ROS homeostasis. Nat Rev Mol Cell Biol **8**: 813-824

Dabrowski A, Boguslowicz C, Dabrowska M, Tribillo I, Gabryelewicz A (2000) Reactive oxygen species activate mitogen-activated protein kinases in pancreatic acinar cells. Pancreas **21**: 376-384

Dalton D A, Langeberg L, Robbins M (1992) Purification and characterization of monodehydroascorbate reductase from soybean root nodules. Arch Biochem Biophys **292**: 281-286

Dat JF, Inzé D, Van Breusegem F (2001) Catalase-deficient tobacco plants: tools for *in planta* studies on the role of hydrogen peroxide. Redox Rep **6**: 37-42

Davletova S, Rizhsky L, Liang H, Shengqiang Z, Oliver DJ, Coutu J, Shulaev V, Schlauch K, Mittler R. (2005) Cytosolic ascorbate peroxidase 1 is a central component of the reactive oxygen gene network of Arabidopsis. Plant Cell **17**: 268-281

De Leonardis S, De Lorenzo G, Borraccino G, Dipierro S (1995) A specific ascorbate free radical reductase isozyme participates in the regeneration of ascorbate for scavenging toxic oxygen species in potato tuber mitochondria. Plant Physiol **109**: 847-851

De Vos M, Van Oosten VR, Van Poecke RMP, Van Pelt JA, Pozo MJ, Mueller MJ, Buchala AJ, Métraux JP, Van Loon LC, Dicke M, et al (2005) Signal signature and transcriptome changes of *arabidopsis* during pathogen and insect attack. Mol Plant Microbe Interact **18**: 923-937

Dean J V, Shah RP, Mohammed LA (2003) Formation and vacuolar localization of salicylic acid glucose conjugates in soybean cell suspension cultures. Physiol Plant **118**: 328-336

Del Río LA, Corpas FJ, Sandalio LM, Palma JM, Gomez M, Barroso JB (2002) Reactive oxygen species, antioxidant systems and nitric oxide in peroxisomes. J Exp Bot **53**: 1255-1272

Del Río LA, López-Huertas E (2016) ROS generation in peroxisomes and its role in cell signaling. Plant Cell Physiol **57**: 1364-1376

Del Río LA, Sandalio LM, Corpas FJ, Palma JM, Barroso JB (2006) Reactive oxygen species and reactive nitrogen species in peroxisomes. production, scavenging, and role in cell signaling. Plant Physiol **141**: 330-335

Demidchik V, Shabala SN, Coutts KB, Tester MA, Davies JM (2003) Free oxygen radicals regulate plasma membrane Ca^{2+}- and K^{+}-permeable channels in plant root cells. J Cell Sci **116**: 81-88

Denness L, McKenna JF, Segonzac C, Wormit A, Madhou P, Bennett M, Mansfield J, Zipfel C, Hamann T (2011) Cell wall damage-induced lignin biosynthesis is regulated by a reactive oxygen species- and jasmonic acid-dependent process in arabidopsis. Plant Physiol **156**: 1364-1374

Dietz, K.J (2003) Plant peroxiredoxins. Annu Rev Plant Biol **54**: 93–107

Dietz KJ, Jacquot JP, Harris G (2010) Hubs and bottlenecks in plant molecular signalling networks. New Phytol **188**: 919-938

Ding H, Wang B, Han Y, Li S (2020) The pivotal function of dehydroascorbate reductase in glutathione homeostasis in plants. J Exp Bot **71**: 3405-3416

Ding X, Jimenez-Gongora T, Krenz B, Lozano-Duran R (2019) Chloroplast clustering around the nucleus is a general response to pathogen perception in *Nicotiana benthamiana*. Mol Plant Pathol **20**: 1298-1306

Dixon DP, Hawkins T, Hussey PJ, Edwards R (2009) Enzyme activities and subcellular localization of members of the Arabidopsis glutathione transferase superfamily. J Exp Bot. **60**: 1207-1218

Dobin A, Davis CA, Schlesinger F, Drenkow J, Zaleski C, Jha S, Batut P, Chaisson M, Gingeras TR (2013) STAR: ultrafast universal RNA-seq aligner. Bioinformatics **29**: 15-21

Dowdle J, Ishikawa T, Gatzek S, Rolinski S, Smirnoff N (2007) Two genes in *Arabidopsis thaliana* encoding GDP-l- galactose phosphorylase are required for ascorbate biosynthesis and seedling viability. Plant J **52**: 673-689

Eastmond PJ (2007) MONODEHYROASCORBATE REDUCTASE4 is required for seed storage oil hydrolysis and post germinative growth in Arabidopsis. Plant Cell **19**: 1376-1387

Eckardt NA, Ainsworth EA, Bahuguna RN, Broadley MR, Busch W, Carpita NC, Castrillo G, Chory J, Dehaan LR, Duarte CM, et al (2023) Climate change challenges, plant science solutions. Plant Cell **35**: 24-66

Edwards K, Johnstone C, Thompson C (1991) A simple and rapid method for the preparation of plant genomic DNA for PCR analysis. Nucleic Acids Res **19**:1349

El Airaj H, Gest N, Truffault V, Garchery C, Riqueau G, Gouble B, Page D, Stevens R (2013) Decreased monodehydroascorbate reductase activity reduces tolerance to cold storage in tomato and affects fruit antioxidant levels. Postharvest Biol Tec **86**: 502-510

Eltayeb AE, Kawano N, Badawi GH, Kaminaka H, Sanekata T, Shibahara T, Inanaga S, Tanaka K (2007) Overexpression of monodehydroascorbate reductase in transgenic tobacco confers enhanced tolerance to ozone, salt and polyethylene glycol stresses. Planta **225**: 1255-1264

Endo T, Mi H, Shikanai T, Asada K (1997) Donation of electrons to plastoquinone by NAD(P)H dehydrogenase and by ferredoxin-quinone reductase in spinach chloroplasts. Plant Cell Physiol **38**: 1272-1277

Eshed Y, Zamir D (1995) An Introgression line population of Lycopersicon pennellii in the cultivated tomato enables the identification and fine mapping of yield-associated QTL. Genetics **141**: 1147-1162

Estavillo GM, Crisp PA, Pornsiriwong W, Wirtz M, Collinge D, Carrie C, Giraud E, Whelan J, David P, Javot H, et al (2011) Evidence for a SAL1-PAP chloroplast retrograde pathway that functions in drought and high light signaling in Arabidopsis. Plant Cell **23**: 3992-4012

Exposito-Rodriguez M, Laissue PP, Yvon-Durocher G, Smirnoff N, Mullineaux PM (2017) Photosynthesis-dependent H_2O_2 transfer from chloroplasts to nuclei provides a high-light signalling mechanism. Nat Commun **8**: 49

Finkemeier I, Goodman M, Lamkemeyer P, Kandlbinder A, Sweetlove LJ, Dietz KJ (2005) The mitochondrial type II peroxiredoxin F is essential for redox homeostasis and root growth of Arabidopsis thaliana under stress. J Biol Chem **280**: 12168-12180

Foreman J, Demidchik V, Bothwell JHF, Mylona P, Miedema H, Torres MA, Linstead P, Costa S, Brownlee C, Jones JDG (2003) Reactive oxygen species produced by NADPH oxidase regulate plant cell growth. Nature **422**: 442-446

Foyer CH, Bloom AJ, Queval G, Noctor G (2009) Photorespiratory metabolism: genes, mutants, energetics, and redox signaling. Annu Rev Plant Biol **60**: 455-484

Foyer CH, Halliwell B (1977) Purification and properties of dehydroascorbate reductase from spinach leaves. Phytochemistry **16**: 1347-1350

Foyer CH, Hanke G (2022) ROS production and signalling in chloroplasts: cornerstones and evolving concepts. Plant J **111**: 642-661

Foyer CH, Kunert K (2024) The ascorbate–glutathione cycle coming of age. J Exp Bot **75**: 2682-2699

Foyer CH, Mullineaux PM (1998) The presence of dehydroascorbate and dehydroascorbate reductase in plant tissues. FEBS Lett **425**: 528-529

Foyer CH, Noctor G (2000) Oxygen processing in photosynthesis: regulation and signalling. New Phytol **146**: 359-388

Foyer CH, Noctor G (2003) Redox sensing and signalling associated with reactive oxygen in chloroplasts, peroxisomes and mitochondria. Physiol Plant **119**: 355-364

Foyer CH, Noctor G (2005) Oxidant and antioxidant signalling in plants: a re-evaluation of the concept of oxidative stress in a physiological context. Plant Cell Environ **28**: 1056-1071

Foyer CH, Noctor G (2005) Redox homeostasis and antioxidant signaling: a metabolic interface between stress perception and physiological responses. Plant Cell **17**: 1866-1875

Foyer CH, Noctor G (2009) Redox regulation in photosynthetic organisms: signaling, acclimation, and practical implications. Antioxid Redox Signal **11**: 861-905

Foyer CH, Noctor G (2011) Ascorbate and glutathione: the heart of the redox hub. Plant Physiol **155**: 2-18

Foyer CH, Noctor G (2016) Stress-triggered redox signalling: What's in pROSpect? Plant Cell Environ **39**: 951-964

Fu D, Calvo JA, Samson LD (2012) Balancing repair and tolerance of DNA damage caused by alkylating agents. Nat Rev Cancer **12**: 104-120

Fujii J, Homma T, Osaki T (2022) Superoxide radicals in the execution of cell death. Antioxidants **11**: 501

Gakière B, Hao J, de Bont L, Pétriacq P, Nunes-Nesi A, Fernie AR (2018) NAD^+ biosynthesis and signaling in plants. CRC Crit Rev Plant Sci **37**: 259-307

Georgiou CD, Papapostolou I, Grintzalis K (2008) Superoxide radical detection in cells, tissues, organisms (animals, plants, insects, microorganisms) and soils. Nat Protoc **3**: 1679-1692

Gest N, Garchery C, Gautier H, Jiménez A, Stevens R (2013) Light-dependent regulation of ascorbate in tomato by a monodehydroascorbate reductase localized in peroxisomes and the cytosol. Plant Biotechnol J **11**: 344-354

Gomez LD, Noctor G, Knight MR, Foyer CH (2004) Regulation of calcium signalling and gene expression by glutathione. J Exp Bot **55**: 1851-1859

Gradogna A, Lagostena L, Beltrami S, Tosato E, Picco C, Scholz-Starke J, Sparla F, Trost P, Caraneto A (2023) Tonoplast cytochrome *b*561 is a transmembrane ascorbate-dependent monodehydroascorbate reductase: functional characterization of electron currents in plant vacuoles. New Phytol **238**: 1957-1971

Gu Z, Eils R, Schlesner M (2016) Complex heatmaps reveal patterns and correlations in multidimensional genomic data. Bioinformatics **32**: 2847-2849

Guptasarma P, Balasubramanian D, Matsugo S, Saito I (1992) Hydroxyl radical mediated damage to proteins, with special reference to the crystallins. Biochemistry **31**: 4296-4303

Hamada A, Tanaka Y, Ishikawa T, Maruta T (2023) Chloroplast dehydroascorbate reductase and glutathione cooperatively determine the capacity for ascorbate accumulation under photooxidative stress conditions. Plant J **114**: 68-82

Han Y, Chaouch S, Mhamdi A, Queval G, Zechmann B, Noctor G (2013b) Functional analysis of arabidopsis mutants points to novel roles for glutathione in coupling H_2O_2 to activation of salicylic acid accumulation and signaling. Antioxid Redox Signal **18**: 2106-2121

Han Y, Mhamdi A, Chaouch S, Noctor G (2013a) Regulation of basal and oxidative stress-triggered jasmonic acid-related gene expression by glutathione. Plant Cell Environ **36**: 1135-1146

Hasanuzzaman M, Borhannuddin Bhuyan MHM, Anee TI, Parvin K, Nahar K, Al Mahmud J, Fujita M (2019) Regulation of ascorbate-glutathione pathway in mitigating oxidative damage in plants under abiotic stress. Antioxidants **8**: 384

Havaux M (2014) Carotenoid oxidation products as stress signals in plants. Plant J **79**:597-606

Hayyan M, Hashim MA, Alnashef IM (2016) Superoxide ion: generation and chemical implications. Chem Rev **116**: 3029-3085

He H, Denecker J, Van Der Kelen K, Willems P, Pottie R, Phua SY, Hannah MA, Vertommen D, Van Breusegem F, Mhamdi A (2021) The Arabidopsis mediator complex subunit 8 regulates oxidative stress responses. Plant Cell **33**: 2032-2057

Heineke D, Riens B, Grosse H, Hoferichter P, Peter U, Flügge UI, Heldt HW (1991) Redox transfer across the inner chloroplast envelope membrane. Plant Physiol **95**: 1131-1137

Herbette S, Lenne C, Leblanc N, Julien JL, Drevet JR, Roeckel-Drevet P (2002) Two GPX-like proteins from Lycopersicon esculentum and Helianthus annuus are antioxidant enzymes with phospholipid hydroperoxide glutathione peroxidase and thioredoxin peroxidase activities. Eur J Biochem **269**: 2414-2420

Hess DT, Matsumoto A, Kim SO, Marshall HE, Stamler JS (2005) Protein *S*-nitrosylation: purview and parameters. Nat Rev Mol Cell Biol **6**: 150-166

Heyno E, Mary V, Schopfer P, Krieger-Liszkay A (2011) Oxygen activation at the plasma membrane: relation between superoxide and hydroxyl radical production by isolated membranes. Planta **234**: 35-45

Höfgen R, Willmitzer L (1988) Storage of competent cells for *Agrobacterium* transformation. Nucleic Acids Res **16**: 9877

Hossain MA, Asada K (1984) Purification of dehydroascorbate reductase from spinach and its characterisation as a thiol enzyme. Cell Physiol **25**: 85-92

Hossain MA, Asada K (1985) Monodehydroascorbate reductase from cucumber is a flavin adenine dinucleotide enzyme. J Biol Chem **260**: 12920-12926

Hossain MA, Nakano Y, Asada K (1984) Monodehydroascorbate reductase in spinach chloroplasts and its participation in regeneration of ascorbate for scavenging hydrogen peroxide. Plant Cell Physiol **25**: 385-395

Hu YQ, Liu S, Yuan HM, Li J, Yan DW, Zhang JF, Lu YT (2010) Functional comparison of catalase genes in the elimination of photorespiratory H_2O_2 using promoter- and 3'-untranslated region exchange experiments in the Arabidopsis *cat2* photorespiratory mutant. Plant Cell Environ **33**: 1656-1670

Iqbal A, Yabuta Y, Takeda T, Nakano Y, Shigeoka S (2006) Hydroperoxide reduction by thioredoxin-specific glutathione peroxidase isoenzymes of *Arabidopsis thaliana*. FEBS Journal **273**: 5589-5597

Jacques S, Ghesquière B, De Bock PJ, Demol H, Wahni K, Willems P, Messens J, Van Breusegem F, Gevaert K (2015) Protein methionine sulfoxide dynamics in *Arabidopsis thaliana* under oxidative stress. Mol Cell Proteomics **14**: 1217-1229

Jammes F, Song C, Shin D, Munemasa S, Takeda K, Gu D, Cho D, Lee S, Giordo R, Sritubtim S (2009) MAP kinases *MPK9* and *MPK12* are preferentially expressed in guard cells and positively regulate ROS-mediated ABA signaling. Proc Natl Acad Sci USA **106**: 20520-20525

Johnston EJ, Rylott EL, Beynon E, Lorenz A, Chechik V, Bruce NC (2015) Monodehydroascorbate reductase mediates TNT toxicity in plants. Science **349**: 1072-1075

Joung JK, Ramm EI, Pabo CO (2000) A bacterial two-hybrid selection system for studying protein-DNA and protein-protein interactions. Proc Natl Acad Sci USA **97**: 7382-7387

Jurado-Flores A, Delgado-Requerey V, Gálvez-Ramírez A, Puerto-Galán L, Pérez-Ruiz JM, Cejudo FJ (2020) Exploring the functional relationship between *y*-type thioredoxins and 2-Cys peroxiredoxins in Arabidopsis chloroplasts. Antioxidants **9**: 1072

Karimi M, Inzé D, Depicker A (2002) GATEWAY vectors for Agrobacterium-mediated plant transformation. Trends Plant Sci **7**: 193-195

Kataya AMR, Reumann S (2010) Arabidopsis glutathione reductase 1 is dually targeted to peroxisomes and the cytosol. Plant Signal Behav **5**: 171-175

Kaya H, Nakajima R, Iwano M, Kanaoka MM, Kimura S, Takeda S, Kawarazaki T, Senzaki E, Hamamura Y, Higashiyama T, et al (2014) Ca^{2+}-activated reactive oxygen species production by Arabidopsis RbohH and RbohJ is essential for proper pollen tube tip growth. Plant Cell **26**: 1069-1080

Kendall A, Keys A, Turner J, Lea P, Miflin B (1983) The isolation and characterisation of a catalase-deficient mutant of barley (*Hordeum vulgare* L.). Planta **159**: 505-511

Kim JJ, Kim YS, Park SI, Mok JE, Kim YH, Park HM, Kim IS, Yoon HS (2017) Cytosolic monodehydroascorbate reductase gene affects stress adaptation and grain yield under paddy field conditions in *Oryza sativa L. japonica*. Mol Breed **37**: 118

Kliebenstein DJ, Osbourn A (2012) Making new molecules - evolution of pathways for novel metabolites in plants. Curr Opin Plant Biol **15**: 415-423

Kobayashi M, Ohura I, Kawakita K, Yokota N, Fujiwara M, Shimamoto K, Doke N, Yoshioka H (2007) Calcium-dependent protein kinases regulate the production of reactive oxygen species by potato NADPH oxidase. Plant Cell **19**: 1065-1080

Koenig D, Weigel D (2015) Beyond the thale: Comparative genomics and genetics of Arabidopsis relatives. Nat Rev Genet **16**: 285-298

Koncz C, Schell J (1986) The promoter of Ti-DNA gene 5 controls the tissue-specific expression of chimeric genes carried by a novel type of Agrobacterium binary vector. Molec Gen Genet **204**: 383-396

Koornneef M, Reuling G, Karssen CM (1984) The isolation and characterization of abscisic acid-insensitive mutants of *Arabidopsis thaliana*. Physiol Plant **61**: 377-383

Korge P, Calmettes G, John SA, Weiss JN (2017) Reactive oxygen species production induced by pore opening in cardiac mitochondria: the role of complex III. J Biol Chem **292**: 9882-9895

Kristensen LG, Holton JM, Rad B, Chen Y, Petzold CJ, Gupta S, Ralston CY (2021) Hydroxyl radical mediated damage of proteins in low oxygen solution investigated using X-ray footprinting mass spectrometry. J Synchrotron Radiat **31**: 4296-4303

Krutmann J (2000) Ultraviolet A radiation-induced biological effects in human skin: relevance for photoaging and photodermatosis. J Dermatol Sci **23**: S22-S26

Kunau W-H, Dommes V, Schulz H (1995) β-Oxidation of fatty acids in mitochondria, peroxisomes, and bacteria: A century of continued progress. Prog Lipid Res **34**: 267-342

Kushnareva Y, Murphy AN, Andreyev A (2002) Complex I-mediated reactive oxygen species generation: Modulation by cytochrome c and $NAD(P)^+$ oxidation-reduction state. Biochem J **368**: 545-553

Kwon S-Y, Choi S-M, Ahn Y-O, Lee H-S, Lee H-B, Park Y-M, Kwak S-S (2003) Enhanced stress-tolerance of transgenic tobacco plants expressing a human dehydroascorbate reductase gene. J Plant Physiol **160**: 347-353

Laloi C, Mestres-Ortega D, Marco Y, Meyer Y, Reichheld JP (2004) The Arabidopsis cytosolic thioredoxin *h5* gene induction by oxidative stress and its W-box-mediated response to pathogen elicitor. Plant Physiol **134**: 1006-1016

Lambert I, Paysant-Le Roux C, Colella S, Martin-Magniette ML (2020) DiCoExpress: a tool to process multifactorial RNAseq experiments from quality controls to co-expression analysis through differential analysis based on contrasts inside GLM models. Plant Methods **16**: 68

Laohavisit A, Richards SL, Shabala L, Chen C, Colaço RDDR, Swarbreck SM, Shaw E, Dark A, Shabala S, Shang Z (2013) Salinity-induced calcium signaling and root adaptation in Arabidopsis require the calcium regulatory protein annexin1. Plant Physiol **163**: 253-262

Leterrier M, Corpas FJ, Barroso JB, Sandalio LM, Del Río LA (2005) Peroxisomal monodehydroascorbate reductase. Genomic clone characterization and functional analysis under environmental stress conditions. Plant Physiol **138**: 2111-2123

Leterrier M, Barroso JB, Valderrama R, Begara-Morales JC, Sánchez-Calvo B, Chaki M, Luque F, Viñegla B, Palma JM, Corpas FJ (2016) Peroxisomal NADP-isocitrate dehydrogenase is required for Arabidopsis stomatal movement. Protoplasma **253**: 403-415

Lew TTS, Koman VB, Silmore KS, Seo JS, Gordiichuk P, Kwak SY, Park M, Ang MCY, Khong DT, Lee MA, et al (2020) Real-time detection of wound-induced H_2O_2 signalling waves in plants with optical nanosensors. Nat Plants **6**: 404-415

Li J, Gorospe M, Hutter D, Barnes J, Keyse SM, Liu Y (2001) Transcriptional induction of *MKP-1* in response to stress is associated with histone H3 phosphorylation-acetylation. Mol Cell Biol **21**: 8213-8224

Li J, Li H, Yang N, Jiang S, Ma C, Li H (2020) Overexpression of a monodehydroascorbate reductase gene from sugar beet M14 increased salt stress tolerance. Sugar Tech **23**: 45-56

Li M, Kim C (2022) Chloroplast ROS and stress signaling. Plant Commun **3**: 100264

Li S (2023) Novel insight into functions of ascorbate peroxidase in higher plants: More than a simple antioxidant enzyme. Redox Biol. **64**: 102789

Li S, Mhamdi A, Clement C, Jolivet Y, Noctor G (2013) Analysis of knockout mutants suggests that Arabidopsis NADP-MALIC ENZYME2 does not play an essential role in responses to oxidative stress of intracellular or extracellular origin. J Exp Bot **64**: 3605-3614

Liao Y, Smyth GK, Shi W (2014) FeatureCounts: an efficient general purpose program for assigning sequence reads to genomic features. Bioinformatics **30**: 923-930

Lisenbee CS, Lingard MJ, Trelease RN (2005) Arabidopsis peroxisomes possess functionally redundant membrane and matrix isoforms of monodehydroascorbate reductase. Plant J **43**: 900-914

Liu X, Hu B, Chu C (2022) Nitrogen assimilation in plants: current status and future prospects. J Genet Genomics **49**: 394-404

Lokdarshi A, Guan J, Urquidi Camacho RA, Cho SK, Morgan PW, Leonard M, Shimono M, Day B, von Arnim AG (2020) Light activates the translational regulatory kinase GCN2 via reactive oxygen species emanating from the chloroplast. Plant Cell **32**: 1161-1178

Lukan T, Coll A (2022) Intertwined roles of reactive oxygen species and salicylic acid signaling are crucial for the plant response to biotic stress. Int J Mol Sci **23**: 5568

Mahaseth T, Kuzminov A (2017) Potentiation of hydrogen peroxide toxicity: from catalase inhibition to stable DNA-iron complexes. Mutat Res Rev Mutat Res **773**: 274-281

Malamy J, Carr JP, Klessig DF, Raskin I (1990) Salicylic acid: A likely endogenous signal in the resistance response of tobacco to viral infection. Science **250**: 1002-1004

Marty, L., Siala, W., Schwarzländer, M., Fricker, M.D., Wirtz, M., Sweetlove, L.J., Meyer Y., Reichheld, J.P., and Hell, R (2009) The NADPH-dependent thioredoxin system constitutes a functional backup for cytosolic glutathione reductase in Arabidopsis. Proc Natl Acad Sci. USA **106**: 9109-9114

Maynard D, Kumar V, Sproß J, Dietz K-J (2020) 12-Oxophytodienoic acid reductase 3 (OPR3) functions as NADPH-dependent α,β-ketoalkene reductase in detoxification and monodehydroascorbate reductase in redox homeostasis. Plant Cell Physiol **61**: 584-595

McNew JA, Goodman JM (1994) An oligomeric protein is imported into peroxisomes in vivo. J Cell Biol **127**: 1245-1257

Mendoza-Aguilar MD, Arce-Paredes P, Aquino-Vega M, Rodríguez-Martínez S, Rojas-Espinosa O (2013) Fate of *Mycobacterium tuberculosis* in peroxidase-loaded resting murine macrophages. Int J Mycobacteriol **2**: 3-13

Mhamdi A, Hager J, Chaouch S, Queval G, Han Y, Taconnat Y, Saindrenan P, Issakidis-Bourguet E, Gouia H, Renou JP, Noctor G (2010b) Arabidopsis GLUTATHIONE REDUCTASE1 plays a crucial role in leaf responses to intracellular hydrogen peroxide and in ensuring appropriate gene expression through both salicylic acid and jasmonic acid signaling pathways. Plant Physiol **153**: 1144-1160

Mhamdi A, Han Y, Noctor G (2013) Glutathione-dependent phytohormone responses: Teasing apart signaling and antioxidant functions. Plant Signal Behav **8**: 24181

Mhamdi A, Mauve C, Gouia H, Saindrenan P, Hodges M, Noctor G (2010c) Cytosolic NADP-dependent isocitrate dehydrogenase contributes to redox homeostasis and the regulation of pathogen responses in Arabidopsis leaves. Plant Cell Environ **33**: 1112-1123

Mhamdi A, Noctor G, Baker A (2012) Plant catalases: peroxisomal redox guardians. Arch Biochem Biophys **525**: 181-194

Mhamdi A, Queval G, Chaouch S, Vanderauwera S, Van Breusegem F, Noctor G (2010a) Catalase function in plants: a focus on Arabidopsis mutants as stress-mimic models. J Exp Bot **61**: 4197-4220

Mhamdi A, Van Breusegem F (2018) Reactive oxygen species in plant development. Development **145**: 1-28

Miller G, Schlauch K, Tam R, Cortes D, Torres MA, Shulaev V, Dangl JL, Mittler R (2009) The plant NADPH oxidase RBOHD mediates rapid systemic signaling in response to diverse stimuli. Sci Signal **2**: 45

Mishra AK, Baek KH (2021) Salicylic acid biosynthesis and metabolism: a divergent pathway for plants and bacteria. Biomolecules **11**: 705

Mittler R, Herr EH, Orvar BL, Van Camp W, Willekens H, Inzé D, Ellis BE (1999) Transgenic tobacco plants with reduced capability to detoxify reactive oxygen intermediates are hyperresponsive to pathogen infection. Proc Natl Acad Sci USA **96**: 14165-14170

Mittler R, Vanderauwera S, Suzuki N, Miller G, Tognetti VB, Vandepoele K, Gollery M, Shulaev V, Van Breusegem F (2011) ROS signaling: the new wave? Trends Plant Sci **16**: 300-309

Mittler R, Zandalinas SI, Fichman Y, Van Breusegem F (2022) Reactive oxygen species signalling in plant stress responses. Nat Rev Mol Cell Biol **23**: 663-679

Miyake C, Asada K (1994) Ferredoxin-dependent photoreduction of the monodehydroascorbate radical in spinach thylakoids. Plant Cell Physiol **35**: 539-549

Mojović M, Vuletić M, Bačić GG, Vučinić Ž (2004) Oxygen radicals produced by plant plasma membranes: An EPR spin-trap study. J Exp Bot **55**: 2523-2531

Moon H, Lee B, Choi G, Shin D, Theertha Prasad D, Lee O, Kwak S-S, Hoon Kim D, Nam J, Bahk J, et al (2002) NDP kinase 2 interacts with two oxidative stress-activated MAPKs to regulate cellular redox state and enhances multiple stress tolerance in transgenic plants. Proc Natl Acad Sci USA **100**: 358-363.

Mou Z, Fan W, Dong X (2003) Inducers of plant systemic acquired resistance regulate NPR1 function through redox changes. Cell **113**: 935-944

Mullen RT, Lee MS, Trelease RN (1997) Identification of the peroxisomal targeting signal for cottonseed catalase. Plant J **12**: 313-322

Muller FL, Liu Y, Van Remmen H (2004) Complex III releases superoxide to both sides of the inner mitochondrial membrane. J Biol Chem **279**: 49064-49073

Murthy SS, Zilinskas BA (1994) Molecular cloning and characterization of a cDNA encoding pea monodehydroascorbate reductase. J Biol Chem **269**: 31129-31133

Myers Jr RJ, Fichman Y, Zandalinas SI, Mittler R (2023) Jasmonic acid and salicylic acid modulate systemic reactive oxygen species signaling during stress responses. Plant Physiol **191**: 862-873

Nakagami H, Soukupová H, Schikora A, Žárský V, Hirt H (2006) A Mitogen-activated protein kinase kinase kinase mediates reactive oxygen species homeostasis in Arabidopsis. J Biol Chem **281**: 38697-38704

Navrot N, Collin V, Gualberto J, Gelhaye E, Hirasawa M, Rey P, Knaff DB, Issakidis E, Jacquot JP, Rouhier N (2006) Plant glutathione peroxidases are functional peroxiredoxins distributed in several subcellular compartments and regulated during biotic and abiotic stresses. Plant Physiol **142**: 1364-1379

Nawrath C, Métraux JP (1999) Salicylic acid induction-deficient mutants of Arabidopsis express *PR-2* and *PR-5* and accumulate high levels of camalexin after pathogen inoculation. Plant Cell **11**: 1393-1404

Nawrath C, Métraux, JP (1999) Salicylic acid induction-deficient mutants of Arabidopsis express *PR-2* and *PR-5* and accumulate high levels of camalexin after pathogen inoculation. Plant Cell **11**: 1393-1404

Njus D, Kelley PM, Tu YJ, Schlegel HB (2020) Ascorbic acid: the chemistry underlying its antioxidant properties. Free Radic Biol Med **159**: 37-43

Noctor G (2015) Lighting the fuse on toxic TNT. Science **349**: 1052-1053

Noctor G, Cohen MC, Trémulot L, Châtel-Innocenti G, Van Breusegem F, Mhamdi A (2024) Glutathione: a key modulator of plant defence and metabolism through multiple mechanisms. J Exp Bot **75**: 4549-4572

Noctor G, Lelarge-Trouverie C, Mhamdi A (2015) The metabolomics of oxidative stress. Phytochemistry **112**:33-53

Noctor G, Mhamdi A (2022) Quantitative measurement of ascorbate and glutathione by spectrophotometry. Methods Mol Biol **2526**: 87-96

Noctor G, Mhamdi A, Chaouch S, Han Y, Neukermans J, Marquez-Garcia B, Queval G, Foyer CH (2012) Glutathione in plants: an integrated overview. Plant Cell Environ **35**: 454-484

Noctor G, Mhamdi A, Foyer CH (2016) Oxidative stress and antioxidative systems: recipes for successful data collection and interpretation. Plant Cell Environ **39**: 1140-1160

Noctor G, Mhamdi A, Queval G, Foyer CH (2013) Regulating the redox gatekeeper: vacuolar sequestration puts glutathione disulfide in its place. Plant Physiol **163**: 665-671

Noctor G, Queval G, Gakière B (2006) NAD(P) synthesis and pyridine nucleotide cycling in plants and their potential importance in stress conditions. J Exp Bot **57**: 1603-1620

Noctor G, Queval G, Mhamdi A, Chaouch S, Foyer CH (2011) Glutathione. The Arabidopsis Book **9**: 1-32

Noctor G, Mhamdi A, Foyer CH (2014) The roles of reactive oxygen metabolism in drought: not so cut and dried. Plant Physiol **164**:1636-1648

Noctor G, Reichheld J, Foyer CH (2018) Seminars in cell & developmental biology ROS-related redox regulation and signaling in plants. Semin Cell Dev Biol **80**: 3-12

Noshi M, Yamada H, Hatanaka R, Tanabe N, Tamoi M, Shigeoka S (2017) Arabidopsis dehydroascorbate reductase 1 and 2 modulate redox states of ascorbate-glutathione cycle in the cytosol in response to photooxidative stress. Biosci Biotechnol Biochem **81**: 523-533

Nyathi Y, Baker A (2006) Plant peroxisomes as a source of signalling molecules. Biochim Biophys Acta **1763**: 1478-1495

Obara K, Sumi K, Fukuda H (2002) The use of multiple transcription starts causes the dual targeting of Arabidopsis putative monodehydroascorbate reductase to both mitochondria and chloroplasts. Plant Cell Physiol **43**: 697-705

Ogata FT, Branco V, Vale FF, Coppo L (2021) Glutaredoxin: Discovery, redox defense and much more. Redox Biol **43**: 101975

Ogasawara Y, Kaya H, Hiraoka G, Yumoto F, Kimura S, Kadota Y, Hishinuma H, Senzaki E, Yamagoe S, Nagata K, et al (2008) Synergistic activation of the Arabidopsis NADPH oxidase AtrbohD by Ca^{2+} and phosphorylation. J Biol Chem **283**: 8885-8892

Paiva CN, Bozza MT (2014) Are reactive oxygen species always detrimental to pathogens? Antioxid Redox Signal **20**:1000-1037

Park AK, Kim IS, Do H, Jeon BW, Lee CW, Roh SJ, Shin SC, Park H, Kim YS, Kim YH, et al (2016) Structure and catalytic mechanism of monodehydroascorbate reductase, MDHAR, from *Oryza sativa L. japonica*. Sci Rep **6**: 33903

Park AK, Kim IS, Do H, Kim H, Choi W, Jo SW, Shin SC, Lee JH, Yoon HS, Kim HW (2019) Characterization and structural determination of cold-adapted monodehydroascorbate reductase, MDHAR, from the antarctic hairgrass *Deschampsia Antarctica*. Crystals **9**: 537

Parwez R, Aftab T, Gill SS, Naeem M (2022) Abscisic acid signaling and crosstalk with phytohormones in regulation of environmental stress responses. Environ Exp Bot **199**: 104885

Pasha A, Subramaniam S, Cleary A, Chen X, Berardini T, Farmer A, Town C, Provart N (2020) Araport lives: an updated framework for Arabidopsis bioinformatics. Plant Cell **32**: 2683-2686

Pastori GM, Kiddle G, Antoniw J, Bernard S, Veljovic-Jovanovic S, Verrier PJ, Noctor G, Foyer CH (2003) Leaf vitamin C contents modulate plant defense transcripts and regulate genes that control development through hormone signalling. Plant Cell **15**: 939-951

Pavet V, Olmos E, Kiddle G, Mowla S, Kumar S, Antoniw J, Alvarez ME, Foyer CH (2005) Ascorbic acid deficiency activates cell death and disease resistance responses in Arabidopsis. Plant Physiol **139**: 1291-1303

Pignocci C, Kiddle G, Hernández I, Foster SJ, Asensi A, Taybi T, Barnes J, Foyer CH (2006) Ascorbate oxidase-dependent changes in the redox state of the apoplast modulate gene transcript accumulation leading to modified hormone signaling and orchestration of defense processes in tobacco. Plant Physiol **141**: 423-435

Queval G, Hager J, Gakière B, Noctor G (2008) Why are literature data for H_2O_2 contents so variable? A discussion of potential difficulties in quantitative assays of leaf extracts. J Exp Bot **59**: 135-146

Queval G, Issakidis-Bourguet E, Hoeberichts FA, Vandorpe M, Gakiere B, Vanacker H, Miginiac-Maslow M, Van Breusegem F and Noctor G (2007) Conditional oxidative stress responses in the Arabidopsis photorespiratory mutant *cat2* demonstrate that redox state is a key modulator of daylength-dependent gene expression, and define photoperiod as a crucial factor in the regulation of H_2O_2-induced cell death. Plant J **52**: 640-657

Queval G, Issakidis-Bourguet E, Hoeberichts FA, Vandorpe M, Gakière B, Vanacker H, Miginiac-Maslow M, Van Breusegem F, Noctor G (2007) Conditional oxidative stress responses in the Arabidopsis photorespiratory mutant *cat2* demonstrate that redox state is a key modulator of daylength-dependent gene expression, and define photoperiod as a crucial factor in the regulation of H_2O_2-induced cell death. Plant J **52**: 640-657

Queval G, Jaillard D, Zechmann B, Noctor G (2011) Increased intracellular H_2O_2 availability preferentially drives glutathione accumulation in vacuoles and chloroplasts. Plant Cell Environ **34**: 21-32

Queval G, Noctor G (2007) A plate reader method for the measurement of NAD, NADP, glutathione, and ascorbate in tissue extracts: application to redox profiling during Arabidopsis rosette development. Anal Biochem **363**: 58–69

Queval G, Thominet D, Vanacker H, Miginiac-Maslow M, Gakière B, Noctor G (2009) H_2O_2-activated up-regulation of glutathione in Arabidopsis involves induction of genes encoding enzymes involved in cysteine synthesis in the chloroplast. Mol Plant **2**: 344-356

Rahantaniaina MS, Li S, Chatel-Innocenti G, Tuzet A, Issakidis-Bourguet E, Mhamdi A, Noctor G (2017) Cytosolic and chloroplastic DHARs cooperate in oxidative stress-driven activation of the salicylic acid pathway. Plant Physiol **174**: 956-971

Reichheld JP, Khafif M, Riondet C, Droux M, Bonnard G, Meyer Y (2007) Inactivation of thioredoxin reductases reveals a complex interplay between thioredoxin and glutathione pathways in Arabidopsis development. Plant Cell **19**: 1851-1865

Rekhter D, Lüdke D, Ding Y, Feussner K, Zienkiewicz K, Lipka V, Wiermer M, Zhang Y, Feussner I (2019) Isochorismate-derived biosynthesis of the plant stress hormone salicylic acid. Science **365**: 498-502

Rhee SG (2006) H_2O_2, a necessary evil for cell signaling. Science **312**: 1882-1883

Rivas-San Vicente M, Plasencia J (2011) Salicylic acid beyond defence: its role in plant growth and development. J Exp Bot **62**: 3321-3338

Rizhsky L, Hallak-Herr E, Van Breusegem F, Rachmilevitch S, Barr JE, Rodermel S, Inzé D, Mittler R (2002) Double antisense plants lacking ascorbate peroxidase and catalase are less sensitive to oxidative stress than single antisense plants lacking ascorbate peroxidase or catalase. Plant J **32**: 329-342

Rouhier N (2010) Plant glutaredoxins: Pivotal players in redox biology and iron-sulphur centre assembly. New Phytol **186**: 365-372

Ruffels J, Griffin M, Dickenson JM (2004) Activation of ERK1/2, JNK and PKB by hydrogen peroxide in human SH-SY5Y neuroblastoma cells: role of ERK1/2 in H_2O_2-induced cell death. Eur J Pharmacol **483**: 163-173

Ruggiero A, Punzo P, Landi S, Costa A, Van Oosten MJ, Grillo S (2017) Improving plant water use efficiency through molecular genetics. Horticulturae **3**: 31

Saleem M, Fariduddin Q, Castroverde CDM (2021) Salicylic acid: a key regulator of redox signalling and plant immunity. Plant Physiol Biochem **168**: 381-397

Salomé PA, Bomblies K, Fitz J, Laitenen RAF, Warthmann N, Yant L, Weigel D (2012) The recombination landscape in *Arabidopsis thaliana* F2 populations. Heredity **108**: 447-455

Sandalio LM, Fernández VM, Rupérez FL, Del Río LA (1988) Superoxide free radicals are produced in glyoxysomes. Plant Physiol **87**: 1-4

Sandalio LM, Rodríguez-Serrano M, Romero-Puertas MC, del Río LA (2013) Role of peroxisomes as a source of reactive oxygen species (ROS) signaling molecules. Subcell Biochem. **69**: 231-255

Sano S, Asada K (1994) cDNA Cloning of monodehydroascorbate radical reductase from cucumber: a high degree of homology in terms of amino acid sequence between this enzyme and bacterial flavoenzymes. Plant Cell Physiol **35**: 425-437

Sano S, Miyake C, Mikami B, Asada K (1995) Molecular characterization of monodehydroascorbate radical reductase from cucumber highly expressed in *Escherichia coli*. J Biol Chem **270**: 21354-2136

Sano S, Miyake C, Mikami B, Asada K (1995) Molecular characterization of monodehydroascorbate radical reductase from cucumber highly expressed in *Escherichia coli*. J Biol Chem **270**: 21354-21361

Sano S, Tao S, Endo Y, Inaba T, Hossain MA, Miyake C, Matsuo M, Aoki H, Asada K, Saito K (2005) Purification and cDNA cloning of chloroplastic monodehydroascorbate reductase from spinach. Biosci Biotechnol Biochem **69**: 762-772

Sanz-Barrio R, Fernández-San Millán A, Carballeda J, Corral-Martínez P, Seguí-Simarro JM, Farran I (2012) Chaperone-like properties of tobacco plastid thioredoxins f and m. J Exp Bot **63**: 365-379

Sarewicz M, Osyczka A (2015) Electronic connection between the quinone and cytochrome *c* redox pools and its role in regulation of mitochondrial electron transport and redox signaling. Physiol Rev **95**: 219-243

Scandalios JG, Guan L, Polidoros AN (1997) Catalases in plants: gene structure, properties, regulation, and expression. Cold Spring Harbor Monograph Archive **34**: 343-406

Schippers JHM, von Bongartz K, Laritzki L, Frohn S, Frings S, Renziehausen T, Augstein F, Winkels K, Sprangers K, Sasidharan R, Vertommen D, Van Breusegem F, Hartman S, Beemster GTS, Mhamdi A, van Dongen JT, Schmidt-Schippers RR (2024) ERFVII-controlled hypoxia responses are in part facilitated by MEDIATOR SUBUNIT 25 in *Arabidopsis thaliana*. Plant J **120**:748-768

Sega GA (1984) A review of the genetic effects of ethyl methanesulfonate. Mutat Res **134**: 113-142

Shannon P, Markiel A, Ozier O, Baliga NS, Wang JT, Ramage D, Amin N, Schwikowski B, Ideker T (2003) Cytoscape: a software environment for integrated models of biomolecular interaction networks. Genome Res **13**: 2498-2504

Shin SY, Kim MH, Kim YH, Park HM, Yoon HS (2013) Co-expression of monodehydroascorbate reductase and dehydroascorbate reductase from *Brassica rapa* effectively confers tolerance to freezing-induced oxidative stress. Mol Cells **36**: 304-315

Singer T, Fan Y, Chang H-S, Zhu T, Hazen SP, Briggs SP (2006) Recombinant inbred lines by whole-genome exon array hybridization. PLOS Genetics **2**: e144

Smirnoff N, Wheeler GL (2000) Ascorbic acid in plants: biosynthesis and function. Crit Rev Biochem Mol Biol **19**: 267-290

Smith EN, Schwarzländer M, Ratcliffe RG, Kruger NJ (2021) Shining a light on NAD- and NADP-based metabolism in plants. Trends Plant Sci **26**: 1072-1086

Snoeren TAL, Mumm R, Poelman EH, Yang Y, Pichersky E, Dicke M (2010) The herbivore-induced plant volatile methyl salicylate negatively affects attraction of the *Parasitoid Diadegma semiclausum*. J Chem Ecol **36**: 479-489

Son Y, Cheong Y-K, Kim N-H, Chung H-T, Kang DG, Pae H-O (2011) Mitogen-activated protein kinases and reactive oxygen species: How can ROS activate MAPK pathways? J Signal Transduct **2011**: 1-6

Stevens R, Page D, Gouble B, Garchery C, Zamir D, Causse M (2008) Tomato fruit ascorbic acid content is linked with monodehydroascorbate reductase activity and tolerance to chilling stress. Plant Cell Environ **31**: 1086-1096

Suzuki N, Koussevitzky S, Mittler R, Miller G (2012) ROS and redox signalling in the response of plants to abiotic stress. Plant Cell Environ **35**: 259-270

Sweetlove LJ, Heazlewood JL, Herald V, Holtzapffel R, Day DA, Leaver CJ, Millar AH (2002) The impact of oxidative stress on Arabidopsis mitochondria. Plant J **32**: 891-904

Szarka A, Bánhegyi G, Asard H (2013) The inter-relationship of ascorbate transport, metabolism and mitochondrial, plastidic respiration. Antioxid Redox Signal **19**: 1036-1044

Takahashi Y, Nagata T (1992) parB: an auxin-regulated gene encoding glutathione S-transferase. Proc Natl Acad Sci USA **89**: 56-59

Tanaka M, Takahashi R, Hamada A, Terai Y, Ogawa T, Sawa Y, Ishikawa T, Maruta T (2021) Distribution and functions of monodehydroascorbate reductases in plants: comprehensive reverse genetic analysis of *Arabidopsis thaliana* enzymes. Antioxidants **10**: 1726

Tarrago L, Laugier E, Zaffagnini M, Marchand C, Le Maréchal P, Rouhier N, Lemaire SD, Rey P (2009) Regeneration mechanisms of *Arabidopsis thaliana* methionine sulfoxide reductases B by glutaredoxins and thioredoxins. J Biol Chem **284**: 18963-18971

Terai Y, Ueno H, Ogawa T, Sawa Y, Miyagi A, Kawai-Yamada M, Ishikawa T, Maruta T (2020) Dehydroascorbate reductases and glutathione set a threshold for high-light–induced ascorbate accumulation. Plant Physiol **183**: 112-122

Tian J, Chen J, Ye X, Chen S (2016) Health benefits of the potato affected by domestic cooking: A review. Food Chem **202**: 165-175

Torres M (2003) Mitogen-activated protein kinase pathways in redox signaling. Front Biosci **8**: 369-391

Torres MA, Dangl JL, Jones JDG (2002) Arabidopsis $gp91^{phox}$ homologues *AtrbohD* and *AtrbohF* are required for accumulation of reactive oxygen intermediates in the plant defense response. Proc Natl Acad Sci USA **99**: 517-522

Triantaphylidès C, Havaux M (2009) Singlet oxygen in plants: production, detoxification and signaling. Trends Plant Sci **14**: 219-228

Truffault V, Gest N, Garchery C, Florian A, Fernie AR, Gautier H, Stevens RG (2016) Reduction of MDHAR activity in cherry tomato suppresses growth and yield and MDHAR activity is correlated with sugar levels under high light. Plant Cell Environ **39**: 1279-1292

Turrens JF (2003) Mitochondrial formation of reactive oxygen species. J Physiol **552**: 335-344

Tuzet A, Rahantaniaina MS, Noctor G (2019) Analyzing the function of catalase and the ascorbate-glutathione pathway in H_2O_2 processing: insights from an experimentally constrained kinetic model. Antioxid Redox Signal **30**: 1238-1268

Vaish S, Gupta D, Mehrotra R, Mehrotra S, Basantani MK (2020) Glutathione S-transferase: a versatile protein family. 3 Biotech **10**: 321

Vanacker H, Guichard M, Bohrer AS, Issakidis-Bourguet E (2018) Redox regulation of monodehydroascorbate reductase by thioredoxin y in plastids revealed in the context of water stress. Antioxidants **7**: 183

Vanacker H, Carver TLW, Foyer CH (2000) Early H_2O_2 accumulation in mesophyll cells leads to induction of glutathione during the hyper-sensitive response in the barley-powdery mildew interaction. Plant Physiol **123**: 1289-300

Vanderauwera S, Suzuki N, Miller G, van de Cotte B, Morsa S, Ravanat JL, Hegie A, Triantaphylidès C, Shulaev V, Van Montagu MC, Van Breusegem F, Mittler R (2011) Extranuclear protection of chromosomal DNA from oxidative stress. Proc Natl Acad Sci USA **108**: 1711-1716

Veljovic-Jovanovic S, Oniki T, Takahama U (1998) Detection of monodehydroascorbic acid radical in sulfite-treated leaves and mechanism of its formation. Plant Cell Physiol **39**: 1203-1208

Voll LM, Zell MB, Engelsdorf T, Saur A, Wheeler MG, Drincovich MF, Weber APM, Maurino VG (2012) Loss of cytosolic NADP-malic enzyme 2 in *Arabidopsis thaliana* is associated with enhanced susceptibility to *Colletotrichum higginsianum.* New Phytol **195**: 189-202

Wanders RJA, Waterham HR, Ferdinandusse S (2016) Metabolic interplay between peroxisomes and other subcellular organelles including mitochondria and the endoplasmic reticulum. Front Cell Dev Biol **3**: 83

Wang LM, Shen BR, Li B Di, Zhang CL, Lin M, Tong PP, Cui LL, Zhang ZS, Peng XX (2020) A synthetic photorespiratory shortcut enhances photosynthesis to boost biomass and grain yield in rice. Mol Plant **13**: 1802-1815

Wang Y, Wei S (2023) Theoretical insights into the reaction mechanism of hydroxyl radicals and guanine in G-quadruplex DNA. Phys Chem Chem Phys **25**:16126-16134

Waszczak C, Akter S, Eeckhout D, Persiau G, Wahni K, Bodra N, Van Molle I, De Smet B, Vertommen D, Gevaert K, De Jaeger G, Van Montagu M, Messens J, Van Breusegem F (2014) Sulfenome mining in *Arabidopsis thaliana*. Proc Natl Acad Sci USA **111**: 11545-11550

Waszczak C, Akter S, Jacques S, Huang J, Messens J, Van Breusegem F (2015) Oxidative post-translational modifications of cysteine residues in plant signal transduction. J Exp Bot **66**: 2923-2934

Weigel D, Mott R (2009) The 1001 genomes project for *Arabidopsis thaliana*. Genome Biol **10**: 107

Wendrich JR, Boeren S, Möller BK, Weijers D, De Rybel B (2017) In vivo identification of plant protein complexes using IP-MS/MS. Methods Mol Biol **1497**: 147-158

Wheeler GL, Jones MA, Smirnoff N (1998) The biosynthetic pathway of vitamin C in higher plants. Nature **393**: 365-369

White RF (1979) Acetylsalicylic acid (aspirin) induces resistance to tobacco mosaic virus in tobacco. Virology **99**: 410-412

Wildermuth MC, Dewdney J, Wu G, Ausubel FM (2001) Isochorismate synthase is required to synthesize salicylic acid for plant defence. Nature **414**: 562-565

Willekens H, Inzé D, Van Montagu M, Van Camp W (1995) Catalases in plants. Mol Breed **1**: 207-228

Xiao M, Li Z, Zhu L, Wang J, Zhang B, Zheng F, Zhao B, Zhang H, Wang Y, Zhang Z (2021) The multiple roles of ascorbate in the abiotic stress response of plants: antioxidant, cofactor, and regulator. Front Plant Sci **12**: 598173

Xu S, Hu E, Cai Y, Xie Z, Luo X, Zhan L, Tang W, Wang Q, Liu B, Wang R, Xie W, Wu T, Xie L, Yu G (2024) Using clusterProfiler to characterize multiomics data. Nat Prot ISSN 1750-2799

Yang Z, Mhamdi A, Noctor G (2019) Analysis of catalase mutants underscores the essential role of CATALASE2 for plant growth and day length-dependent oxidative signalling. Plant Cell Environ **42**: 688-700

Yeh HL, Lin TH, Chen CC, Cheng TX, Chang HY, Lee TM (2019) Monodehydroascorbate reductase plays a role in the tolerance of *Chlamydomonas reinhardtii* to photooxidative stress. Plant Cell Physiol **60**: 2167-2179

Yoon HS, Lee H, Lee IA, Kim KY, Jo J (2004) Molecular cloning of the monodehydroascorbate reductase gene from *Brassica campestris* and analysis of its mRNA level in response to oxidative stress. Biochim Biophys Acta **1658**: 181-186

Zamocky M, Furtmüller PG, Obinger C (2008) Evolution of catalases from bacteria to humans. Antioxid Redox Signal **10**: 1527-1548

Zandalinas SI, Fritschi FB, Mittler R (2021) Global warming, climate change, and environmental pollution: recipe for a multifactorial stress combination disaster. Trends Plant Sci **26**: 588-599

Zhang T, Ma M, Chen T, Zhang L, Fan L, Zhang W, Wei B, Zhang D, Li S, Xuan W, Noctor G, Han Y (2020) Arabidopsis S-NITROSOGLUTATHIONE REDUCTASE1 coordinates glutathione-mediated activation of the salicylic acid pathway in response to intracellular oxidative stress. Plant Cell Environ **43**: 1175-1191

Zhou F, Zheng B, Wang F, Cao A, Xie S, Chen X, Schick JA, Jin X, Li H (2021) Genome-wide analysis of mdhar gene family in four cotton species provides insights into fiber development via regulating asa redox homeostasis. Plants **10**: 227

université PARIS-SACLAY

ÉCOLE DOCTORALE
Sciences du végétal : du gène à l'écosystème (SEVE)

Titre : Étude sur les rôles de réductases monodéshydroascorbate spécifiques (MDHAR) chez *Arabidopsis thaliana*

Mots clés : stress oxydatif; antioxydants; ascorbate; glutathion; catalase; acide salicylique

Le peroxyde d'hydrogène (H_2O_2) est une molécule de signalisation importante chez les plantes, et son contenu est contrôlé par divers systèmes, notamment les catalases (CAT) et les ascorbate peroxydases (APX). Le fonctionnement continu de l'APX nécessite la régénération de l'ascorbate, pour laquelle plusieurs possibilités existent. Un type d'enzyme régénérant l'ascorbate est la monodéshydroascorbate réductase (MDHAR), une protéine dépendante du NAD(P)H qui est codée par cinq *MDAR* gènes chez Arabidopsis. Ce travail visait à examiner l'importance de ces gènes en utilisant des mutants à perte de fonction spécifiques alliés à d'autres techniques. L'analyse des transcrits a révélé que des mutants knock-out pouvaient être obtenus pour tous les gènes. Les dosages de l'activité de MDHAR dans des extraits de feuilles ont révélé que la *MDAR1* peroxysomale codait la majeure partie de l'activité dépendante du NADH, tandis que l'activité dépendante du NADPH était principalement codée par *MDAR1*, aux côtés de la *MDAR2* cytosolique. À l'exception du mutant *mdar4*, qui nécessitait du sucre pour la germination et la croissance post-germinative précoce, tous les mutants montraient un phénotype de type sauvage lorsqu'ils étaient cultivés dans des conditions standard. Pour explorer si l'absence d'impact phénotypique des mutations était due à la redondance des gènes, deux approches ont été utilisées. Dans la première, les mutants ont été croisés avec le mutant *cat2*, qui présente une activité de catalase foliaire fortement réduite, afin de tester les interactions entre différents systèmes d'élimination du H_2O_2. Dans la seconde, nous avons cherché à explorer une redondance entre les deux gènes *MDAR* codant des isoformes peroxysomales en produisant des mutants doubles *mdar1 mdar4*. Sur la base de l'analyse moléculaire et biochimique de toutes ces lignées, il peut être conclu que l'expression d'au moins une isoforme peroxysomale pourrait être nécessaire à la viabilité des plantes et que la *MDAR2* cytosolique semble coder la MDHAR la plus importante dans les conditions de stress oxydatif. Il est intéressant de noter que, l'introduction du mutant *mdar2* dans le fond génétique *cat2* a affaibli, plutôt que renforcé, certaines réponses au stress oxydatif, ce qui suggère des mécanismes de signalisation inédits liés à l'activité de la MDHAR.

Title : A study of the roles of specific monodehydroascorbate reductases (MDHARs) in *Arabidopsis thaliana*

Keywords : Oxidative stress; antioxidants; ascorbate; glutathione; catalase; salicylic acid

Hydrogen peroxide (H_2O_2) is an important signalling molecule in plants, and contents are controlled by various systems, notably catalases (CAT) and ascorbate peroxidases (APX). Continued function of APX requires regeneration of ascorbate, for which several possibilities exist. One type of ascorbate-regenerating enzyme is monodehydroascorbate reductase (MDHAR), an NAD(P)H-dependent protein which is encoded by five *MDAR* genes in Arabidopsis. This work aimed to examine the importance of these genes using specific loss-of-function mutants allied to other techniques. Transcript analysis showed that knockout mutants could be obtained for all the genes. Assays of MDHAR activity in leaf extracts revealed that the peroxisomal *MDAR1* encoded most of the NADH-dependent activity while NADPH-dependent activity was chiefly encoded by *MDAR1* alongside cytosolic *MDAR2*. Apart from *mdar4*, which required sugar for germination and early post-germinative growth, all mutants showed a wild-type phenotype when grown in standard conditions. To explore whether the lack of phenotypic impact of the mutations was caused by gene redundancy, two approaches were undertaken. In the first, mutants were crossed with the *cat2* mutant, which has greatly decreased leaf catalase activity, to test for interactions between different H_2O_2-removing systems. In the second, we sought to examine redundancy between the two *MDAR* genes encoding peroxisomal isoforms by producing double *mdar1 mdar4* mutants. Based on molecular and biochemical analysis of all these lines, it can be concluded that expression of at least one peroxisomal isoform might be required for plant viability and that the cytosolic *MDAR2* seems to encode the most important MDHAR in oxidative stress conditions. Intriguingly, introduction of *mdar2* into the *cat2* background weakened rather than enforced some responses to oxidative stress, pointing to novel signalling mechanisms related to MDHAR activity.